

**Interfacial Enhancement of Polypropylene -Zeolite  
Composites**



**By**

**Dildare METİN**

**A Dissertation Submitted to the  
Graduate School in Partial Fulfillment of the  
Requirements for the Degree of**

**MASTER OF SCIENCE**

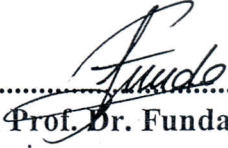
**Department: Chemical Engineering  
Major: Chemical Engineering**

**İzmir Institute of Technology  
İzmir, Turkey**

**April, 2002**

We approve the thesis of **Dildare METİN**

Date of Signature



.....  
**Asst. Prof. Dr. Funda TIHMINLIOĞLU**  
Supervisor  
Department of Chemical Engineering

26.04.2002



.....  
**Prof. Dr. Devrim BALKÖSE**  
Co-Supervisor  
Department of Chemical Engineering

26.04.2002



.....  
**Prof. Dr. A. Semra ÜLKÜ**  
Co-Supervisor  
Department of Chemical Engineering

26.04.2002



.....  
**Asst. Prof. Dr. S. Fehime ÖZKAN**  
Department of Chemical Engineering

26.04.2002



.....  
**Asst. Prof. Dr. Metin TANOĞLU**  
Department of Mechanical Engineering

26.04.2002



.....  
**Prof. Dr. Devrim BALKÖSE**  
Head of Department

26.04.2002

## ACKNOWLEDGEMENTS

I would like to thank and express my gratitude to Assistant Professor Funda Tihminliođlu for her supervision, guidance and support during my studies. I am also grateful to Professor Devrim Balköse and Professor Semra Ülkü for their valuable comments and recommendations.

I would like to thank the Technical and Scientific Research Council of Turkey (TÜBİTAK) and Government Planning Institute (DPT) for the financial support. I am very grateful to Petkim Petrochemicals Company for the supply of polypropylene used in this study.

I would like to thank Research Specialist Filiz Özmihçı for the thermal analyses, Research Specialist Özlem Çađlar for the FTIR analyses and Rahim İşler, Ali Öziş and Feridun Şenol from Petkim Petrochemicals Co. for the mechanical tests. I am also indebted to the laboratory technicians Şerife Şahin, Belgin Tunçel, and Tülin Burhanođlu for their helps in the laboratory work. I would like to appreciate deeply to my officemates, research assistants: Ayben Top, Hilal Pehlivan and Ulaş Atikler for their friendships and understandings. I would like to thank Semih Elbir for his help in the maintenance of the extruder.

Finally, I am grateful to my family for their supports and understandings during this thesis as in all stages of my life.

## ABSTRACT

The objective of this study was to improve the properties of polypropylene-zeolite composites by enhancement of the interphase between polypropylene and zeolite. Surface treatment of zeolite was applied for modification of interfacial interactions between zeolite and polypropylene. Surface treatment of natural zeolite was carried out with (3 wt%) polyethyleneglycol (PEG) and three different silane coupling agents namely, 3-aminopropyltriethoxysilane (AMPTES), methyltriethoxysilane (MTES), and 3-mercaptopropyltrimethoxysilane (MPTMS) at four different concentrations (0.5, 1, 1.5 and 2 wt%) to find suitable surface modifier for improving filler compatibility and mechanical properties. PP composites containing (2, 4 and 6 wt%) untreated or treated zeolite and plasticizers: dioctylphthalate (DOP) or epoxidized soybean oil (EPS) were prepared by extrusion technique. The effects of the modifications and zeolite content on the thermal, mechanical, structural and physical properties of PP composite were investigated.

The contact angle measurements and FTIR analyses of untreated and silane treated zeolite samples and water sorption results of PP-zeolite composites showed that hydrophobicity of zeolite significantly increases with surface modification.

Thermal analyses indicated that the addition of zeolite and silane treatment to the PP-EPS matrix did not change the melting and degradation temperature of the composites. However, these modifications were found to increase the crystallinity and crystallization temperature of the composites due to the nucleating effect of the zeolite.

The mechanical properties of PP composites containing silane treated zeolite indicated significant improvements compared to the composites containing untreated filler. The most enhanced dry and wet mechanical properties were observed for 1 wt% AMPTES treated zeolite containing PP composites. The effect of interfacial interactions and adhesion between zeolite and PP was evaluated by various semiempirical equations: Pukanszky model, Nicholais and Narkis model and Nielsen model. The improvement in adhesion between silane treated zeolite and PP was also confirmed from these models.

Moreover, the water sorption and mechanical test results, as well as scanning electron micrographs and optical micrographs of the composites verify that silane coupling agents enhanced compatibility and interfacial adhesion between zeolite particles and PP matrix strongly led to an improvement of the mechanical properties of

the composites. Consequently, 1 wt% AMPTES was proposed to be the most appropriate surface modifier by considering the water sorption results, thermal, mechanical and microstructure analyses of PP-zeolite composites.

## ÖZ

Bu çalışmada, polipropilen ve zeolit ara yüzeyi iyileştirilerek polipropilen-zeolit kompozitlerinin özelliklerinin geliştirilmesi amaçlanmıştır. Polipropilen ve zeolit arasındaki ara yüzey etkileşimleri zeolit yüzeyi kaplanarak modifiye edilmiştir. Kompozitlerin mekanik özelliklerini ve dolgu maddesiyle polipropilen arasındaki etkileşimi en uygun geliştiren yüzey etkin maddenin bulunabilmesi amacıyla zeolit yüzeyi (ağırlıkça % 3) polietilen glikol (PEG) ve dört farklı derişimde (ağırlıkça % 0.5, 1, 1.5 ve 2) üç farklı silan bağlayıcıyla: 3-aminopropiltrioksasilan (AMPTES), metiltrioksasilan (MTES), ve 3-merkaptopropiltrimetoksasilan (MPTMS) kaplanmıştır. Yüzeyi modifiye edilmiş ve işlem görmemiş zeolit (ağırlıkça % 2, 4, ve 6) ve plastikleştirici olarak dioktilfitalat (DOP) yada epokside soya yağı (EPS) içeren polipropilen kompozitler ekstrüzyon tekniğiyle hazırlanmıştır. Yüzey modifikasyonunun ve zeolit miktarının kompozitlerin ısıl, mekanik, yapısal ve fiziksel özellikleri üzerine etkileri incelenmiştir.

İşlem görmemiş ve silan bağlayıcılarla modifiye edilen zeolit örneklerinin kontak açısı ölçümleri ve FTIR analizleri ve PP-zeolit kompozitlerin su sorpsiyon sonuçları, zeolit hidrofobik özelliğinin yüzey modifikasyonu ile belirgin bir şekilde arttığını göstermiştir.

Isıl analiz sonuçları, PP-EPS matrisine zeolit ilavesi ve silan muamelesinin kompozitlerin erime ve bozunma sıcaklıklarını değıştirmedini göstermiştir. Buna karşın, bu modifikasyonların zeolit aş kristali etkisinden dolayı kompozitlerin kristalliğı ve kristalleşme sıcaklığını arttırdığı bulunmuştur.

Silanla modifiye edilen zeolit içeren PP kompozitlerin mekanik özellikleri işlem görmemiş zeolit içeren kompozitlere oranla belirgin ölçüde gelişme göstermiştir. En iyi kuru ve yaş mekanik özellikler ağırlıkça %1 AMPTES ile muamele edilmiş zeolit içeren kompozitlerde gözlenmiştir. PP ve zeolit arasındaki ara yüzey etkileşimleri ve yapışma Pukanszky, Nicholais-Narkis ve Nielsen modelleri kullanılarak değılendirilmiştir. Silan bağlayıcılarla işlem görmüş zeolit ve PP arasındaki yapışmadaki gelişme bu modellerle doğrulanmıştır.

Kompozitlerin su sorpsiyon ve mekanik test sonuçları, elektron taramalı mikroskop ve optik mikroskop fotoğraflarında da gözlendiğı gibi silan bağlayıcıların zeolit ve PP matrisi arasındaki uyumluluğı ve ara yüzeydeki yapışmayı iyileştirdiğı,

kompozitlerin mekanik özelliklerini geliştirdiğini desteklemektedir. Sonuç olarak, kompozitlerin su sorpsiyon sonuçları ısı, mekanik ve yapısal analiz sonuçları göz önüne alındığında en uygun yüzey aktif madde AMPTES (ağırlıkça % 1) olarak ön görülmüştür.

# TABLE OF CONTENTS

## LIST OF FIGURES

## LIST OF TABLES

Chapter 1. INTRODUCTION.....	1
Chapter 2. POLYMER COMPOSITES.....	5
2.1. Matrix: Polypropylene .....	7
2.2. Filler : Natural Zeolite .....	9
2.2.1. Clinoptilolite .....	11
Chapter 3. POLYMER - FILLER INTERFACE.....	12
3.1. Surface Modification of Filler .....	13
3.1.1. Non-reactive Treatment .....	13
3.1.2. Reactive Treatment .....	14
3.2. Modification of Polymer.....	15
3.3. Introduction of Elastomer .....	16
Chapter 4. SURFACE MODIFICATION OF FILLER.....	18
4.1. Coupling Agents .....	19
4.1.1. Silane Coupling Agents .....	21
4.2. Surface Modification Methods .....	25
Chapter 5. CHARACTERIZATION OF POLYMER COMPOSITES .....	27
5.1. Particle Size Analysis .....	27
5.2. Contact Angle Measurements .....	28
5.3. Thermal Analyses .....	31
5.3.1. Characterization of PP-Zeolite Composites by TGA .....	31
5.3.1. Characterization of PP-Zeolite Composites by DSC.....	32
5.4. Characterization of PP-Zeolite Composites by FTIR Spectroscopy.....	36
5.5. Mechanical Properties of Polypropylene Composites .....	38
5.6. Microstructure Analysis.....	43
Chapter 6. EXPERIMENTAL .....	44
6.1. Materials .....	44
6.2. Methods .....	45
6.2.1. Size Reduction of Zeolite .....	45
6.2.2. Surface Modification of Zeolite.....	46
6.2.3. Preparation of PP-Zeolite Composites.....	49
6.2.4. Characterization of Zeolite .....	50
6.2.4.1. Particle Size Measurement of Zeolite.....	50
6.2.4.2. FTIR Analysis of Zeolite .....	51
6.2.4.3. TGA of Zeolite.....	51
6.2.4.4. Contact Angle Measurements .....	51
6.2.5. Characterization of PP- Zeolite Composites .....	51
6.2.5.1. Infrared Analyses.....	51
6.2.5.2. Thermal Analyses .....	52
6.2.5.3. Water Sorption of PP-Zeolite Composites.....	52

6.2.5.4. Mechanical Characterization of PP-Zeolite Composites .....	52
6.2.5.5. Morphology of PP-Zeolite Composites .....	53
6.2.5.6. Density Measurements.....	53
Chapter 7. RESULTS AND DISCUSSION .....	54
7.1. Particle Size Measurement of Natural Zeolite .....	54
7.2. Contact Angle Measurements .....	55
7.3. Water Sorption of PP-Zeolite Composites .....	57
7.4. FTIR Spectroscopy Results.....	60
7.4.1. Characterization of Zeolite.....	60
7.4.2. Characterization of PP-Zeolite Composites .....	63
7.5. Thermal Analyses.....	65
7.5.1. Characterization of PP-Zeolite Composites by TGA .....	66
7.5.2. Characterization of PP-Zeolite Composites by DSC .....	69
7.5.2.1. Melting and Degradation Behaviour of PP-Zeolite Composites.....	69
7.5.2.2. Crystallization Behaviour of PP-Zeolite Composites .....	72
7.5.2.3. Crystallization Kinetics of PP-Zeolite Composites .....	76
7.6. Mechanical Properties of PP-Zeolite Composites.....	80
7.6.1. Young's Moduli of PP-Zeolite Composites .....	80
7.6.2. Tensile Yield Stress of PP-Zeolite Composites .....	84
7.6.3. Tensile Stress at Break .....	90
7.6.4. Elongation at Break .....	93
7.7. Microstructure Analyses .....	96
7.7.1 Optical Microscopy .....	96
7.7.1 Scanning Electron Microscopy (SEM).....	99
7.8. Density Measurements .....	101
Chapter 8. CONCLUSIONS AND RECOMMENDATIONS .....	104
REFERENCES .....	107
APPENDIX.....	112

## LIST OF FIGURES

Figure 2.1. Tacticity of Polypropylene .....	8
Figure 2.2. The 3D Structure of Zeolite.....	10
Figure 4.1. Examples of Non-silane Coupling Reactions in Polypropylene Composites .....	20
Figure 4.2. Bonding Siloxane to Polymer through Diffusion.....	22
Figure 4.3. Tensile Yield Strength of PP/CaCO <sub>3</sub> Against (a) Filler Content, (b) Amount of Coupling Agent .....	23
Figure 5.1. Surface Tensions in The Contact Angle Measurement .....	29
Figure 6.1. Surface Treatment Process of Gördes 1 Zeolite with PEG .....	47
Figure 6.2. Surface Treatment Process of Gördes 1 Zeolite with Silane Coupling Agents.....	48
Figure 6.3. Extrusion and Film Drawing Unit.....	49
Figure 6.4. Flow sheet of the Preparation of PP-Gördes 1 Zeolite Composites .....	50
Figure 7.1. Particle Size Measurements of Untreated and PEG Treated Zeolite.....	55
Figure 7.2. The Contact Angle Measurements of Treated Zeolites with AMPTES, MTES, and MPTMS .....	56
Figure 7.3. Water Sorption of PP – Untreated and PEG Treated Zeolite Composites with Different Plasticizers .....	57
Figure 7.4. Water Sorption of PP – Zeolite Composites as a Function of Zeolite Loading at Three Different Surface Modifiers .....	58
Figure 7.5. Chemical Reactions of Silane Coupling Agents with Zeolite Surface .....	59
Figure 7.6. FTIR Spectrum of AMPTES.....	60
Figure 7.7. FTIR Spectrum of MTES .....	61
Figure 7.8. FTIR Spectrum of MPTMS.....	61
Figure 7.9. FTIR Spectra of Untreated and Treated Zeolite with 1 wt% AMPTES, MTES, and MPTMS.....	62
Figure 7.10. Variation of b/a with Respect to Silane Coupling Agents.....	63
Figure 7.11. FTIR Spectra of PP Composites Containing 6 wt % Zeolite with DOP and EPS .....	64
Figure 7.12. FTIR Spectra of PP – EPS Composites Containing 6 wt% Untreated and Treated Zeolite with 1 wt % AMPTES.....	64

Figure 7.13. FTIR Spectra of PP – EPS Composites Containing 6 wt % Untreated and Treated Zeolite with 1 wt % MTES .....	65
Figure 7.14. FTIR Spectra of PP - EPS Composites Containing 6 wt % Untreated and Treated Zeolite with 1 wt % MPTMS .....	65
Figure 7.15. TGA Curve of Gördes 1 zeolite .....	67
Figure 7.16. TGA Curves of PP – EPS Composites Containing 2 wt % Untreated and Treated Zeolite.....	69
Figure 7.17. DSC Curves of PP – EPS Composites Containing 2 wt % Untreated and Treated Zeolite.....	71
Figure 7.18. DSC Curves of Composites Containing 4 wt % MPTMS Treated Zeolite at Different Cooling Rates.....	73
Figure 7.19. The Curves $\log q$ versus $1/\Delta T^2$ for Unfilled and Filled PP–EPS Composites Containing 4 wt % Untreated and Treated Zeolites with Silane Coupling Agents.....	76
Figure 7.20. Avrami Plots of Unfilled and Filled PP – EPS Composites with 4 wt % Untreated and Treated Zeolite with Different Silane Coupling Agents ....	77
Figure 7.21. Avrami Plot of The PP – EPS Composites Containing 4 wt % Treated Zeolite with 1 wt % MTES at a Cooling Rate of 10°C/min .....	78
Figure 7.22. Kissinger Plot of PP – EPS.....	79
Figure 7.23. Young’s Modulus of Dry and Wet PP – Zeolite Composites with Respect to Plasticizers and Zeolite Content .....	81
Figure 7.24. Effect of Silane Coupling Agents on The Young’s Modulus of Dry PP Composites Containing 6 wt % Zeolite.....	83
Figure 7.25. Effect of Silane Coupling Agents on The Young’s Modulus of Wet PP Composites Containing 6 wt % Zeolite.....	83
Figure 7.26. Experimental and Theoretical Young’s Modulus Values of PP – EPS with Respect to Zeolite Content .....	84
Figure 7.27. Dry and Wet Tensile Yield Stress of PP – Zeolite Composites with Respect to Zeolite Content for two Different Plasticizers.....	85
Figure 7.28. Effect of Silane Coupling Agents on The Dry Yield Stress of PP Composites Containing 6 wt % Zeolite .....	86
Figure 7.29. Effect of Silane Coupling Agents on The Wet Yield Stress of PP Composites Containing 6 wt % Zeolite.....	86

Figure 7.30. Effect of Surface Modifiers on the Experimental and Theoretical Dry Yield Stress of PP Composites with Respect to Zeolite Content and Pukanszky Model .....	88
Figure 7.31. Effect of Surface Modifiers on The Experimental and Theoretical Wet Yield Stress of PP Composites with Respect to Zeolite Content and Pukanszky Model .....	88
Figure 7.32. Experimental and Theoretical Dry Yield Stress Values of PP Composites Containing Treated Zeolite with 0.5 wt% MPTMS .....	90
Figure 7.33. Dry Tensile Yield Stress at Break of PP Composites with Respect to Zeolite Content .....	92
Figure 7.34. Wet Tensile Yield Stress at Break of PP Composites with Respect to Zeolite Content .....	92
Figure 7.35. Experimental and Theoretical Dry Tensile Stress at Break Values of PP Composites Containing Treated Zeolite with 1 wt % AMPTES.....	93
Figure 7.36. Effect of Silane Coupling Agents on The Elongation at Break of PP Composites with Respect to Zeolite Content .....	94
Figure 7.37. Effect of Silane Coupling Agents on The Elongation at Break of PP Composites Containing 4 wt % Zeolite.....	95
Figure 7.38. Experimental and Theoretical Elongation at Break Values of The Composites Containing Treated Zeolite with 1.5 wt% MPTMS .....	96
Figure 7.39. Optical Micrographs of Untreated and PEG Treated Zeolite.....	97
Figure 7.40. Optical Micrographs of AMPTES, MTES, and MPTMS Treated Zeolite.....	98
Figure 7.41. Optical Micrographs of 50 Times Magnified PP Composites Containing EPS and 4 wt % (a) Untreated Zeolite and (b) PEG Treated Zeolite .....	98
Figure 7.42. Optical Micrographs of 50 Times Magnified PP Composites Containing EPS and 4 wt % Treated Zeolite and (a) 1 wt % AMPTES, (b) 1 wt % MTES, and (c) 0.5 wt % MPTMS.....	99
Figure 7.43. SEM Micrographs of The Fracture Surfaces of PP Composites Containing 4 wt% (a) Untreated Zeolite and Treated Zeolite with (b)1 wt% AMPTES, (c) 1 wt % MTES, (d) 1 wt % MPTMS.....	100
Figure 7.44. Effect of Surface Treatment on The Experimental Densities of PP Composites with Respect to Zeolite Content .....	102

Figure 7.45. Effect of Silane Coupling Agents on The Void Fractions in PP-Zeolite Composites..... 103

Table 2.1.

Table 2.2.

Table 2.3.

Table 4.1.

Table 4.2.

Table 4.3.

Table 5.1.

Table 5.2.

Table 5.3.

Table 6.1.

Table 6.2.

Table 6.3.

Table 7.1.

Table 7.2.

Table 7.3.

Table 7.4.

Table 7.5.

Table 7.6.

Table 7.7.

Table 7.8.

Table 7.9.

Table 7.10.

Table A.1.

Table A.2.

Table A.3.

## LIST OF TABLES

Table 2.1. Common Polymers Used in Composites .....	5
Table 2.2. Common Fillers and Reinforcements for Polymers .....	6
Table 2.3. Properties of Typical Filled and Unfilled Polypropylene.....	9
Table 4.1. Miscellaneous Coupling Agents for Polypropylene Composites .....	20
Table 4.2. Commonly Used Silane Coupling Agents.....	22
Table 4.3. Comparison of Pre-Treatment with In-Situ Treatment.....	25
Table 5.1. Characteristic Peaks of Polypropylene .....	36
Table 5.2. Characteristic Peaks of Natural Zeolite .....	37
Table 5.3. Characteristic Peaks of Silane Coupling Agents .....	38
Table 6.1. Chemical Composition of MH-418 PP .....	44
Table 6.2. Chemical Structures of Surface Modifiers .....	46
Table 6.3. Experimental Conditions of the Extrusion Process .....	49
Table 7.1. TGA Results of PP-Untreated Zeolite Composites .....	66
Table 7.2. TGA Results of PP-2 wt % Treated Zeolite Composites .....	68
Table 7.3. DSC Results of PP-Untreated Zeolite Composites.....	70
Table 7.4. DSC Results of PP-2 wt % Treated Zeolite Composites.....	72
Table 7.5. Crystallization Results of PP-EPS Composites Containing 4 wt% Zeolite .....	74
Table 7.6. Avrami Parameters of the PP-Zeolite Composites for Non-isothermal Crystallization.....	79
Table 7.7. Activation Energy Values of the PP-Zeolite Composites for Non-isothermal Crystallization.....	80
Table A.1. Density and Water Sorption Results of PP- Zeolite Composites .....	112
Table A.2. Contact Angle Measurements.....	114
Table A.3. Experimental Dry Tensile Test Results of PP- Zeolite Composites.....	115
Table A.4. Experimental Wet Tensile Test Results of PP- Zeolite Composites .....	117
Table A.5. B values in Pukanszky Model for Dry and Wet Yield Stress of PP-Zeolite Composites.....	119
Table A.6. Values of Adhesion Parameter “a” in Nicolais Nartis Model for Dry and Wet Yield Stress of PP-Zeolite Composites.....	120

Table A.7. Values of Stress Concentration Parameter “S” in Nielsen Model for Dry and Wet Tensile Stress at Break Values of PP-Zeolite Composites.....	121
Table A.8. Values of Interaction Parameter “K” for Dry and Wet Elongation at Break Values of PP-Zeolite Composites.....	122
Table A.9. Theoretical Dry Tensile Tests Results of PP Composites .....	123
Table A.10. Theoretical Wet Tensile Tests Results of PP Composites.....	125

# Chapter 1

## INTRODUCTION

Polypropylene is one of the most important commercial polymers for its superior intrinsic properties such as high melting temperature, high chemical resistance, and low density. However, polypropylene in many applications is never used alone, but always in combination with other materials such as fillers or reinforcing agents to extend the polymer, to decrease the price of the compound and to provide functional properties to the polymer such as flame retardant or conductivity.

CaCO<sub>3</sub>, talc, mica, Mg(OH)<sub>2</sub> or glass fibers are extensively used fillers to enhance the properties of polypropylene in many fields of application such as household, electronic, automotive industry, etc.. Mostly interfacial properties between PP and filler strongly influence the properties of the composite. For that reason, the interface between PP and the filler is modified to improve wettability and adhesion between filler and PP by the modification of the PP or surface treatment of the filler. Modification of the polymer can be done by three different methods: plasma, corona discharge and ion beam irradiation methods. Modification of the polymer depends on surface properties of the polymers that leads to the rough surface and surface damage such as bond scission, carbonization and crosslinking. Generally, corona treatment is used to increase dye printing in the packaging industry. Surface treatment of the filler with surface modifiers such as fatty acids, silane coupling agents and titanate coupling agents has been widely used for the modification of the interface in particulate filled polymers, that does not lead to the surface damage of the polymer. Silane coupling agents are widely used for the modification of the interface that provide better improved properties than the other surface modifiers (Khunava, 1998, Koh et al., 2001).

Silane coupling agents modify the interface by interacting with both the filler and PP, thus forming a link between the components. In the literature, there are many studies dealing with the characterization of interfaces and their influence on the mechanical properties of particulate filled composites. Surface modification with silane coupling agents has given satisfactory results for CaCO<sub>3</sub>, silica, mica, talc and glass fibers (Demjen et al, 1997 and 1998, Khunava, 1998, Nakatsuka, 1985, Ulutan and Balköse 1996, Xavier and Schultz, 1990).

Demjen et al. (1997) investigated the influence of interfacial interactions on the polypropylene-CaCO<sub>3</sub> composites. Interfacial interactions were modified by surface treatment of the filler. Polypropylene composites were prepared by different amounts of filler treated with eight functional trialkoxy silane coupling agents and stearic acid. Tensile properties of the composites were determined and the effect of interfacial interactions was evaluated by semiempirical equations. Amino functional silanes increased the strength of the interaction considerably. The other coupling agents reduce the surface tension of the filler, which leads to a decrease in the tensile strength of the composites.

Ulutan and Balköse (1996) studied the effects of surface modification of the silica with  $\gamma$ -aminopropyltrimethoxysilane coupling agent and water sorption on the interfacial properties of flexible PVC-silica composites. Liquid water and water vapor sorption of the PVC composites by silane application were decreased about 24 % and 11.9 % respectively. Also they studied the ultimate tensile strength of the composites (UTS) under wet conditions. While the untreated silica composite reduced its UTS by about 21.2 %, silanized silica composite reduced its UTS by only about 13.6 % under wet conditions. The improvement of the interface by silane treatment had been observed through the tensile tests, water and water vapor uptake results.

Domka (1994) investigated surface modification of CaCO<sub>3</sub>, kaolin and synthetic CaCO<sub>3</sub>. These fillers were modified with many types of surface active substances, fatty acids and their derivatives, silane coupling agents and titanate coupling agents. The modified fillers were tested in rubber mixtures based on butadiene-styrene rubber and in polyurethanes. The surface hydrophobization of these fillers increased using all surface modifiers. Hydrophobization degree was found to be closely dependent on the amount of surface modifier. Strong hydrophobization led to increasing of the polymer-filler adhesion.

Xavier and Schultz (1990) studied the influence of mica surface treatments in polypropylene composites at constant mica content (40 wt%). They used isopropyl triisostearoyl titanate and 3-aminopropyl triethoxy silane and investigated the effect of surface treatment on the microstructure and fracture propagation in the composites. Improved interfacial adhesion was observed in the case of silane treated mica composites.

Levita et al. (1989) investigated the effect of modifiers on the strength and fracture properties of polypropylene filled with calcium carbonate. CaCO<sub>3</sub> was modified

with stearic acid and titanate coupling agent. The untreated filler caused a decrease of toughness whereas 10 % increase was observed for the titanate treated filler.

Although different fillers such as  $\text{CaCO}_3$ , talc, mica, glass fiber were used as in PP matrix, not many work was cited in the literature about the use of zeolite as a filler. Zeolite can be used as an alternative material instead of calcium carbonate, talc and mica in polypropylene composites. Zeolites are inorganic, microporous, crystalline solids widely used as catalysts, adsorbents, ion exchangers and also fillers. Khunava and Sain (1995) investigated the effect of 3-phenylene bismaleimide (BMI) as a modifier for 17.3–53.3 wt% talc and zeolite filled polypropylene composites. The tensile strength of zeolite filled composites demonstrates a maximum 41.4 MPa for the highest concentrations of 2.6 wt% BMI and 53.3 wt% zeolite. This fact indicates that the degree of interaction between polypropylene and zeolite is directly proportional to the concentration of filler for a BMI concentration 2.6 wt%. A maximum tensile strength was obtained as 44.5 MPa by the composites filled with only 40 wt% talc containing 3 wt% BMI. These results indicate that polypropylene shows a variable degree of filling capacity depending on the type of filler and concentration of surface modifier.

Özmiğci (1999) and Pehlivan (2001) studied the preparation and characterization of polypropylene–zeolite composites. They concluded that zeolite loading increases the thermal stability of polypropylene and decreases the mechanical properties of polypropylene because of poor interfacial adhesion between the filler and polypropylene.

The objective of this study is to improve the properties of the polypropylene-zeolite composite by enhancement of the interphase between polypropylene and zeolite. For that reason, zeolite was treated with four different surface modifiers: polyethyleneglycol (PEG) and three different silane coupling agents 3-aminopropyltriethoxysilane (AMPTES), methyltriethoxysilane (MTES) and 3-mercaptopropyltrimethoxysilane (MPTMS) to improve the compatibility of zeolite and PP and corresponding mechanical properties of the composites.

In this thesis, interfacial enhancement of polypropylene-zeolite composite is outlined. Chapter 2 presents general information on polymer composites and introduces polypropylene as the matrix and zeolite as the filler to be used in this study. Chapter 3 presents the polymer-filler interface and the modification methods of the polymer-filler interface. Chapter 4 deals with surface modification of the filler. In Chapter 5, the characterization methods of polypropylene-zeolite composites are given. In Chapter 6

and 7, the experimental study and the results and discussions are given. Finally, Chapter 8 presents the conclusions of this study with the recommendations for future studies.

### Composites

physical and chemical

Composites are

primary phase

Matrix can be

form of fibers

inorganic, polymeric

### Polymer

composites are

cost and ease of

polymers used

Table 2.1. Classification of Composites

Classification	Subclassification
Polymeric matrix	Polyester
	Polyepoxy
	Polyvinyl
	Polyurethane
	Polyacrylate
	Polyimide
	Polyamide
	Polyether

### Many

thermal, optical

## Chapter 2

### POLYMER COMPOSITES

Composite is defined as a combination of two or more components that differ in physical and chemical properties to provide specific characteristics for particular uses. Composites have two main phases, matrix and filler or reinforcing agent. Matrix is the primary phase and filler or reinforcing agent is the secondary phase in the composite. Matrix can be polymer, metal or ceramic. Fillers or reinforcing agents may be in the form of fibers, wires, powders, granules, or whiskers which are made of organic, inorganic, metallic or ceramic material.

Polymers are usually preferred as a matrix instead of metal or ceramic for composites because of their low density, low electrical and thermal conductivity, low cost and easy processability. Table 2.1 shows the common thermoplastic or thermoset polymers used as matrix in composites.

Table 2.1. Common Polymers Used in Composites.

Thermoplastics	Thermosets
Polypropylene (PP)	Alkyds
Polyethylene (PE)	Amino plastics
Polyvinyl chloride (PVC)	Cyanate esters
Polystyrene (PS)	Epoxy resins
Polyethylene terephthalate (PET)	Phenolic plastics
Polymethyl methacrylate (PMMA)	Polyimides
Polytetrafluoroethylene (PTFE)	Elastomers

Many kinds of fillers as listed in Table 2.2 are used to improve the mechanical, thermal, optical and processing properties and to reduce cost of a polymeric product in

different industries such as packaging, automotive or wire coatings. The main reasons related to the use of fillers in polymers are:

- Increased stiffness, strength and dimensional stability
- Increased toughness or impact strength
- Increased heat distortion temperature
- Increased mechanical damping
- Possibility to vary permeability of the composites to gas and liquids
- Modified electrical properties
- Reduced cost

However, all of these desirable features may not be found in any single composite. The properties of composite materials are determined by the properties of components such as the shape, particle size and composition of the filler phase, by the morphology of the system, and by the nature of the interface between the phases (Nielsen, 1974).

Table 2.2. Common Fillers and Reinforcements for Polymers.

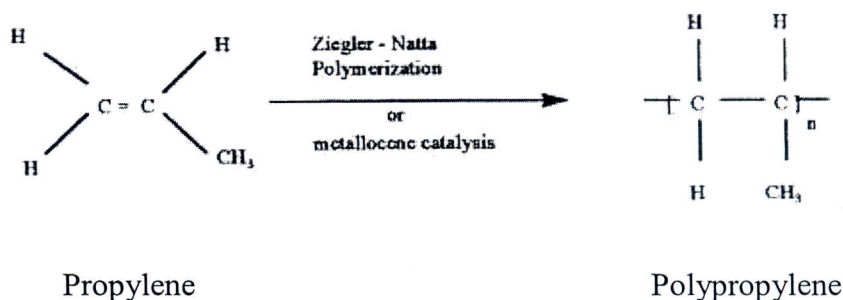
Filler	Chemical composition
Calcium carbonate	$\text{CaCO}_3$
Talc	$\text{MgSiO}_3$
Kaoline	$\text{Al}_2\text{O}_3 \cdot 2\text{SiO}_2 \cdot 2\text{H}_2\text{O}$
Mica	$\text{KFeMgAlSiO}_n$
Silica	$\text{SiO}_2$
Wollastonite	$\text{CaSiO}_3$
Magnesium hydroxide	$\text{Mg(OH)}_2$
Alumina	$\text{Al}_2\text{O}_3$
Glass fibers	
Cellulose	
Starch	

In the present study, polypropylene as the matrix material and clinoptilolite type zeolite as the filler was used.

## 2.1. Matrix: Polypropylene

Polypropylene is one of the most important commercial polymers for its superior intrinsic properties such as high melting temperature, high chemical resistance to acids alkalies and salt solutions, low water absorption, easy reprocessing and low density (Moore, 1996).

Polypropylene is a high molecular weight organic material. Its semicrystalline form is enabled by the regularity of the polymer chain. The regularity is controlled by the use of mostly Ziegler-Natta or metallocene catalyst technology in polymerization processes as shown below.



Propylene

Polypropylene

Polypropylene is a highly versatile material for the following reasons (Galli et al., 1984):

- The polymer with different morphological and molecular structures can be synthesized using high yield catalysts and new processes
- The polymer can contain high amount of filler and reinforcing agent, can be blended with other polymeric materials, and can be treated with flame-, light-, and thermal resistant products, processing aids, etc.
- The polymer can be modified by grafting with functional groups to produce polar polymers, multilayer composite structures, and anticorrosion systems for metal items.

The structure of polypropylene determines the physical properties of polypropylene and its processability. The most two critical features of a base polypropylene are its molecular weight and its tacticity (polymer-chain configuration). The molecular weight and tacticity have the strongest influence on physical and process properties of polypropylene. Typical commercial polypropylene has molecular weights

ranging between 10,000 and 1,000,000 grams per mole. In general, a broader molecular weight will tend to improve crystalline properties such as tensile strength, stiffness, and heat distortion temperature (HDT), while it decreases impact. In addition, the broader molecular weight polypropylene exhibits lower viscosity at high shear rates, which provides improved performance in processes such as injection molding.

The tacticity of polypropylene results in its semicrystalline form. It determines the amount of the material that can crystallize, but not the amount that will crystallize. Tacticity is introduced due to the various arrangements of the methyl groups in the general formula of polypropylene as given in Figure 2.1. Typically, isotactic structure forms over 90% of the chains in polypropylene to provide the regularity necessary for the formation of crystals. In isotactic structure, the methyl groups occur on one side of the molecules. The remainder of the chains has an atactic or random arrangement. This portion of polypropylene can not crystallize and is soft and soluble in a number of solvents.

Isotactic polypropylene (PP) is one of the most important commodity polymers widely used in technical applications because of its good mechanical properties, facile processing, versatility to accept numerous types of filler, and relatively low cost (Tjong et al., 1997).

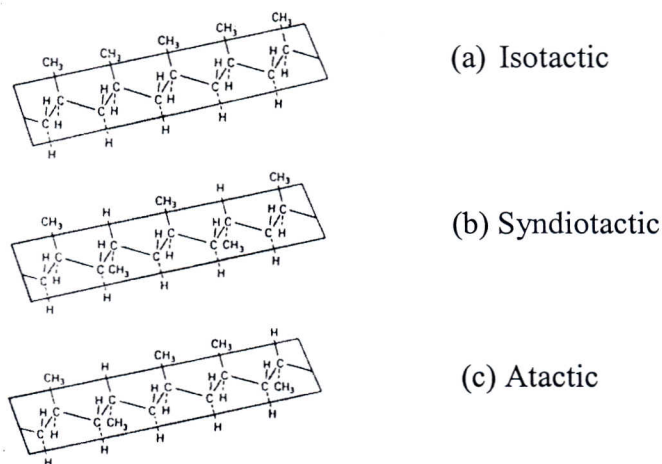


Figure 2.1. Tacticity of Polypropylene.

The properties of polypropylene can be enhanced dramatically by the addition of fillers and reinforcements such as  $\text{CaCO}_3$ , talc, mica, silica, zeolites carbon fiber or glass fiber. One of these fillers and reinforcements,  $\text{CaCO}_3$  is used extensively in

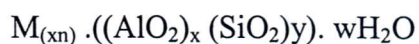
polypropylene matrix. The properties of typical filled and unfilled polypropylene depend on chemical composition and shape of the fillers as shown in Table 2.3. (Seymour, 1990). Especially, chemical composition and purity of the filler have a direct effect on its application possibilities and performance. Insufficient purity leads to discolouration of the product and limits the application of the filler (Karger-Kocsis, 1995).

Table 2.3. Properties of Typical Filled and Unfilled Polypropylene (Seymour, 1990).

	Unfilled PP	40% Talc PP	40% Ca CO <sub>3</sub> PP	40% Glass PP	30% Graphite PP
T <sub>m</sub> (°C)	170	168	168	163	168
Heat deflection temperature at 1.82MPa (°C)	55	100	80	160	120
Max. resistance to continuous heat (°C)	100	120	110	135	125
Coefficient of linear expansion (cm/cm°Cx10 <sup>-5</sup> )	9	6	4	3	3
Tensile strength (MPa)	35	32	26	82	47
% Elongation	150	5	15	2	0.5
Flexural strength (MPa)	48	60	45	100	62
Compressive strength (MPa)	45	52	35	64	55
Specific gravity	0.90	1.25	1.23	1.22	1.04

## 2.2. Filler: Natural Zeolite

Zeolites are porous crystalline, hydrated aluminasilicates of alkaline and alkaline earth elements such as sodium, potassium, calcium, and barium. The structural formula of a zeolite is shown below:



M is the cation of valance n, w is the number of water molecules and the ratio  $y/x$  refers to the Si/Al, usually has the values of 1-5 depending upon the structure. Structurally the zeolites are framework aluminosilicates based on infinitely extending three-dimensional network of  $AlO_4$  and  $SiO_4$  tetrahedra linked to each other by shearing all of the oxygens. 3D structure of zeolites is shown in Figure 2.2. (Breck, 1974).

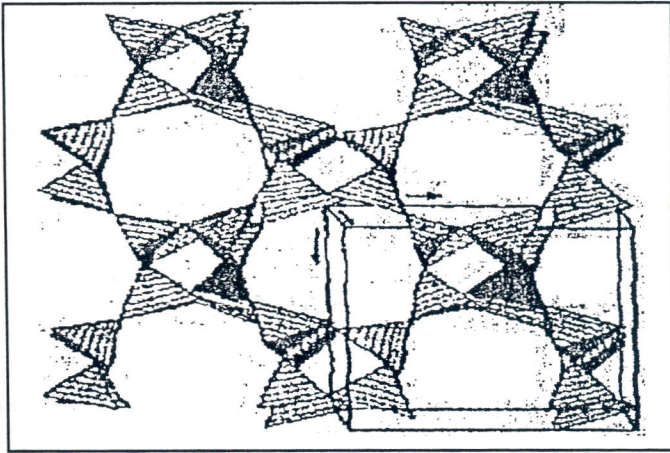


Figure 2.2. The 3D Structure of Zeolite.

Natural zeolites form as a result of the chemical reaction between volcanic glass and saline water and also by alteration of pre-existing feldspars, poorly crystalline clays, and biogenic silica (Palaban, 1994). Nowadays, 50 types of natural zeolite and more than 120 types of synthetic zeolites have been reported in the literature. The variety of zeolites types is resulted from differences in the way in which the tetrahedra may link in one, two or three dimensions and from the type of other ions that substitute within the interstices. The most common natural zeolites are clinoptilolite, analcime, heulandite, laumontite and phillipsite (Dwyer and Dyer, 1984, Dyer, 1984, Van et al., 1991, Vasant, 1990). In Turkey, mostly clinoptilolite from heulandite group and analcime type zeolites are available (Özkan and Ülkü, 1997).

Physical and chemical properties of zeolite vary among zeolite types. The differences are primarily due to differences in crystal structure and chemical composition such as particle density, cation selectivity, void volume, molecular pore size, and crystal shape vary depending on the zeolite type (Dwyer and Dyer, 1984).

Zeolites take place in various applications due to their inherently regular pore dimensions on the molecular scale and high thermal stability. In particular, zeolites are

widely used as catalysts, adsorbents, ion exchangers and fillers. Some applications of zeolites are removal of SO<sub>2</sub> and CO<sub>2</sub> from industrial waste gas, production of O<sub>2</sub> and N<sub>2</sub> from air, removal of heavy metals and ammonium ions from wastewater and usage as fillers in phenolic resins, plastics and papers. In addition, silver exchanged natural zeolites are used as antibacterial agents. However, naturally occurring zeolites are rarely phase-pure and are contaminated to varying degrees by other species such as Fe<sup>++</sup>, SO<sub>4</sub><sup>-</sup>, quartz, other zeolites and amorphous glass. For this reason, naturally occurring zeolites are limited in many important commercial applications where uniformity and purity are essential (Berry, 2000, Dyer, 1984).

### 2.2.1. Clinoptilolite

Clinoptilolite, a member of heulandite group of natural zeolites, is the most abundant and commonly used zeolite mineral. Idealized formula of clinoptilolite is in the form of (Na,K)<sub>6</sub>(Al<sub>6</sub>Si<sub>30</sub>O<sub>72</sub>)20H<sub>2</sub>O. Although major exchangeable cations in clinoptilolite are Na and K, Ca and Mg may also present in the clinoptilolite. Si/Al ratio is between 4.25 – 5.25 and the density range of clinoptilolite is 1.7-2.3g/cc. Clinoptilolite has high thermal resistance up to 750 °C due to the high silicon concentration. (Gottari and Galli, 1985).

Although, clinoptilolite is colorless or white, it may be colored as brick red due to the presence of finely oxides of iron or similar impurities. The composition and purity of clinoptilolite are dependent on mineral deposits.

## Chapter 3

### POLYMER - FILLER INTERFACE

Interface can be defined as a boundary between components in the composite. However, interphase refers to the transient region of components in the composite. Interphase in the polymer composites is a region such as diffusion zone, or a chemical reaction zone where filler or reinforcement and matrix phases are chemically or mechanically combined (Tang and Kardos; 1997).

Interfaces in multicomponent polymer systems containing fillers, reinforcing materials, flame retardants, elastomers, pigments, etc. play an important role in the mechanical and physical properties of the composite materials. Properties of polymer composites are significantly influenced by interfacial interactions. The interactions in the interface of polymer composites can be formed by chemical bonding or secondary bonding such as ionic bonding, dipolar interactions, dispersion forces, covalent bonding and hydrogen bonding. Ionic bonding results in the electrostatic attraction between oppositely charged ions. Dipolar bonding is caused by the interaction of permanent dipoles within the material. Dispersion force bonding results in the attraction between local electron density fluctuations in the material caused by electron mobility. Covalent bonding is due to the formation of chemical bonds within the material. Hydrogen bonding is similar to ionic bonding and results in sharing of an adjacent hydrogen atom by two other atoms. Physical and chemical interactions across the phase boundaries control the overall performance of polymer composites. Strong interactions such as covalent bonding and hydrogen bonding cause good adhesion and efficient stress transfer from the polymer matrix to the fillers and reinforcements in the composites (Wightman, 1993, Xanthos, 1988).

Interfacial properties of polymer composites depend on the polymer matrix, the additives, filler content, and the compounding technologies (Bertalan et al., 2001). Interface in polymer composites can be improved by three different methods:

- Surface modification of filler
- Modification of polymer

## Chapter 3

### POLYMER - FILLER INTERFACE

Interface can be defined as a boundary between components in the composite. However, interphase refers to the transient region of components in the composite. Interphase in the polymer composites is a region such as diffusion zone, or a chemical reaction zone where filler or reinforcement and matrix phases are chemically or mechanically combined (Tang and Kardos; 1997).

Interfaces in multicomponent polymer systems containing fillers, reinforcing materials, flame retardants, elastomers, pigments, etc. play an important role in the mechanical and physical properties of the composite materials. Properties of polymer composites are significantly influenced by interfacial interactions. The interactions in the interface of polymer composites can be formed by chemical bonding or secondary bonding such as ionic bonding, dipolar interactions, dispersion forces, covalent bonding and hydrogen bonding. Ionic bonding results in the electrostatic attraction between oppositely charged ions. Dipolar bonding is caused by the interaction of permanent dipoles within the material. Dispersion force bonding results in the attraction between local electron density fluctuations in the material caused by electron mobility. Covalent bonding is due to the formation of chemical bonds within the material. Hydrogen bonding is similar to ionic bonding and results in sharing of an adjacent hydrogen atom by two other atoms. Physical and chemical interactions across the phase boundaries control the overall performance of polymer composites. Strong interactions such as covalent bonding and hydrogen bonding cause good adhesion and efficient stress transfer from the polymer matrix to the fillers and reinforcements in the composites (Wightman, 1993, Xanthos, 1988).

Interfacial properties of polymer composites depend on the polymer matrix, the additives, filler content, and the compounding technologies (Bertalan et al., 2001). Interface in polymer composites can be improved by three different methods:

- Surface modification of filler
- Modification of polymer

- Introduction of elastomer

### 3.1. Surface Modification of Filler

Many kinds of fillers used for incorporation into polymers are treated with various surface modifiers in order to modify the characteristics of the filler-matrix interface. Surface modification of the filler prevents the agglomerations of the particles by decreasing the strength of the interactions between particles. This may lead to improvements in the dispersion of the fillers during compound preparation and the mechanical properties of filled polymer composites (Hornsby and Watson, 1995, Mareri, 1997).

Surface modification of fillers changes the surface free energy of the fillers. Surface free energy of the fillers determines both matrix-filler and particle-particle interactions. While matrix-filler interactions depend on adhesion and affinity of the components, this type of interactions significantly influence the mechanical properties, particularly yield stress, tensile strength, and impact resistance. Particle-particle interactions determine aggregation. Both interactions can be modified by surface treatment.

Surface modification can be classified in two groups according to interactions between polymer and filler; non-reactive treatment and reactive treatment. Interaction between the surface modifier and the filler surface is generally strong for all types of surface modifier. In most cases, this is a chemical bond in the form of a carboxylate linkage with a fatty acids or strong hydrogen bond with coupling agents. There is also interactions between the adsorbed and non-adsorbed surface modifier and the polymer matrix. If the modification of the filler is resulted in weak interactions, this type of treatment is called as non-reactive treatment. If this interaction and a mutual interaction between the absorbed and non-absorbed surface modifier molecules are strong, this type of treatment is called as reactive treatment (Liauv, 2000).

#### 3.1.1. Non-reactive Treatment

Non-reactive treatment of a filler surface with a surfactant is widely used to influence both particle-particle and particle-matrix interaction. Non-treated fillers and reinforcements have high energy surfaces while polymers have low surface free energy.

The surface energy of the fillers is closely related to the hydrophilicity of the filler. The hydrophobicity of the fillers can be increased by chemisorption of surface active agents such as fatty acids. Non reactive treatment depends on acid-base reactions between filler surface and surface modifier. Polar (-COOH) functional groups of fatty acids react with the filler surface, which combine within their structure similarities with the polymer. Surface free energy of the treated filler with fatty acids such as stearic acid decreases. Change in surface free energy of the fillers provides wettability of the filler with polymer. Non-reactive surface treatment of the filler modifies only the van der Waals forces between the surface of the filler and the matrix. This type of treatment leads to decreased aggregation, improved homogeneity and ease of processing, but decreased matrix-filler interaction (Bledzki and Gassan, 1999, Demjen et.al.,1998, Hornsby and Watson, 1995, Karger-Kocsis,1995, Pukansky, 1989).

Rao et al. (1998) studied the interfacial interactions and mechanical properties of wollastonite filled polymethylmethacrylate (PMMA) composites. In general, wollastonite is modified by reactive coupling agents (silanes, titanates) to improve the interfacial bonding between the filler and the matrix. However, the wollastonite was treated with stearic acid, a cheap non-reactive coupling agent, to disperse the particles in the matrix in this study. The PMMA filled with 20 wt% treated and untreated wollastonite composites were prepared in a twin screw extruder and an injection molding machine. The tensile modulus of the composites containing untreated and treated wollastonite increased by 66 and 78 % respectively, when compared to the unfilled PMMA. However, the tensile strength of PMMA filled with treated wollastonite increased by 17 % when compared to the unfilled PMMA. The mechanical results indicated that a strong interfacial bonding between stearic acid and the filler taken place because of acid-base interactions between the filler and stearic acid.

Anionic and cationic hydrophobic wetting agents are also used for non-reactive treatment. These amine salts of fatty acids encapsulate the filler with a hydrophobic monomolecular layer, which displaces air and water on the filler surface (Whelan and Craft, 1985).

### **3.1.2. Reactive Treatment**

In the case of reactive treatment, surface free energy of the filler also decreases because of the presence of an organic substance on its surface. Reactive coupling agents

(silanes or titanates) can create covalent bonds between the reactive groups of the polymer matrix and those of the filler.

Acid functionalized polymers with an unsaturated chain structure such as maleanized or acrylic acid modified polyolefins are also considered as effective coupling agents for basic and amphoteric surface fillers in polyolefin matrix materials. Modification of the polymer composite can be carried out by incorporation of reactive sites such as carboxylic acid or anhydride groups on to the polymer chain either during polymerization or by subsequent reactive modification in the molten state (Hornsby and Watson, 1995). Maleanized or acrylic acid modified polyolefins can also be used for fillers with acidic surface, such as clays and glasses after the treatment of these fillers with aminosilane. Both the use of functionalized polyolefins and surface treatment of filler with aminosilane provide high strength to the polymer composite (Liau, 2000).

### 3.2. Modification of Polymer

Surface characteristics of polymers determine their interfacial and adhesion properties in technological applications. There have been many attempts to modify the surface of polymers to improve wettability, dye printing, and adhesion to other polymers and fillers. Plasma technology, corona discharge, and ion beam irradiation have been used for modifications of the polymers. These treatments depend on electric discharge and surface properties of the polymers. However, rough surface and/or surface damage such as bond scission, carbonization, and cross-linking are produced by the above methods and thereby influence the bonding to the polymers. These methods are effectively used to improve mechanical properties of polypropylene and polyethylene composites (Koh et.al., 2001, Bledzki and Gassan, 1999, Akovali and Dilsiz, 1996).

Corona treatment is one of the most interesting techniques for surface oxidation and activation. Corona treatment involves passing a polymeric solid through a gap between a grounded and charged electrode. Under this situation, atmospheric gases such as oxygen and nitrogen are ionized and able to interact strongly with the substrate to be treated. The chemistry initiated by corona discharges is complex and depends not only on the variables of the corona, but also the substrate being treated. The most common application of corona is the surface treatment of polyolefins. These are significantly oxidized in corona discharges. This process changes the surface energy of the polymer

(Schreiber, 1993). Corona treatment is the most applicable method in the packaging industry to increase the adhesion of polymeric films.

Plasma is defined as an ionized gas with an essentially equal density of positive and negative charges. Plasma treatment depends on type and nature of the used gases, and a variety of surface modifications. Plasmas in inorganic vapors, such as nitrogen, ammonia, oxides of sulfur, nitrogen, and carbon, can be used to modify surfaces by implementing chemical groups derived from the active species of the plasma discharge. These plasmas are capable of chemically modifying treated surfaces, without encapsulating them in polymeric layers. Surface crosslinkings can be introduced, surface energy can be increased or decreased, reactive free radicals and groups can be produced (Bledzki and Gassan, 1999, Schreiber, 1993).

Akovağlı (1997) studied the mechanical and thermal properties of polypropylene composites containing (10, 20 and 30 wt%) modified calcium carbonate with plasma polymerized acetylene. Although no significant change was observed in crystalline melting points of unfilled, unmodified and modified  $\text{CaCO}_3$  filled polypropylene samples, some changes in the heat of fusion values were obtained depending on the differences in plasma- operational parameters used. Some of the composite samples prepared with surface-modified  $\text{CaCO}_3$  are found to yield higher percentage elongations and are mechanically superior compared to those prepared with unmodified filler.

### **3.3. Introduction of Elastomer**

Elastomers are incorporated to pure polymers or particulate filled polymers to improve the properties of polymeric materials such as impact resistance. In particulate filled ternary polymers, filler was encapsulated by the elastomer. The presence of elastomer improves the processability and the mechanical properties of particulate filled polymers. Ethylene-propylene-diene-terpolymer (EPDM) or elastomer blend (EPDM-PE) are commonly used in polypropylene composites. Ternary composites of PP containing both filler and elastomer provide stiffer and tougher materials than the PP matrix (Jancar and Dibenedetto, 1994 and 1995).

Schaefer et al. (1993) studied mechanical properties of the ternary systems consisting of PP, EPDM and different types of inorganic fillers (kaolin,  $\text{BaSO}_4$ ). They concluded that the influence of EPDM on the mechanical properties was dependent on the filler and EPDM concentrations and on the filler type. A strong polymer-filler

interaction, as in kaolin-containing systems, led to an immobilization of EPDM in the interphase. In addition, poor interaction occurred in BaSO<sub>4</sub> containing systems, in which the interphase has properties similar to the bulk material.

## Chapter 4

### SURFACE MODIFICATION OF FILLER

Interfacial interactions are often modified by the surface modification of reinforcements or fillers. Modification of the filler involves coating of fillers with surface modifiers that carry suitable functional groups, in order to make the filler surface more compatible or reactive with the matrix material. The surface modification of fillers reduces the interaction between the filler particles and the extent of agglomeration. In particulate filled composites, various surface modifiers such as coupling agents and surfactants are used. Surface modifiers have to be properly selected for a particular polymer-filler system (Pukanszky et al., 1989, Wang et al., 1999).

Surface treatment causes the filler surface to become hydrophobic and moisture adsorption of particulate filled polymer composites is significantly reduced during storage. Inorganic fillers mostly contain hydroxyl groups on the surface, owing to reactions with atmospheric water or simply due to strong adsorption forces resulting from the high surface energy. The hydrophilic nature of inorganic fillers makes it easy for atmospheric water to accumulate at the interface by diffusing through the matrix. As a result, interfacial bonds of thermoplastics/filler systems are either intrinsically weak or deterioratable on ageing, when the composite is exposed to humid environments. For this reason, the majority of particulate fillers are coated with coupling agents to form hydrophobic nature. In particulate filled polypropylene composites, since polypropylene is nonpolar, hydrophobic substance, only limited amount of untreated hydrophilic filler can be added to it (Chiang and Yang, 1988, Liauv, 2000, Mascia, 1989).

Polymers, organic materials exhibit little tendency to wet and cover the surface of inorganic filler particles during processing. Optimum properties in composites usually can not be obtained with fillers in the agglomerated form. Maximum performance of a polymer composite can be achieved only if wetting of the filler or reinforcement by the polymer is perfect. Wetting agents or coupling agents are significantly different from each other, which are used to improve the polymer-filler compatibility. A wetting agent provides wetting of the filler particles with the polymer by changing of the surface tension of the filler. Treatment of fillers with wetting agents such as fatty acids or stearic acids improves wettability of the filler by polymer due to

changing polarity of the fillers. However, a coupling agent is a bifunctional molecule having an organic end and an inorganic end. The inorganic end bonds to the filler, and the organic end bonds to the polymer. Therefore, a chemical bond can be obtained between filler particles and polymer. A wide variety of coupling agents has been used in particulate filled thermoplastics (Xavier et. al., 1990, Liauv, 2000).

#### 4.1. Coupling Agents

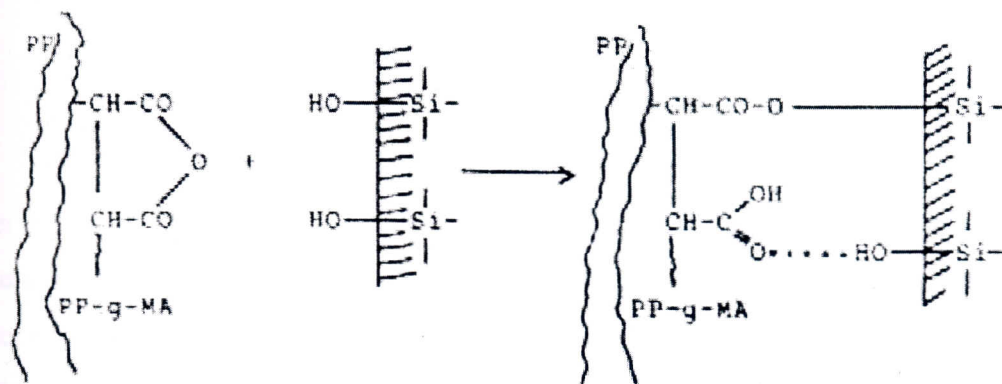
Coupling agents are bifunctional molecules containing organic and inorganic ends, improve the mechanical properties and chemical resistance of composites by enhancing adhesion across the polymer-filler interface. Surface modification of the filler with a coupling agent has been widely used for enhancing polymer-filler interface. Coupling agents used for polypropylene composites are listed in Table 4.1. The most widely used coupling agents are silane and titanate based compounds, whose chemical composition allows them to react with both the surface of the filler and the polymer matrix. The reaction of the fillers with non-silane coupling agents is shown in Figure 4.1. The reactions of maleated PP as coupling agent in PP/silicate composite and sulfonylazides as coupling agents in PP/CaCO<sub>3</sub> are shown in Figure 4.1.(a) and (b) respectively (Xanthos, 1988, Whelan and Craft, 1985 ).

There are several mechanisms of coupling agents during enhancement of polymer composites (Bledzki and Gassan, 1999, Mascia, 1989):

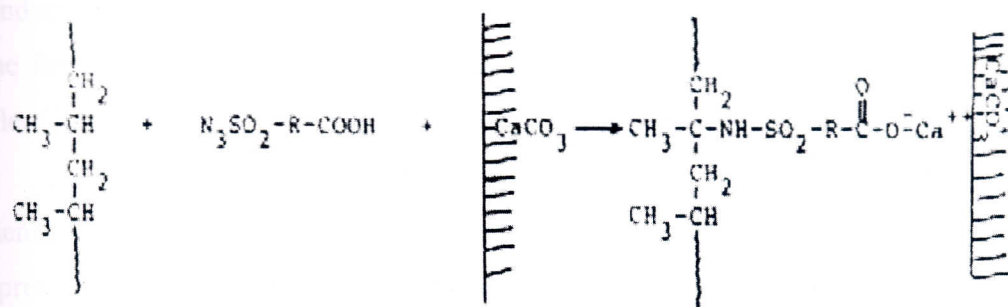
- Weak boundary layers: coupling agents eliminate weak boundary layers,
- Deformable layers: coupling agents produce a tough and flexible layer,
- Restrained layers: coupling agents develop a highly crosslinked interphase region,
- Wettability: coupling agents improve the wetting between polymer and substrate ,
- Chemical bonding: coupling agents form covalent bonds with polymer and filler,
- Acid – base effect: coupling agents alter acidity of substrate surface

Table 4.1. Miscellaneous Coupling Agents for Polypropylene Composites (Xanthos, 1988).

Filler / Reinforcement	Coupling Agent
Calcium Carbonate, Glass, Graphite, Mica, Talc, Wood, etc.	Carboxyl or anhydride functional PP or aminofunctional silane
Calcium Silicate	Aminofunctional silane + maleic anhydride + peroxide
Mica, Glass, Calcium Carbonate	Sulfonylazide based compounds
Mica, Wood, Glass	Bismaleimide or bismaleamic acid based compounds
Mica, Talc	Titanate coupling agents



(a)



(b)

Figure 4.1. Examples of Non-silane Coupling Reactions in Polypropylene Composites: (a) Graft Copolymers as Coupling Agents in PP/Silicate Composite (b) Sulfonylazides as Coupling Agents in PP/CaCO<sub>3</sub>.

### 4.1.1. Silane Coupling Agents

The general formula of silane coupling agents is  $Y(\text{CH}_2)_n \text{Si} (\text{OR})_3$ , where R stands for most frequently methyl, ethyl or isopropyl group while Y denotes a functional group capable of interaction with polymers such as amino, mercapto or vinyl group. The functional groups are chosen for reactivity or compatibility with the polymer, while the hydrolyzable groups (methoxy or ethoxy groups) are merely intermediates in formation of silanol groups for bonding to mineral surfaces. The modification reaction develops as follows (Plueddemann, 1991, Jesionowski and Krysztafkiewicz, 2000):

Hydrolysis reaction:



Condensation reaction:



The hydrolyzable group of silane coupling agents can be hydrolyzed mostly with water but in some systems acid or a base catalyst in a protic solvent is used. The presence of water in the system is one of the most significant parameters in the reaction. Water molecules cause hydrolysis and formation of silanols ( $\equiv\text{Si-OH}$ ). Silanols can then combine to form a siloxane linkage ( $\equiv \text{Si-O-Si} \equiv$ ) between two silane molecules and production of a new water molecule which can then react further. Silanol groups condense to form siloxane groups depending on drying conditions and treatment time. The formation of siloxane groups allows the bonding of the coupling agent with the filler (Jo and Blum, 1999, Ogasawara et al, 2001).

The functional groups of coupling agents can be bonded physically or chemically to a polymer matrix to enhance the interphase of a composite. Figure 4.2 is a representation of the bonding of the siloxane to the polymer through a combination of interpenetration and chemical reaction. The exact mechanism of bonding will depend on several factors including: the relative acidity or basicity at the interface (pH), the thermodynamic compatibility of the polymer with organosilane and its condensation products, the temperature dependence of hydrolysis and condensation, the temperature

dependence of polymer chain disentanglement (to facilitate interpenetration) and the activation energy for providing a covalent bond between the polymer matrix and the organic functional group of the silane coupling agent (Dibenedetto, 2001, Parker, 2001).

Silane coupling agents are generally considered to be adhesion promoters between mineral fillers and organic matrix that improve mechanical strength and chemical resistance of composites. The improved adhesion between the surfaces of inorganic materials treated with silane coupling agents and organic polymers is caused by:

- Improved wetting of the treated inorganic surface by the polymer
- Improved compatibility between the treated inorganic surface and the polymer
- Hydrogen bonding between the treated inorganic surface and the polymer
- Multiple covalent bonds between the treated inorganic surface and the polymer

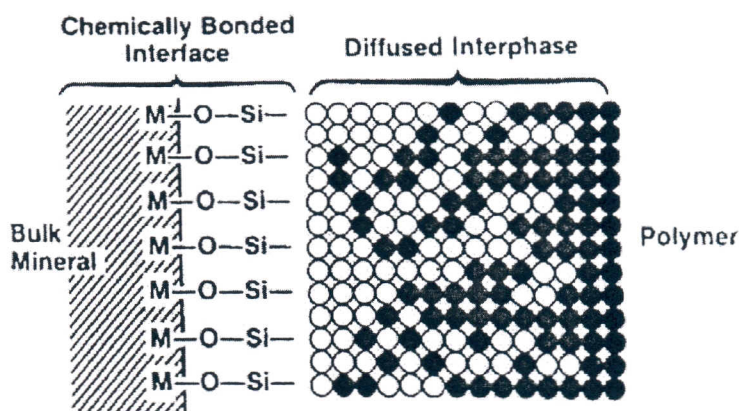


Figure 4.2. Bonding Siloxane to Polymer through Diffusion (Dibenedetto, 2001).

Commonly used silane coupling agents are listed in Table 4.2. In the literature reviews, improvements in the mechanical properties of the polymer composites were observed using modified silica, talc or CaCO<sub>3</sub> with aminofunctional silane coupling agents.

Table 4.2. Commonly Used Silane Coupling Agents.

	Chemical Formula
(3-methacryloxypropyl)trimethoxy silane	$\text{CH}_2=\text{C}(\text{CO}-\text{O}-\text{CH}_2-\text{CH}_2-\text{CH}_2-\text{Si}-(\text{O}-\text{CH}_3)_3)$
(3-aminopropyl)triethoxy silane	$\text{NH}_2-\text{CH}_2-\text{CH}_2-\text{CH}_2-\text{Si}-(\text{O}-\text{CH}_2-\text{CH}_3)_3$
Vinyl triethoxysilane	$\text{CH}_2=\text{CH}-\text{Si}-(\text{O}-\text{CH}_2-\text{CH}_3)_3$
(3- mercaptopropyl)trimethoxy silane	$\text{HS}-\text{CH}_2-\text{CH}_2-\text{Si}-(\text{O}-\text{CH}_3)_3$

Demjen et al. (1997 and 1998) investigated the effect of silane treatment on the tensile properties of polypropylene- $\text{CaCO}_3$  composites. Polypropylene composites used were composed of different amounts of filler treated with eight functional trialkoxy silane coupling agents and stearic acid. The effects of surface modification with stearic acid and silane coupling agents such as 3-aminopropytriethoxy silane (AMPTES), 3-methacryloxytrimethoxy silane (MPTMS) and N-(4-vinyl benzene)-N-(3-trimethoxysilylpropylene)diamine, hydrochloride (CVBS) are shown in Figure 4.3. AMPTES and CVBS have a clear reactive coupling effect, and both of these coupling agents increase the tensile strength of the composite by enhancement of the interfacial interaction. MPTMS exerts a non-reactive surfactant effect, forming an inefficient coupling agent. The other coupling agents reduce the surface tension of the filler, which leads to a decrease in the tensile strength of the composites. AMPTES has the strong coupling effect because of catalytic effect of amine group. Also, optimum amount of coupling agents can be found by comparison of tensile strengths of the composites as seen in Figure 4.3.(b).

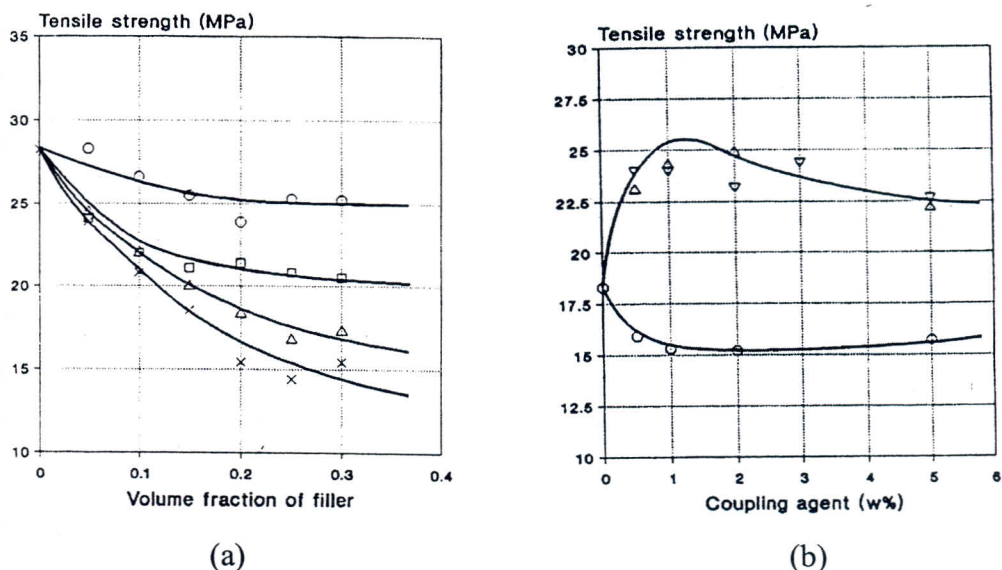


Figure 4.3. Tensile Yield Strength of PP/ $\text{CaCO}_3$  Against (a) Filler Content, ( $\Delta$ ) Non-treatment, (o) 0.8 wt% AMPTES, ( $\square$ ) 0.7 wt% CVBS and ( $\times$ ) 1.3 wt% MPTMS, (b) Amount of Coupling Agent (o) STAC, ( $\Delta$ ) CVBS and ( $\nabla$ ) AMPTES (Demjen et al., 1997 and 1998).

Jesionowski and Krysztafkiewicz (2000) investigated effect of the modification techniques and efficiency of silane coupling agents in hydrated silicas. Two techniques were used to modify the surface of the hydrated silicas. The new wet technique of silica surface modification was involved in a direct reaction of the modifying agent with the

surface groups of the just forming hydrated silica. In the other technique, after the hydrated silicas are obtained, coupling agents were added. Eight different silane coupling agents were used for the modification of the hydrated silicas in each technique. It was concluded that hydrophobization and agglomeration size of modified hydrated silicas with silane coupling agents in wet technique was higher and lower than others respectively.

Lee et al. (2000) proposed that the improvement in the wettability of epoxy matrix with natural zeolite could be obtained by the modification of the zeolite with silane coupling agents. For that reason, the surface tensions of the untreated and silane treated natural zeolite to be used in polymer composites were investigated. The surface treatment of the natural zeolite was carried out with  $\gamma$ -aminopropyltriethoxysilane coupling agent. 0.5 wt% the silane coupling agent to the natural zeolite was hydrolyzed in the mixture of ethanol/water:95/5 v% for 15 min at room temperature, and then the natural zeolite was treated with the hydrolyzed solutions for 30 min at 50 °C and dried for 24 hours at 120°C. The dried zeolite was ground and sieved into 325 mesh under. The polar group of surface tension for untreated zeolite decreased from 15.27 to 12.23 mJ/ m<sup>2</sup>. The decrease in polar group of surface tension for the treated zeolite was observed due to the increasing effect of alkyl group (hydrophobic) in the silane coupling agent.

Hertl (1968) studied the reactions of methyltrimethoxysilane with silica gel in the range from room temperature to 200°C using IR spectroscopy. At room temperature silica gel physically adsorbed the silane, at 120-200°C the adsorbed silane reacted with isolated silanol groups on the silica described by third order reaction kinetics with the activation energy of 30.5 kcal/mol. For every three isolated silanol groups on silica that reacted, 1.56 formed SiOSi with the methoxysilane, 0.45 formed hydrogen bonds with unreacted methoxy groups of silane that had formed siloxane bonds with adjacent silanol groups, and 1.08 formed SiOCH<sub>3</sub> with methanol. Hertl also studied the stability of these bonds with respect to water vapor and thermal behaviour. These bonds were found to be stable to water vapor at room temperature and to resist to thermal changes up to 300°C in vacuum (Plueddemann, 1991).

Although silane coupling agents is used for enhancement of the interphase in filled polymers, they may provide important improvements in rheology of filled thermoplastics and in protecting the filler against mechanical damage during high shear operations such as mixing, extrusion, and injection molding (Plueddemann, 1991).

## 4.2. Surface Modification Methods

Surface treatment of filler can be carried out in two different ways: pre-treatment and in-situ treatment. In pre-treatment, surface treatment of the filler is done before incorporation of the filler into the polymer. However, in-situ treatment requires the surface modification of the filler directly by mixing of the filler, surface modifier and the polymer during melt blending. The surface treatment diffuses to the filler surface through the polymer melt. Advantages and disadvantages of the two procedures are summarized in Table 4.3. The importance of the various factors depend on the nature of the coating and filler, and the composite processing conditions (Rothon, 1995).

Table 4.3. Comparison of Pre-Treatment with In-Situ Treatment.

Pre-Treatment	In-Situ Treatment
Often more expensive due to the extra processing step.	Less expensive but higher additive levels may be required due to the less efficient adsorption process.
Volatile/flammable condensation products (water/CO <sub>2</sub> from fatty acids and alcohols from silanes) can be easily removed.	Volatile flammable condensation products can be a problem in non-vented extruders.
Filler stability to water adsorption and carbonation is ensured.	Filler stability problems not overcome, in-situ treatment can be good in limited stability conditions.
The treated surface is available at the earliest stages of incorporation, minimization of wear on processing equipment.	Untreated surface is available before the diffusion process becomes effective.
Interpenetration of coating and matrix may be limited.	Increased opportunities for coating matrix interpenetration.
Fresh surfaces generated by break down of filler particles during compounding will remain untreated.	Fresh surfaces will be readily treated by diffusion of surface modifier through the melt.

Various methods may be used depending on the nature of the filler, the surface modifier and the filler preparation procedure in precoating of the filler. When the filler is produced from aqueous solution it is often advantageous to add a water-dispersible form of the coating prior to drying. In most cases, dry coating is often achieved by use of a high shear mixer. In the dry-milling procedures, the conditions must be carefully chosen to ensure complete coverage and surface reaction. Non-reactive and reactive surface modifiers such as fatty acids (stearic acid) and silane coupling agents are usually applied by pretreatment, while functionalized polymers such as maleated polypropylene are generally applied according to in-situ treatment (Domka, 1994, Pukanszky, 1989, Rother, 1995).

Demjen and Pukanszky (1997) prepared polypropylene surface treated  $\text{CaCO}_3$  with different coupling agents composites according to the pretreatment method. In this study,  $\text{CaCO}_3$  was dry blended with 0.5, 1, 2, 3 and 5 wt% silane coupling agents for 1min at room temperature in a high speed internal mixer. Prehydrolysis of silanes was carried out by adsorbed water on the filler surface. The surface treated filler was left standing at room temperature for two days then kept in polyethylene bags for about a month. Demjen et al. (1998) also modified  $\text{CaCO}_3$  with the same coupling agents with a different method. In this study, surface treatment of  $\text{CaCO}_3$  was carried out in an internal mixer by dropwise of butanol and coupling agent solution. Mixing time was adjusted as 3 hours at room temperature. The suspension was left standing in the flask for three days, then n-butanol was removed by distillation at 60 °C.  $\text{CaCO}_3$  was dried, then stored under saturated water vapour conditions for 10 days. Polypropylene composites were prepared from each surface treated  $\text{CaCO}_3$  in an internal mixer and a compression molding. The results indicate that there were no significant differences in tensile strengths of polypropylene composite with the same coupling agents at constant filler content according to the different treatment methods.

## Chapter 5

### CHARACTERIZATION OF POLYMER COMPOSITES

The incorporation of fillers or reinforcements into polymers causes substantial changes in terms of their thermal and mechanical properties. These changes can be explained by characterization of polymer composites. For characterization of polymer composites, spectroscopic methods, thermal analyses and microstructure analysis are generally used. Fourier Transform Infra-red Spectroscopy (FTIR), Thermal Gravimetric Analysis (TGA), Differential Scanning Calorimetry (DSC), Scanning Electron Microscopy (SEM) and Optical Microscopy are the commonly employed techniques for characterization of the polymer composites. The properties of polymer composites depend on several factors, such as variation in the mobility of the polymers, filler-polymer interactions, and the effect of fillers on the chemical composition and structure of the polymers. The mobility of polymer composites depends on the shape and the particle size of the filler. In addition, the filler-polymer interactions depend on the wettability or adhesion of the filler with polymer. For those reasons, the particle size and contact angle of the filler are important variables that can be measured in the characterization of polymer composites (Fuad et al., 1995, Hunt and James, 1993).

Measurement of mechanical properties of polymer composites such as tensile or impact strength is not usually regarded as polymer characterization, but it should be included. Because mechanical properties give information about the ultimate end use of polymer composites (Hunt and James, 1993).

#### 5.1. Particle Size Analysis

Particle size of the filler is one of the major factors that determines the ultimate use of a particulate composite. Hence, there is considerable interest in its measurement, especially of particle size distributions rather than single average values. Particle size analysis can be done using a variety of techniques including sieving, sedimentation, optical scattering and diffraction from particulate suspensions. Particle sizing techniques attempt to break down powders to primary sizes by use of intensive mixing, ultrasonics, and dispersants (Rothon, 1995).

The most common technique for measuring the particle size distribution of a fine powder is the monitoring of the change in concentration of a sedimenting suspension. The concentration of a homogeneous suspension of particles can be determined by their attenuation of a beam of low energy X-rays which scans the sedimentation vessel from bottom to top. The particle size is obtained from Stokes' Law as a function of particle and fluid densities, fluid viscosity and settling velocity of the particles (Lowell and Shields, 1991).

## 5.2. Contact Angle Measurements

The contact angle determines the wettability that can be defined as an affinity of a liquid for a solid surface. When a liquid spreads spontaneously along a solid surface it is said to wet the surface. If the liquid in the form of a drop remains stationary and appears spherical it is non-wetting (Lowell and Shields, 1991). This drop will have an angle between itself and the solid that is indicative of the interaction between the two materials. The contact angle can be defined as the angle formed between the solid surface and a tangent drawn to the liquid surface at the point of contact with the solid surface. The contact angle is greater than  $90^\circ$  for non-wetting liquids and less than  $90^\circ$  for wetting liquids (Akova, 1993, Myers, 1988).

The forces in the drop are balanced as shown in Figure 5.1. These forces include the tendency of the drop to minimize its surface area by forming a sphere, and the tendency to spread on the solid surface and thus increase the extent of interfacial contact. This balance of forces has been described by the Young equation:

$$\gamma_{sv} - \gamma_{sl} = \gamma_{lv} \cos \theta \quad (5.1)$$

where  $\gamma_{sl}$  is the surface tension between solid and liquid,  $\gamma_{sv}$  is the surface tension between the solid and vapor,  $\gamma_{lv}$  is the surface tension between the liquid and vapor, and  $\theta$  is the angle of the drop between solid and liquid. By measuring the angle between the liquid drop and the solid surface and surface tension of the liquid, the interaction between the solid and liquid ( $\gamma_{sl}$ ) can be calculated.

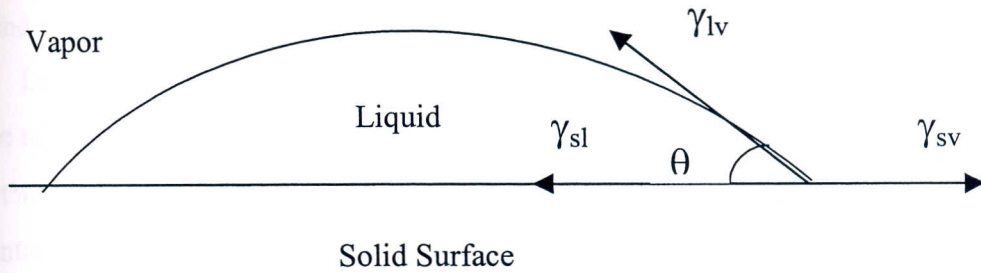


Figure 5.1. Surface Tensions in the Contact Angle Measurement.

Contact angles are often used to estimate fiber-matrix bond strength. The energy needed to separate the fiber from the matrix that can be expressed by work of adhesion in Equation 5.2.

$$W_A = \gamma_{sv} + \gamma_{lv} - \gamma_{sl} \quad (5.2)$$

Work of adhesion can be calculated also using surface tension of the liquid and contact angle by combining Equation 5.1 and 5.2 (Karger and Kocsis, 1995).

$$W_A = \gamma_{lv} (1 + \cos \theta) \quad (5.3)$$

Moyer and Wightman (1984) studied the effect of oxygen plasma treatment on the wettability of carbon fiber/polyamide matrix composite. Contact angles of water were measured against the polyamide composite before and after short time exposures to oxygen plasma. The contact angle was decreased dramatically with only short exposures to oxygen plasma. This indicates that wettability of the polyamide composite enhances due to an increase in surface oxygen functionality by oxygen plasma.

Koltuksuz (2002) studied the removal of benzene, toluene and o-xylene from wastewater by natural zeolite. Polar zeolite surface was made more hydrophobic using cationic surfactants as dodecyl amine (DA), tetramethylammonium (TMA<sup>+</sup>) and an anionic surfactant as sodium dodecyl sulfate (SDS). Hydrophobic properties of untreated and treated zeolite surface with different surfactants were found by measurement of contact angles. DA was found to be more effective compared to others and increased the mean contact angle degree from 7.76° to 51.13° at a concentration of

$1 \times 10^{-3} \text{M}$ . This indicates that hydrophobicity of zeolite surface is a function of surfactant type and surfactant concentration.

Lee et al. (2000) investigated the surface tension of untreated and silane treated zeolite to be used in epoxy composites. In this study, surface tensions of untreated and 0.5 wt%  $\gamma$ -aminopropyltriethoxysilane treated zeolite surface were found by calculation of contact angle according to the wicking method. Wicking method depends on the contact angle formed between a liquid and a fine powder at the powder filled column. The contact angles were calculated by determination of the rate of penetration of different liquids such as methylene iodide, water and formamide from Washburn's Equation 5.4. In the Washburn's equation,  $h$  is the penetrated distance of the liquid in a selected time  $t$  (sec),  $R$  (cm) is the effective interstitial pore radius between the packed particles in column and  $\eta$ (cP) is the viscosity of the probe liquid.

$$h^2 = \frac{tR\gamma_{LV} \cos \theta}{2\eta} \quad (5.4)$$

$R$  and  $\cos\theta$  are two unknowns in the Washburn's equation.  $R$  can be calculated by using spreading liquids such as n-alkanes. Generally, n-alkanes are used as spreading liquids that can completely wet the solid surface, so that the contact angle  $\theta$  is equal to zero. After the calculation of the  $R$  by using n-alkanes the contact angle for each liquid with the solid powder is calculated via Equation 5.4. The contact angles between the untreated natural zeolite and methylene iodide, water and formamide were found  $76.7^\circ$ ,  $68.8^\circ$ , and  $54.2^\circ$  respectively. The contact angles between the treated natural zeolite and methylene iodide, water and formamide were found  $62.6^\circ$ ,  $68.4^\circ$ , and  $64.2^\circ$  respectively. The total surface tension of the zeolite is the sum of the surface tensions of polar and apolar component of the zeolite. The apolar component of the untreated zeolite was  $19.22 \text{ mJ/m}^2$  and the polar one was  $15.27 \text{ mJ/m}^2$ . The apolar component of the treated zeolite was  $27.08 \text{ mJ/m}^2$  and the polar one was  $12.23 \text{ mJ/m}^2$ . The surface tension of the apolar component increased, while the surface tension of polar component decreased with silane treatment. This effect was due to that the surface of the zeolite was more affected by hydrophobic alkyl group than amine or hydroxyl groups. The apolar component of untreated zeolite was a little larger than the polar and this means that the untreated zeolite is some hydrophobic. This result is different from the general surface

characteristics of zeolites whose surface is hydrophilic due to the hydroxyl groups located on the surface of the zeolite in the form of Al-OH or Si-OH.

### **5.3. Thermal Analyses**

Thermal analysis is frequently used to investigate the behavior of a sample as a function of temperature. There is a wide array of thermal analysis techniques that are commonly employed for the study of polymer composites. Thermal properties of polymer composites are very important in end use applications and the processing methods that used to make polymer products. Generally, thermal properties of polymer composites can be analysed by thermogravimetric analysis (TGA), differential scanning calorimetry (DSC) analysis, thermomechanical analysis (TMA), and dynamic mechanical analysis (DMA). TGA is used for thermal degradation study while DSC analysis is used for oxidative stability and crystallinity studies. TMA is employed for linear coefficient of thermal expansion determination and DMA characterises the viscoelastic properties of the polymer composites. (Fuad and et al., 1995, Hatakeyama and Quinn, 1994, Grulke, 1994).

In this study, DSC and TGA were used for the thermal characterization of polypropylene-zeolite composites.

#### **5.3.1. Characterization of PP-Zeolite Composites by TGA**

Thermogravimetric analysis (TGA) is the simplest and the oldest thermal analysis technique. TGA is based on the weight loss of a sample due to the formation of volatile products as a function of temperature. TGA is used to characterize the decomposition and thermal stability of materials under a variety of conditions. TGA take place in determination of additives such as plasticizer or filler and evaluation of moisture, volatiles and residues in a material ((Hunt and James, 1993, Hatakeyama and Quinn, 1994).

Thermal characterization of polypropylene-zeolite composites and their components can be done by TGA that gives information about degradation kinetics and weight loss of the samples. Filler content in the composite can be found by comparing the weight loss of the samples. TGA determines the water content and types of water in the zeolite structure. Knowlton and White (1981) studied the types of water in

clinoptilolite. They concluded that the nature of water in clinoptilolite is predominantly dependent on the interactions of water molecules with the Si, Al framework. They reported that the three types of water are present in natural zeolite; external water, loosely bound water, and tightly bound water that remove from the structure of zeolite at around 75°C, 171°C, and 271°C respectively.

Özmihçi (1999) studied the effect of zeolite on the thermal degradation of polypropylene by TGA. The degradation temperature of polypropylene-zeolite (2, 4, and 6 wt %) composites shifts to higher values due to zeolite content in the composites. The composites were heated until 1000°C at a heating rate of 10°C/min. Polypropylene started degradation at 220°C but the composites started 10-20°C later. Termination of degradation of polypropylene is at 550°C and for the zeolite filled composites were at 575 °C. Also, Özmihçi found that filler content of 2, 4, and 6 wt% zeolite filled polypropylene composites were lower than the expected values because of uneven dispersion of zeolite in the composite.

### 5.3.2. Characterization of PP-Zeolite Composites by DSC

Differential Scanning Calorimetry (DSC) is used to determine the thermal transition of a polymer such as melting, degradation, crystallization and glass transition temperatures. DSC takes place in a variety of applications such as determination of the heat of fusion, the specific heat as a function of temperature, the degree of crystallinity, kinetic parameters and the oxidative stability of a polymer. Thus DSC is appropriate for investigating both changes in physical properties as well as chemical changes (Schnabel, 1981).

The addition of various types of fillers such as CaCO<sub>3</sub>, talc or zeolite to the polymer influences the crystallinity of polymers. The change in the crystallinity of the polymer affects the mechanical properties of the composite. For that reason, the crystallinity of the composite should be known. The crystallinity of the composites can be calculated from DSC measurements. The crystallinity index ( $\chi$ ) is the ratio of the measured melting enthalpy ( $\Delta H_m$  (J/g)) of the polypropylene composite to the value of enthalpy of 100 % crystalline polypropylene ( $\Delta H_0=209$  J/g) (Horrocks and D'Souza, 1991 and Gutierrez et al., 1999).

$$\chi = \frac{\Delta H_m}{\Delta H_o} \quad (5.5)$$

Linear correction factor should be used to calculate the crystallinity index of polypropylene composites in equation (5.5), because of the different weight of polypropylene in each composite. So the crystallinity index of the composites can be written in the following equation.

$$\chi = \frac{\Delta H_m \frac{m_c}{m_p}}{\Delta H_o} \quad (5.6)$$

where  $m_c$  denotes the mass of the composite and  $m_p$  denotes the mass of the polymer (Gutierrez et al., 1999).

The crystallization kinetics of polymers can be described by Avrami equation given in Equation 5.7.

$$\alpha(t) = 1 - \exp(-Kt^n) \quad (5.7)$$

where;

$\alpha(t)$ : fraction of the transformed material in the time  $t$

$n$  : a constant that is a function of the crystal growth and nucleation mechanism

$K$  : characteristic function of the process (describes the rate of crystallization)

Kissinger method can be also used for the determination of the crystallization kinetics parameters given in Equation 5.8.

$$\frac{d\alpha(t)}{dt} = A \exp(-E/RT)(1 - \alpha)^n \quad (5.8)$$

where;

$\alpha$ : reaction rate

$A$ : frequency factor

$E$ : activation energy

T: temperature

n: reaction order

Kissinger equation is used to obtain the activation energy of crystallization from the variation in the peak temperature with heating rate. Kissinger's method assumes that the maximum in the DSC curve occurs at the same temperature as the maximum reaction rate. Equation 5.8 can be written in the form of Equation 5.9 when the maximum reaction rate occurs at  $d/dt(d\alpha/dt)=0$ .

$$\frac{E\phi}{RT_p^2} = An(1-\alpha)^{n-1} \exp(-E/RT_p) \quad (5.9)$$

where  $\phi$  is the cooling rate and  $T_p$  is the temperature at which the maximum conversion rate occurs in the DSC curve. Also Equation 5.9 can be written in the form of Equation 5.10 to obtain activation energy from the slopes of  $\ln(\phi/T_p^2)$  versus  $1/T_p$  plots.

$$\ln\left(\frac{\Phi}{T_p^2}\right) = -\frac{E}{RT_p} + \ln\left(\frac{AR}{E}\right) \quad (5.10)$$

Dobrevá and Gutzow (1993) studied the crystallization kinetics of molten polymers in the presence of nucleating agents. They concluded that the overall crystallization rate coefficient  $K$  depends on:

$$K(T) = \omega G^{n-1} I \quad (5.11)$$

Where  $I$  is the nucleation rate and  $G$  represents the linear growth velocity. On the other hand, the non-isothermal crystallization process is also defined with the method developed by Dobrevá and Gutzow for the study of the crystallization kinetics of molten polymers in the presence of nucleating agents. Dobrevá and Gutzow have proposed the following relationship:

$$\log q \approx \text{const} - \frac{B}{2.3\Delta T^2} \quad (5.12)$$

where  $q$  is the rate of crystallization,  $\Delta T$  is equal to  $T_m - T_p$  ( $T_m$  is the melting temperature and  $T_p$  is the temperature at which the peak value of the  $d\alpha/dT$  curve is reached) and  $B$  a parameter which can be calculated from the Equation 5.13.

$$B = \omega \frac{\sigma^3 V_m^2}{3kT_m \Delta S_m^2 n} \quad (5.13)$$

where;

$V_m$  : molar volume of the crystallizing substance

$\Delta S_m$  : entropy of melting

$k$  : Boltzman constant

$\sigma$  : specific surface tension

$\omega$  : geometrical factor

The activity of filler ( $\phi$ ) is defined as Equation 5.14.  $B^*$  is the value of  $B$  when the polymer is filled and  $B^0$  when it is unfilled.

$$\phi = \frac{B^*}{B^0} \quad (5.14)$$

Thus, from the experimental slopes in the representation  $\log q$  versus  $1/\Delta T^2$ , according to Equation 5.12, it is possible to obtain the  $B$  values. Finally, by using Equation 5.14, the parameter  $\phi$  can be estimated. The activity is related to the parameter  $\phi$  so that a lower value of  $\phi$  deals with a higher value of activity.

Gutierrez et al. (1999) and Alonso et al. (1997) investigated the effect of silane coupling agents on the activity of talc in the polypropylene-talc composites using DSC. They concluded that the value of the treated filler is closer to zero, so the treated filler is more active than the untreated filler. Consequently, the interaction between the filler and the matrix will be higher and the filler will influence the matrix structure to a greater extent because of the high activity of the filler. This higher interaction can be used to explain the improvement in the mechanical performance of the composite. As a result of these studies, the parameter  $\phi$  is adequate to quantify in a form of the matrix-

filler interaction. The properties of the composite can be changed by varying this activity with different treatments.

#### 5.4. Characterization of PP-Zeolite Composites by FTIR Spectroscopy

Infrared spectroscopy gives information about the chemical composition and structure of the materials such as chain structure, degrees of branching, geometric isomerism, and functional groups present in the material. FTIR spectroscopy is ideal for analyzing surface modified filler. It gives information about the effect of surface modifiers on the chemical composition of the filler. (Cahn et al., 1992, Demjen et al., 1999).

Characteristic peaks of polypropylene and zeolite should be known to characterize PP-zeolite composites by FTIR spectroscopy. Characteristic peaks of polypropylene and zeolite are given in Table 5.1 and 5.2 respectively ( Polymer Handbook, Braundrup et al., 1976, Banwell et al., 1983, Goryainov et al. 1995).

Table 5.1. Characteristic Peaks of Polypropylene (Polymer Handbook, Braundrup et al., 1976, Banwell et al., 1983).

Vibration	Wave Number (cm <sup>-1</sup> )
i-polypropylene	790, 1158
s-polypropylene	1131, 1199, 1230
t-polypropylene	997, 995
-CH <sub>2</sub> asymmetric stretching	2930
-CH <sub>2</sub> symmetric stretching	2860
-CH <sub>2</sub> deformation	1470
-CH <sub>3</sub> asymmetric stretching	2970
-CH <sub>3</sub> symmetric stretching	2870
-CH <sub>3</sub> asymmetric deformation	1460
CH <sub>3</sub> symmetric deformation	1375

According to Breck, infrared spectrum of zeolites can be divided two classes. The first class of vibrations arises due to internal vibrations of the TO<sub>4</sub> tetrahedron

which is the primary unit of the structure and the second class is related to the external linkages between tetrahedra. The internal vibrations T-O is sensitive to the Si/Al ratio of the framework. Internal T-O bonding is between 450-500  $\text{cm}^{-1}$ . The water vibrations of zeolite are also observed at 3700, 3400, and 1620  $\text{cm}^{-1}$  (Fuentes, 1997 and Goryainov et al. 1995).

Table 5.2.Characteristic Peaks of Natural Zeolite (Goryainov et al. 1995).

Vibration	Wave Number ( $\text{cm}^{-1}$ )
T-O stretching (T:Al or Si)	1065
Internal T-O double ring	450
External T-O (symetric stretching)	790
External T-O double ring	609
Isolated OH stretching	3700
H bonded H <sub>2</sub> O, O-H stretching	3400
H <sub>2</sub> O bending	1620

The characteristic peaks of silane coupling agents should be known to identify the chemical reactions between zeolite and the coupling agents. Characteristic peaks of silane coupling agents are listed in Table 5.3. The Si-O-R group has at least one strong band at 1110-1000  $\text{cm}^{-1}$  due to an asymmetric Si-O-C stretching vibration. Silanol (SiOH) and siloxanes (Si-O-Si) groups formed as the result of the hydrolysis and condensation reactions between silane coupling agents and mineral surface are observed by FTIR spectroscopy. The silanol groups absorb at 3700-3200  $\text{cm}^{-1}$ . A strong band due to Si-O stretching vibration occurs at 910-830  $\text{cm}^{-1}$ . In the condensed state a broad medium-weak intensity band occurs near 1030  $\text{cm}^{-1}$  which shifts appropriately on deuteration and may be described as Si-OH deformation. Siloxanes are characterized by at least one strong band at 1130-1000  $\text{cm}^{-1}$  due to asymmetric Si-O-Si stretching. In infinite siloxane chains, absorption maxima occur near 1085 and 1020  $\text{cm}^{-1}$  (Colthup et al., 1990).

FTIR spectroscopy also gives information about the interactions between filler, polymer and surface modifier. Demjen et al. (1999) studied the reactions of aminofunctional silane coupling agents in the polypropylene-CaCO<sub>3</sub> composite. In this

study, FTIR spectroscopy was used to determine the mechanism of interaction between the silane coupling agents and the apolar polypropylene which does not contain reactive groups. FTIR analysis demonstrated that during processing, oxidation of the polymer takes place in spite of the presence of stabilizers. Reactive groups formed as a result of oxidation of polypropylene enter into chemical reactions with amino functionality of the silane. As a result of the reactions between polypropylene and silane, the strong coupling was formed between and polypropylene and  $\text{CaCO}_3$ .

Table 5.3.Characteristic Peaks of Silane Coupling Agents (Colthup et al., 1990).

Vibration	Wave Number ( $\text{cm}^{-1}$ )
Si-O-R stretching	1110-1000
Si-O-C symmetric stretching	850-800
Si-O-C asymmetric stretching	1100
Si-O- $\text{CH}_3$	1190
Si-O- $\text{CH}_3$ symmetric stretching	2840
Si-O- $\text{C}_2\text{H}_5$	1175-1160
Si-O- $\text{C}_2\text{H}_5$ symmetric stretching	970-940
Si-O- $\text{C}_2\text{H}_5$ double bond	1100-1075
Si- $\text{CH}_3$	860-760
Si- $\text{CH}_3$ symmetric stretching	1280-1255

### 5.5. Mechanical Properties of Polypropylene Composites

The mechanical properties of particulate filled composites depend on the properties of the components, the shape, size and volume content of the filler phase, and the nature of the interphase between the filler and polymer. The incorporation of particulate mineral fillers into a thermoplastic polymer can improve some mechanical properties such as the Young's Modulus or the heat deflection temperature, but it affects some other properties, like the impact strength, adversely. However, these negative effects can be minimized by the use of very fine particles. Because of their small size, these particles tend to agglomerate. In this situation, surface treatment is applicable for obtaining a good particle dispersion in the matrix (Mareri, 1998).

Modulus, yield stress, tensile strength and ultimate elongation are generally used to characterize the mechanical properties of the composites. Young's modulus is the ratio of stress to strain below the elastic limit, gives information about rigidity of the composite. Tensile yield stress is a very important property of the composites that gives information on the maximum allowable load before plastic deformation occurs. It is a measure of the strength of a polymeric material at the yield point. Tensile strength is the ultimate strength of the composite. Polymers are used under loads approaching their ultimate strength in many applications such as film and pipe production, for that reason tensile strength is also an important parameter. The tensile yield strength and tensile strength can be increased or decreased by the addition of fillers and reduced by the addition of plasticizers. The increase in yield strength with increase in filler content is due to the filler carrying higher loads than the matrix. The evaluation of modulus is easier than tensile or yield strength because while modulus is a bulk property, the other depends on polymer filler interaction. There are many semiempirical models for the prediction of properties such as elastic modulus and yield strength of particulate filled polymeric composites.

The relative modulus of a particulate filled polymer is given by Halphin- Tsai equation as follows

$$E_c / E_m = (1 + \xi \eta \Phi_f) / (1 - \eta \Phi_f) \quad (5.15)$$

where  $\eta$  can be calculated as

$$\eta = (E_f / E_m - 1) / (E_f / E_m + \xi) \quad (5.15)$$

where  $E_c$ ,  $E_f$  and  $E_m$  are the modulus of the composite, the filler and the polymer respectively.  $\Phi_f$  is the volume fraction of the filler and  $\xi$  is a geometrical factor that depends on the filler geometry and loading conditions.  $\xi$  is equal to 2 for spherical particles. Radosta suggested that this equation is versatile enough to be used in the prediction of relative moduli for flexural and tensile tests (Ulutan and Gilbert, 2000).

The Kerner equation is also used to calculate the modulus of a polymer composite containing nearly spherically particles in the case of some adhesion between the phases.

$$E_c / E_m = 1 + \left[ \frac{15(1 - \nu_p)}{8 - 10\nu_p} \right] \left[ \frac{\Phi_f}{1 - \Phi_f} \right] \quad (5.16)$$

where  $\nu_p$  is the Poisson's ratio of the polymer, taken as 0.35 for isotactic polypropylene (Maiti and Sharma, 1992, Nielsen and Landel, 1994).

The Kerner-Nielsen or modified Kerner model expresses the effect of filler concentration on Young's modulus of the polymer composite. This model takes into account the maximum packing fraction of the filler particles (Jancar et al. 1993). Kerner-Nielsen model for polymer composites containing spherical fillers is given as following equation.

$$E_c / E_m = (1 + AB\Phi_f) / (1 - B\psi\Phi_f) \quad (5.17)$$

and

$$A = \frac{7 - 5\nu_p}{8 - 10\nu_p} \quad (5.18)$$

$$B = \frac{E_f / E_m - 1}{E_f / E_m + A} \quad (5.19)$$

$$\psi = 1 + \left[ \frac{1 - \Phi_{\max}}{\Phi_{\max}^2} \right] \Phi_f \quad (5.20)$$

where  $A$  is a function of the geometry of the particles and the factor  $\psi$  depends on the maximum packing fraction  $\Phi_{\max}$  of the filler. The factor  $\psi$  is given as  $(1 + 0.89\Phi_f)$  for spherical  $\text{CaCO}_3$  fillers (Ulutan and Gilbert, 2000, Nielsen and Landel, 1994, Jancar et al., 1993).

Interfacial adhesion between the fillers and the matrix is an important factor affecting the tensile strength of the composites. For that reason, theoretical tensile yield

strength and tensile strength of the composites are formulated corresponding to the cases of adhesion and no adhesion between the filler particles and the matrix. In the case of no adhesion between the matrix and the filler, the interfacial layer can not transfer stress. The Nielsen and the Nicholais and Narkis models predict tensile strengths of the composites are formulated in Equations 5.21 and 5.22 respectively (Liang and Li 2000, Nielsen and Landel, 1994, Maiti and Sharma, 1992)

$$\sigma_c / \sigma_p = (1 - \Phi_f^{2/3})S \quad (5.21)$$

$$\sigma_c / \sigma_p = (1 - a\Phi_f^b) \quad (5.22)$$

where  $\sigma_c$  and  $\sigma_m$  are tensile strengths of the composite and matrix respectively. The parameter S in the Nielsen's model describes weakness in the structure created through stress concentration at the filler-matrix interphase. Unity in the value of S means a 'no stress concentration effect', whereas the lower the value the 'greater the stress concentration effect or poorer the adhesion'. a and b parameters in the Nicholais and Narkis model are the constants related to filler-matrix interaction, adhesion and geometry of the filler respectively. For spherical particles having no adhesion to the polymer matrix, Equation 5.22 becomes

$$\sigma_c / \sigma_p = (1 - 1.21\Phi_f^{2/3}) \quad (5.23)$$

In the case of no adhesion between polymer and filler a and b are equal to 1.21 and 2/3 respectively as shown in Equation 5.23. In general for spherical fillers, the value of a is lower than 1.21 the better the adhesion and a=0 represents the upper limit with the unfilled polymer. In addition, a value of a = 1.1 describes dense hexagonal packing in the plane of highest density.

The Pukanszky model describes the effects of composition and the interfacial interaction on tensile yield stress or tensile strength of particulate filled polymers is given in Equation 5.24. The parameter B is an interaction parameter that is related to the macroscopic characteristics of the filler-matrix interface and interphase.

$$\sigma_y / \sigma_{y0} = \frac{1 - \Phi_f}{1 + 2.5\Phi_f} \exp(B_{\sigma} \Phi_f) \quad (5.24)$$

The first term in Equation 5.24 is related to the decrease in effective load bearing cross section, while the second one is concerned with the interfacial interaction between filler and matrix. Interfacial interaction depends on the area of the interphase, and the strength of the interaction as shown in Equation 5.25.  $A_f$  is the specific surface area of the filler,  $\rho_f$  is its density, and  $t$  is the thickness of the interface. From the  $B_{\sigma}$  values, strength of interaction  $\sigma_{yi}$  can be calculated as follows.

$$B_{\sigma} = (1 + A_f \rho_f t) \ln(\sigma_{yi} / \sigma_{ym}) \quad (5.25)$$

In the case of perfect adhesion between filler and matrix, Nielsen proposed a simple model for the elongation at break of polymer composites as shown by the following Equation 5.26.

$$\varepsilon_c / \varepsilon_m = (1 - \Phi_f^{1/3}) \quad (5.26)$$

where  $\varepsilon_c$  and  $\varepsilon_m$  are the elongations of break of the composite and matrix respectively. The model assumes that spherical particles are uniformly dispersed and that there exists strong adhesion at the polymer-filler interface.

Mitsuishi et al (1985) have developed an equation to estimate the effect of filler-polymer interaction on elongation

$$\varepsilon_c / \varepsilon_m = (1 - K\Phi_f^{2/3}) \quad (5.27)$$

where, the interaction parameter,  $K$ , has a constant value which depends on filler size and the modification of fillers. When adhesion is poor, and the specimen is subjected to elongational deformations, separation at particle/matrix contacts occurs due to the formation of voids. As a result, well-dispersed but weakly adhering particulates produce compounds with higher ultimate elongations (Boluk and Schreiber, 1990, Maiti and Sharma, 1992).

Interfacial adhesion between the fillers and the matrix is an important factor affecting strength of particulate filled polymer composites. Pukanszky et al. (1989 and 1998) studied the interfacial interaction in polypropylene/ $\text{CaCO}_3$  composites. In these studies eight different silane coupling agents and maleated polypropylene are used for modification of the interface between polypropylene and  $\text{CaCO}_3$ . The maximum values of Parameter B in Pukanszky model depend on the strength of the interaction were found as 2 and 3.4 for aminofunctional silane treatment and maleated polypropylene respectively. According to the Pukanszky's result, the strength of the interaction is better for the case of maleated PP. Pukanszky's results also showed that the size of the interface and the strength of the interaction significantly influence ultimate tensile properties. Jancar and Kucera (1990) believed that poor adhesion between PP and  $\text{CaCO}_3$  accounted for a decrease of the tensile yield stress with increasing volume fraction of  $\text{CaCO}_3$ .

## 5.6. Microstructure Analysis

Microstructure analysis is used for examination of surfaces. Scanning electron microscopy (SEM) and optical microscopy give information about the state of dispersion of particles in the matrix and effects of surface treatment on the fillers.

SEM is a surface technique that can be done on samples of any thickness. It analyzes electrons that are scattered from the sample's surface. Optical microscopy depends on light transmission through or reflection from matter. Optical microscopy can be used to show structures about the size of the wavelength of visible light, near one micron. Electron microscopy has resolutions to several nanometers. For these reasons, optical microscopy is of limited value in examining the interface region, therefore SEM is used to study details of fracture surfaces, but can not be resolve to monomolecular coverage of silane treatment (Grulke, 1994, Plueddeman, 1991, Sabilia et al., 1988).

## Chapter 6

### EXPERIMENTAL

#### 6.1. Materials

In this study, MH-418 polypropylene in pellet form supplied from PETKİM Petrochemical Co. and natural zeolite from Gördes 1 mine, rich in clinoptilolite mineral from Western Anatolia, were used. The composition of the additives present in the polypropylene is given in Table 6.1. The additives such as calcium stearate and antioxidants are incorporated into PP for providing specific properties such as color stability, processing ease, high heat resistance and oxidation stability (Quality Control Laboratory of Petkim, 2001).

Table 6.1. Chemical Composition of MH-418 PP (Quality Control Laboratory of Petkim, 2001).

Additive	Chemical Formula	Amount (wppm)
Calcium Stearate	$\text{Ca}(\text{H}_{35}\text{C}_{17}\text{CO})_2$	750
Primary Antioxidant	$\text{C}_{73}\text{H}_{108}\text{O}_{12}$	470
Antioxidant (Aryl Phosphite)	Tris(2,4-di-ter-butyl-phenyl)phosphite	312
Secondary Antioxidant	Tris(3,5-di-tert-butyl-4-hydroxy-benzyl)isocyanurate	312

The surface treatment agents employed were 3-aminopropyltriethoxysilane (Fluka), methytriethoxysilane and 3-mercaptopropyltrimethoxysilane (Merck) and polyethyleneglycol (PEG-4000, Merck). Dioctylphthalate (Aldrich) and epoxidized soybean oil (Akdeniz Kimya) were used as plasticizers.

## 6.2. Methods

Experimental methods can be summarized in five groups:

- Size reduction of zeolite
- Surface modification of zeolite
- Preparation of polypropylene-zeolite composites
- Characterization of zeolite
- Characterization of polypropylene-zeolite composites

### 6.2.1. Size Reduction of Zeolite

Natural zeolites from Gördes 1 mine were first crushed into small particles using a hammer. Powder form of the zeolites was prepared by grinding in Multifix Ball Mill. Zirconia balls were used as grinding media during ball-milling. The cylinder size was 59.5 mm radius and 76 mm height. The particle size of zirconia balls was 9.48 mm. After the 50 % of the cylinder volume were filled with the balls, 50 gr small particulate zeolites were ground at a speed of 100 rpm for 5 hour. After the grinding process, the zeolites were obtained in size range of  $-45\mu\text{m}$  by sieving. Particles less than  $1\mu\text{m}$  in size were separated according to Stoke's Law in a zeolite-water suspension. Stoke's law as given by Equation 6.1, states that under fixed conditions the time  $t$  taken for a particle to settle to a fixed depth is inversely proportional to the square root of its spherical diameter,  $d$ .

$$d = 10^4 \left[ \frac{18\eta l}{(\rho_s - \rho_f)gt} \right]^{1/2} \quad (6.1)$$

where  $d$  is the diameter,  $\eta$  is the viscosity of water,  $\rho_s$  and  $\rho_f$  are the densities of the zeolite and water,  $g$  is the gravitational constant and  $t$  is the time for the particle to settle a distance,  $l$  (Rothon, 1995).  $\rho_s$  and  $\rho_f$  were taken as  $1800 \text{ g/cm}^3$  and  $1000\text{g/cm}^3$  respectively. The time required for the  $1\mu\text{m}$  zeolite particles to settle down could easily be determined using Equation 6.1. After the sedimentation process, the suspension was then separated from the solids settled to the bottom of the container. This suspension was dried in an air dried oven at  $110^\circ\text{C}$  and the zeolite was again dried in a vacuum oven at  $110^\circ\text{C}$  and 400 mbar for 4 hours.

## 6.2.2. Surface Modification of Zeolite

Surface modification of zeolite was carried out in order to decrease the hydrophilic nature of their surface and to make them more compatible with the hydrophobic PP. For that reason, a homogeneous dispersion of particles in PP composite can be obtained by preventing agglomerations of particles. Zeolite particles were modified with polyethyleneglycol (PEG-4000) and three different silane coupling agents: 3-aminopropyltriethoxysilane (AMPTES), 3-mercaptopropyltrimethoxysilane (MPTMS) and methyltriethoxysilane (MTES). Chemical structures of surface modifiers used are shown in Table 6.2. The silane coupling agents were chosen since no external acid or base catalysts are required for hydrolysis reaction. Additionally, MTES was used for investigating the effect of functional groups of silane coupling agents.

Table 6.2. Chemical Structures of Surface Modifiers.

Surface Modifier	Chemical Formula	Producer
PEG	$\text{HO}(\text{C}_2\text{H}_4\text{O})_n\text{H}$	Aldrich
AMPTES	$\text{NH}_2\text{-CH}_2\text{-CH}_2\text{-CH}_2\text{-Si}(\text{O-CH}_2\text{-CH}_3)_3$	Fluka
MPTMS	$\text{SH-CH}_2\text{-CH}_2\text{-CH}_2\text{-Si}(\text{O-CH}_3)_3$	Merck
MTES	$\text{CH}_3\text{-Si}(\text{O-CH}_2\text{-CH}_3)_3$	Merck

Surface modifications of zeolite with non-ionic surface modifier PEG and silane coupling agents were performed by two different methods. In the first method, zeolite surface was modified during the zeolite grinding process. In this method, only PEG surface modifier was used as a grinding aid of zeolite. In the second method, surface modification of grinded zeolite with surface modifier was carried out in solution. Silane coupling agents were used as a surface modifier in this method.

In the first method, zeolite was dry blended with 3 wt% PEG for 5 hrs at 100 rpm in the ball mill. After the grinding process, zeolite sieved from the 45  $\mu\text{m}$  sieve. Particles below 1 $\mu\text{m}$  in size were obtained at the end of 35 hrs at 25°C. After the following sedimentation process, 1 $\mu\text{m}$  PEG treated zeolite particles as shown in chemical reaction were obtained by drying in a vacuum oven at 110 °C and 400 mbar for 4 hours. During the drying process, PEG melts and acts as a lubricant coating the

particles. Surface treatment process of Gördes 1 zeolite with PEG is shown schematically in Figure 6.1.

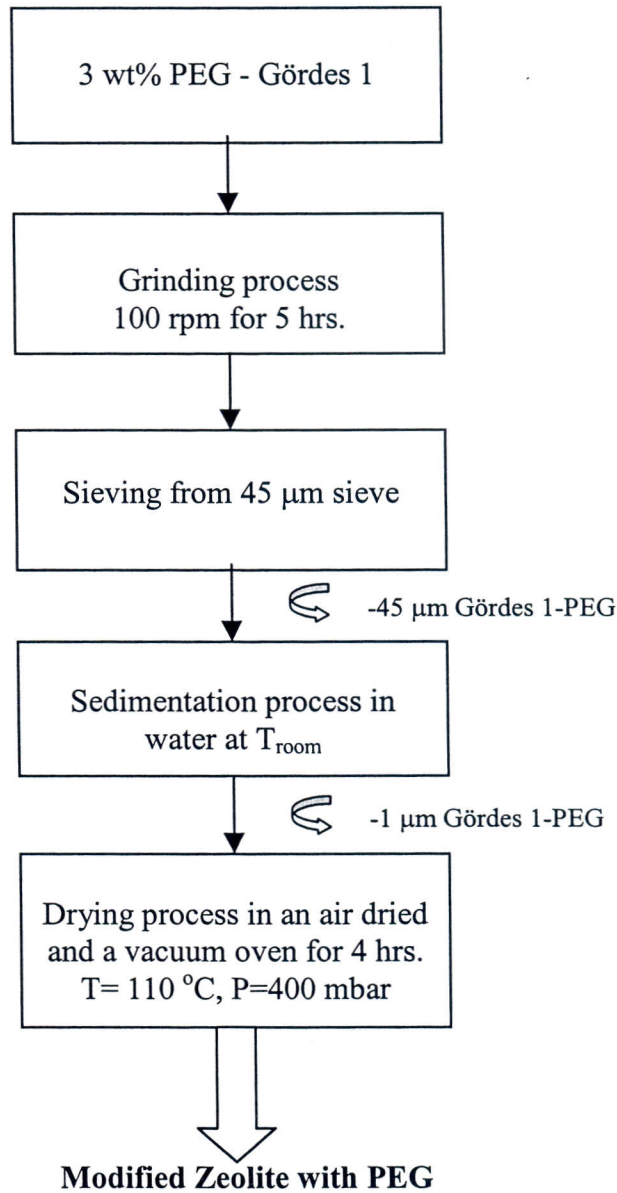
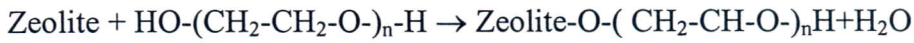
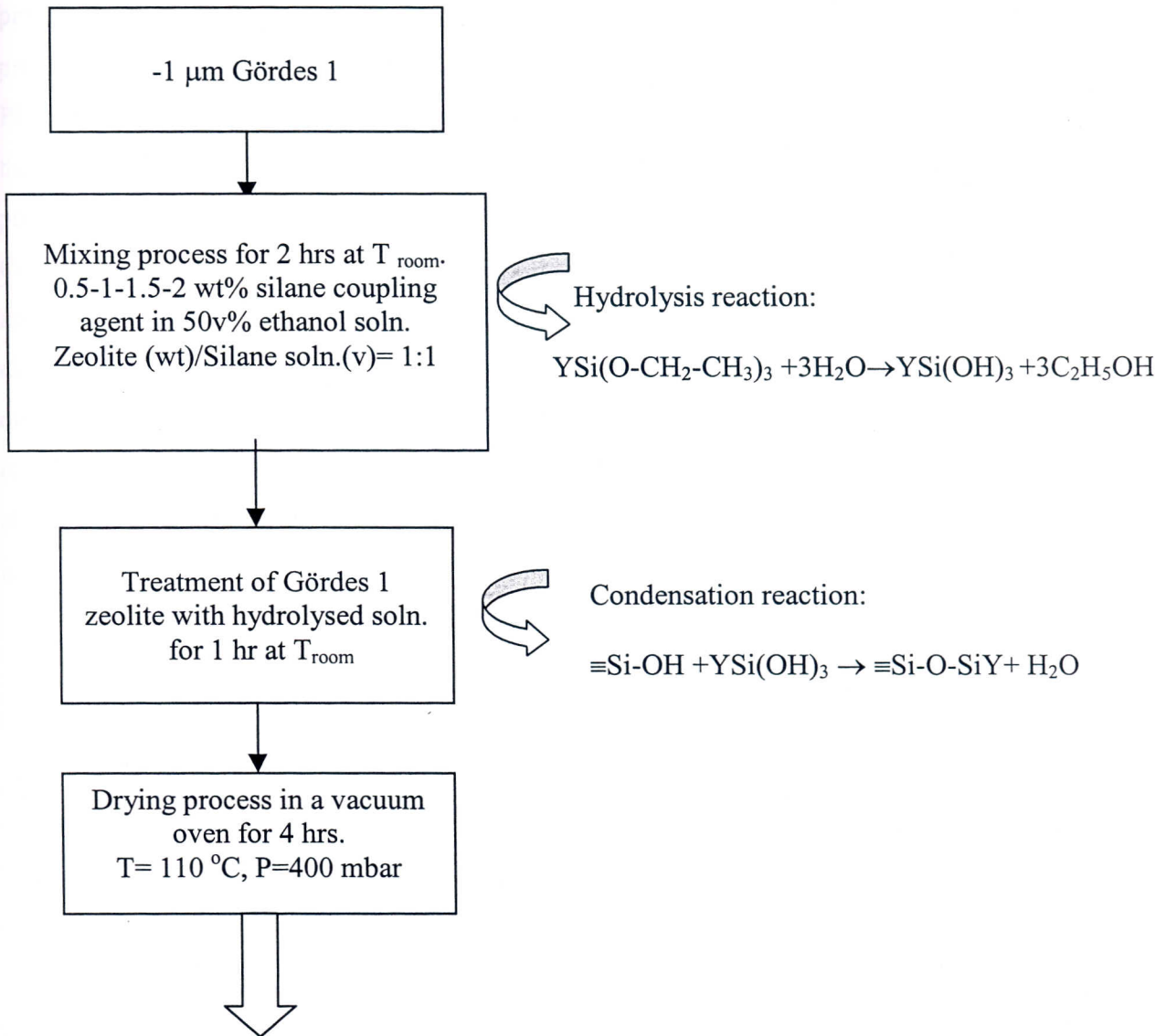


Figure 6.1. Surface Treatment Process of Gördes 1 with PEG.

In the second method, -1µm zeolite was added to a solution of silane coupling agent (0.5, 1, 1.5, and 2 wt%) in 50 v% aqueous ethanol solution. Zeolite to solution ratio was taken as 1:1 on weight/ volume basis. Hydrolysis reaction was carried out by mixing of silane-ethanol solution. The slurry was stirred for 2 hrs by a magnetic stirrer

and then kept for 1hr at room temperature for treatment of the zeolite with hydrolysed solution. Then, the resulting slurry was dried in a vacuum oven at 110 °C and 400 mbar pressure for 4 hrs. Surface treatment process of Gördes 1 zeolite with silane coupling agents is shown in Figure 6.2.



### Modified Zeolite with Silane Coupling Agents

Figure 6.2. Surface Treatment Process of Gördes 1 Zeolite with Silane Coupling Agents. Y denotes the organofunctional group of silane coupling agents;  $\text{NH}_2-\text{CH}_2-\text{CH}_2-\text{CH}_2$  for AMPTES,  $\text{SH}-\text{CH}_2-\text{CH}_2-\text{CH}_2$  for MPTMS and  $\text{CH}_3$  for MTES.

### 6.2.3. Preparation of PP-Zeolite Composites

PP composites were prepared by blending of PP pellets and 2, 4, and 6 wt % untreated or treated zeolite using an Axon BX-18 single screw extruder and then drawing through an Axon 2R-180 two roll mill shown in Figure 6.3. Plasticizers such as dioctylphthalate (DOP) and epoxidized soybean oil (EPS) were used to improve processability of the PP-zeolite composites in the extruder. Before the extrusion process, surface treated or untreated forms of zeolite (2, 4, and 6 wt%) were mixed with PP pellets and plasticizer. Plasticizer was used as 5 v/w % of total weight of the PP and the zeolite. These blends were conditioned in a vacuum oven at 80 °C under 400 mbar pressure for an hour to provide effective filler dispersion and devolatilization. Compositions containing a premix of PP, zeolite and plasticizer conditioned were fed into the extruder that has an L/D of 20, and a diameter of 18 mm, and a flat die of dimensions (50x1mm). The PP composite cast film taken from the flat die was quenched using a polished drum cooled by tap water and then stretched between casting rolls in the calender. Flow sheet of the preparation of PP- Gördes 1 zeolite composites is shown in Figure 6.4 and the experimental conditions of the extrusion process are given in Table 6.3.

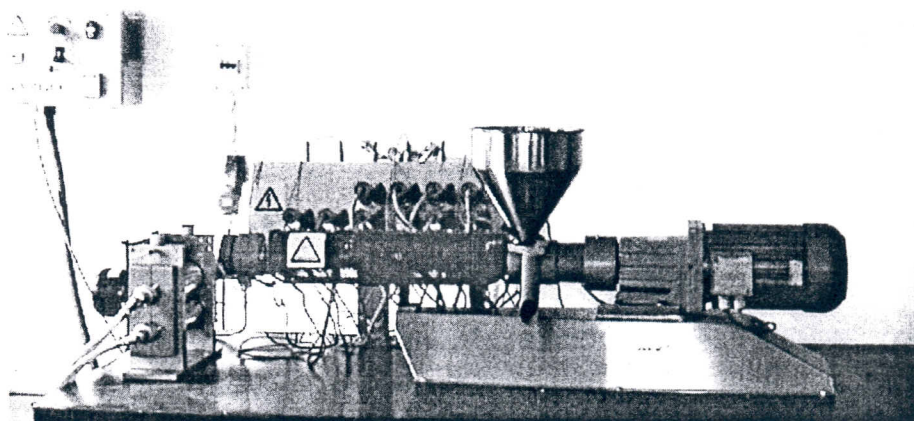


Figure 6.3. Extrusion and Film Drawing Unit (BX-18, AXON).

Table 6.3. Experimental Conditions of the Extrusion Process.

Screw Frequency (Hz)	Motor Voltage (V)	Motor Current (A)	Roller Frequency (Hz)	Zone Temperatures (°C)					
				1	2	3	4	5	6
20	38	4.5	4-7	200	220	220	220	220	220

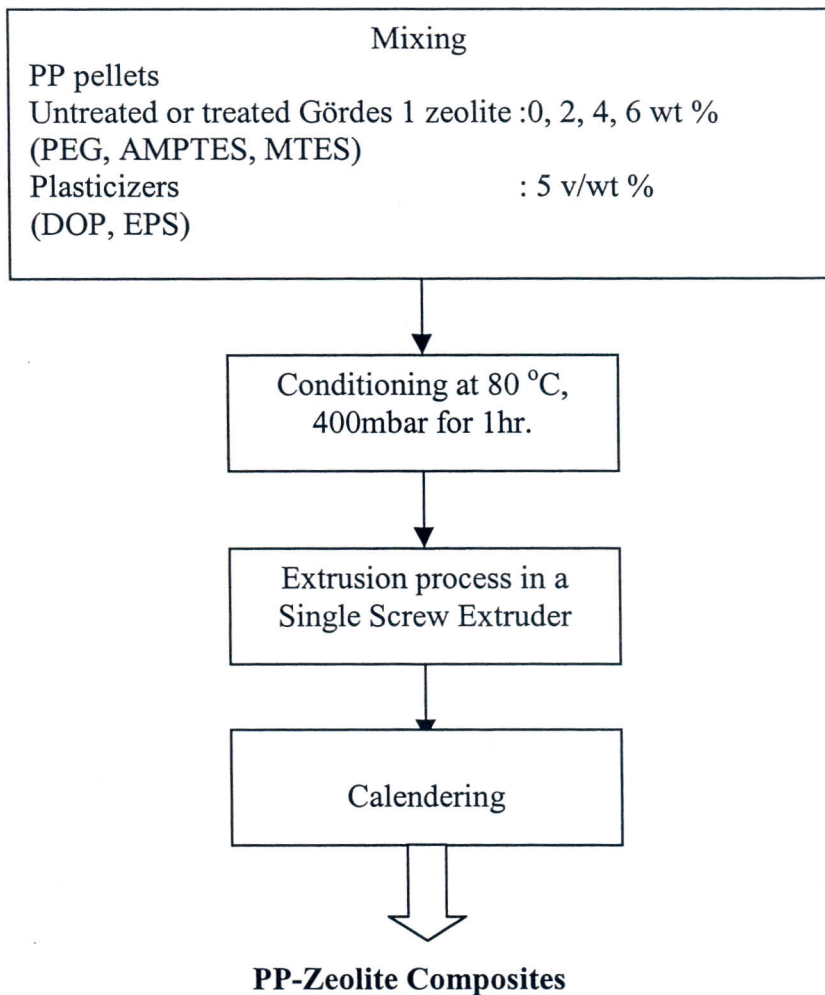


Figure 6.4. Flow Sheet of the Preparation of PP-Gördes 1 Zeolite Composites.

#### 6.2.4. Characterization of Zeolite

Zeolite was characterized by particle size analysis, Fourier Transform Infra-red Spectroscopy (FTIR), thermal gravimetric analysis (TGA) and contact angle measurements.

##### 6.2.4.1. Particle Size Measurement of Zeolite

Particle size measurement provides the determination of the size distribution of particles. Particle size analyses of  $1\mu\text{m}$  untreated and PEG treated zeolite are measured in the range of  $100 - 1\mu\text{m}$  by Micromeritics X-ray Sedigraph 5100.

#### **6.2.4.2. FTIR Analysis of Zeolite**

FTIR analysis gives information about the chemical structure of zeolites and the chemical reactions between silane coupling agents and zeolite. Untreated and treated zeolites with different modifiers were analyzed by KBr pellet technique. The pellets were prepared by pressing of 0.004 gr zeolite samples with 0.2 gr of KBr. FTIR analyses of liquid silane coupling agents were obtained by dropping of the coupling agents over KBr pellets. IR spectra were made up of 20 scans from  $400\text{ cm}^{-1}$  to  $4400\text{ cm}^{-1}$  with a Shimadzu FTIR 8201 model instrument.

#### **6.2.4.3. TGA of Zeolite**

TGA of zeolite was carried out using Shimadzu Thermal Gravimetric Analyzer (TGA-51) from room temperature to  $600\text{ }^{\circ}\text{C}$  at a heating rate of  $10\text{ }^{\circ}\text{C}/\text{min}$ . Nitrogen was used as a carrier gas with a constant flow rate of  $40\text{ ml}/\text{min}$ .

#### **6.2.4.4. Contact Angle Measurements**

Hydrophobicity of zeolite surface can be determined by contact angle measurements. Untreated zeolite surface were polished using silicon carbide papers such as P500, P800 and P1200 respectively. After the zeolite surface perfectly polished, it was treated with different silane coupling agents according to the surface modification method given in the previous section. Contact angles of water on the zeolite surface were measured by Krüss-G10 goniometer. Five contact angle measurements were done for each zeolite samples.

### **6.2.5. Characterization of PP-Zeolite Composites**

#### **6.2.5.1. Infrared Analyses**

The IR Spectra of the polypropylene composite films were obtained by placing the samples on the path of the IR light beam using the transmission technique. The liquid plasticizers dioctylphthate (DOP), epoxidized soybean oil (EPS) were analyzed

by preparing KBr pellets. All spectra were taken between  $400\text{ cm}^{-1}$  and  $4400\text{ cm}^{-1}$  with a Shimadzu FTIR 8201 model instrument.

### 6.2.5.2. Thermal Analyses

Thermal analyses of the PP-Gördes I zeolite films were conducted using Shimadzu Thermal Gravimetric Analyzer (TGA-51) and Shimadzu Differential Scanning Calorimeter (DSC-50). Thermal gravimetric analyser was used for the thermal degradation study of polypropylene composites. The experiments were carried out from room temperature to  $600\text{ }^{\circ}\text{C}$  at a heating rate of  $10\text{ }^{\circ}\text{C}/\text{min}$ . The analyses were performed in dry nitrogen atmosphere with a flow rate of  $40\text{ ml}/\text{min}$ .

Shimadzu Differential Scanning Calorimeter (DSC-50) was used to study the thermal degradation and crystallization behavior of polypropylene composites. Thermal degradation analyses were carried out from room temperature up to  $500\text{ }^{\circ}\text{C}$  at a heating rate of  $10\text{ }^{\circ}\text{C}/\text{min}$ . In the crystallization analyses, each sample was hold at  $200\text{ }^{\circ}\text{C}$  for 4 min in order to erase any previous thermal history. The measurements were made from  $200\text{ }^{\circ}\text{C}$  to  $50\text{ }^{\circ}\text{C}$  at the cooling rates of 5, 10 and  $20\text{ }^{\circ}\text{C}/\text{min}$ . Flow rate of nitrogen gas used as a purge gas was  $40\text{ ml}/\text{min}$  and kept constant throughout the experiments.

### 6.2.5.3. Water Sorption of PP-Zeolite Composites

Water sorption experiments were carried out by immersion of PP film and PP-zeolite composite films having different zeolite loadings (2,4, and 6 wt %) in distilled water for 24 hours at room conditions. The samples removed from the water were wiped with a tissue paper and weighed. These experiments gave the amount of water sorbed at the end of 24 hrs. The water uptakes were plotted for various PP-zeolite films as a function zeolite content.

### 6.2.5.4. Mechanical Characterization of PP-Zeolite Composites

Tensile tests of dry and wet PP composites containing (0, 2, 4, and 6 wt%) untreated and treated zeolite were performed on an Instron Universal Testing Machine Model 4411 under the conditions that the load cell was at 50 kgf, crosshead speed at  $500\text{ mm}/\text{min}$  and the gauge length was 50 mm. Wet samples were obtained from water

sorption experiments. Tensile tests were done at room conditions (23 °C and 50 % relative humidity). Tensile test specimens were prepared as strips of 0.5 cm width according to ASTM D-882. Minimum three specimens were tested for each PP composites, the mean values were reported.

#### 6.2.5.5. Morphology of PP-Zeolite Composites

SEM and optical microscopy were used to examine the morphology of PP-zeolite composites. Fracture surfaces of polypropylene matrix filled with 4 wt% untreated, treated with 1 wt% AMPTES, 1 wt% MTES and 1 wt% MPTMS zeolite composites and the tensile specimens of these composites were observed with Philips XL-30S FEG scanning electron microscope (SEM).

Optical micrographs of untreated and treated zeolite samples, and PP-zeolite composites with different surface modifiers and zeolite loadings were taken using transmission mode with a camera fitted to Olympus BX-60 microscope at different magnifications.

#### 6.2.5.6. Density Measurements

Density measurements of the PP composites were measured using the density kit of Sortorius YDK 01 balance depending on Archimed's principle. Both the sample weight ( $W_a$ ) and the weight of the water displaced by the sample ( $W_f$ ) were recorded to calculate the density of the sample using the equation below.

$$\rho_c = \frac{W_a \rho_f}{(W_a - W_f) 0.99983} + 0.0012 \quad (6.2)$$

where  $\rho_c$  and  $\rho_f$  are the densities of the composite and water, respectively.

## Chapter 7

### RESULTS AND DISCUSSION

In this study, interfacial enhancement of polypropylene-zeolite composites was studied. For this reason, polypropylene composites containing two different types of plasticizers such as dioctylphthalate (DOP) and epoxidized soybean oil (EPS) and untreated and treated zeolite with four types of surface modifiers were prepared to investigate the effects of plasticizers and surface modifiers on the interfacial properties of the composites. In this study, surface treatment of the filler, Gördes 1 zeolite, was carried out with a non-ionic surface modifier, polyethyleneglycol (PEG), and three different types of silane coupling agents: 3-aminopropyltriethoxysilane (AMPTES), 3-mercaptopropyltrimethoxysilane (MPTMS) and methyltriethoxysilane (MTES) to improve the interfacial properties of the PP composites. Four different surface treatment concentrations were studied to determine the optimum treatment concentration of the surface modifiers.

In the scope of this study, the effects of number of parameters such as zeolite content, type of surface modifiers and plasticizers and modifier concentration on the interfacial properties of PP-zeolite composites were investigated.

#### 7.1. Particle Size Measurement of Natural Zeolite

Particle size distribution of zeolite is an important parameter affecting the mechanical properties of polypropylene composites. Particle size analyses of  $-1\ \mu\text{m}$  untreated and PEG treated zeolite samples obtained by size reduction were carried out in the range of 100 and  $1\ \mu\text{m}$ . Figure 7.1 shows the particle size distributions of untreated and treated zeolite. As shown in the figure, particle sizes of 99.9 and 99.6 % of untreated and PEG treated zeolite samples were lower than  $100\ \mu\text{m}$  and also 99.5 and 95.5 % of particle sizes of untreated and PEG treated zeolite samples were lower than  $10\ \mu\text{m}$  respectively. In addition,  $-1\ \mu\text{m}$  particles constitute 23.1 and 18.4 % of untreated and PEG treated zeolite samples respectively. Mean particle size values of untreated and PEG treated zeolite were found as 1.507 and  $4.168\ \mu\text{m}$  respectively. The results

indicated that the modification of zeolite with PEG in the ball mill did not lead to the decrease in the particle size of zeolite.

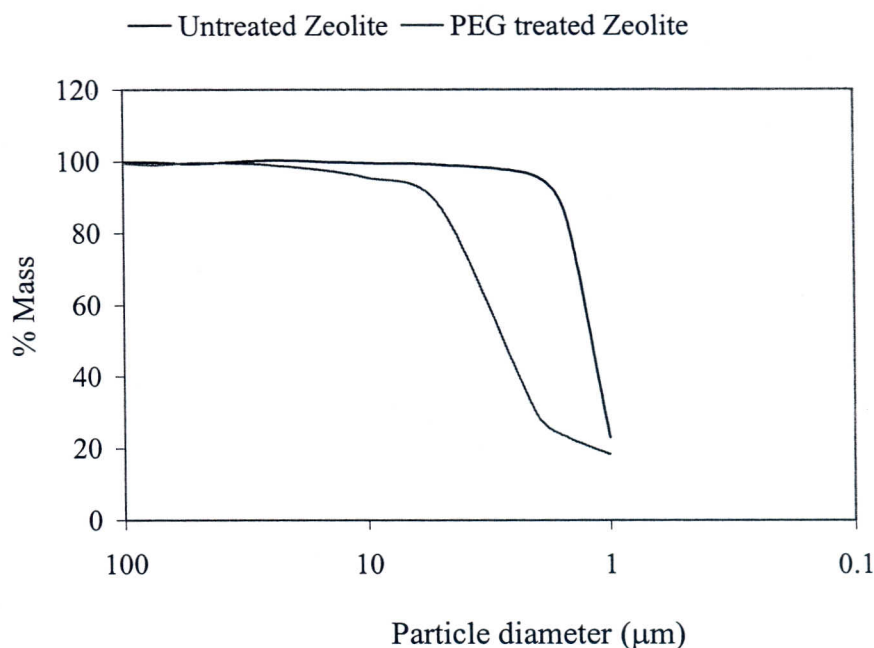


Figure 7.1. Particle Size Measurements of Untreated and PEG treated Zeolite.

Large zeolite particles affect appearance and the deformation of the polymer composites. On the other hand, aggregation tendency of small particles is higher than that of large particles. Extensive aggregation leads to insufficient homogeneity of fillers in polymer matrix. For that reason, zeolite was modified by silane coupling agents in order to prevent the aggregation of small zeolite particles.

## 7.2. Contact Angle Measurements

Contact angles of untreated and treated zeolite with silane coupling agents (AMPTES, MTES and MPTMS) were measured to investigate the effects of silane treatment on the zeolite surface and the wettability between polypropylene and zeolite. The mean contact angles of untreated and treated zeolite samples were obtained from five different measurements given in Table A.2 in Appendix. Figure 7.2 shows the mean contact angles of untreated and silane treated zeolites with water as a function of silane concentration for three types of silane treated zeolites. The contact angle of untreated zeolite was measured as  $0^\circ$  indicating strong hydrophilicity of the zeolite. As seen in the figure, the contact angles of the treated zeolites were higher than that of the

untreated ones. Although the increase in contact angles of treated zeolites was obtained for all silane coupling agents, the change in contact angles of the treated zeolites was found to be dependent on the silane type and concentration. The contact angles of amino-functional and merkapto silane coupling agents consist of terminal functional groups such as  $H_2N-$  and  $HS-$  are higher than that of MTES which has no functional group, because the introduction of a polar terminal functional group causes the formation of more ordered layers around filler. The maximum mean contact angles of the silane treated zeolites were measured as 39, 30.6 and  $90^\circ$  for 1 wt% AMPTES, 1 wt% MTES and 0.5 wt% MPTMS respectively. The increase in contact angle of water on the filler shows the increase in hydrophobicity of the filler. It was found that the hydrophobicity of zeolite significantly increased by surface modification and 0.5 wt% MPTMS was determined as the most effective coupling agent for hydrophobization of the zeolite.

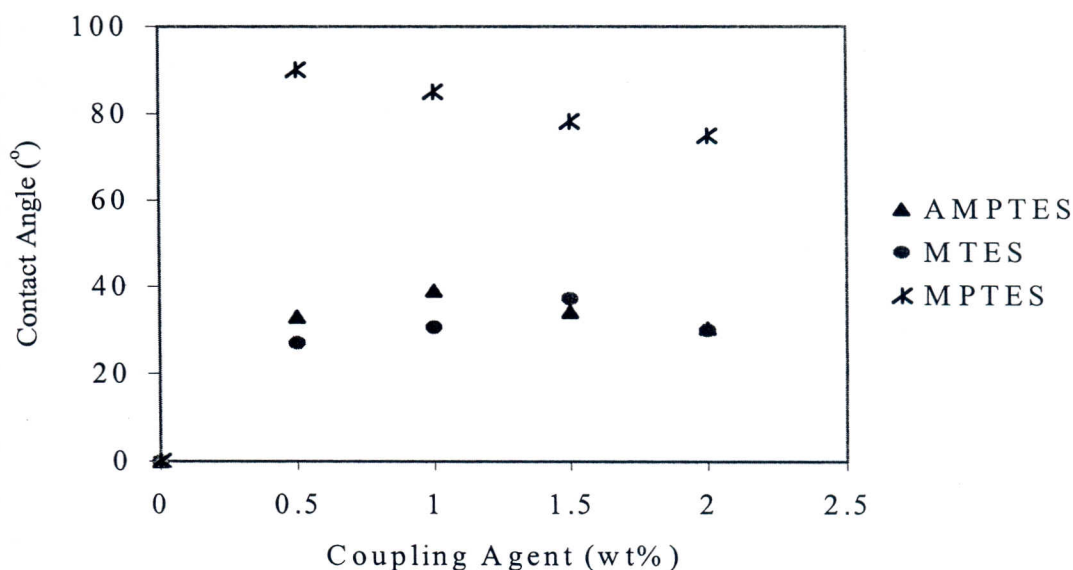


Figure 7.2. The Contact Angle Measurements of Treated Zeolites with AMPTES, MTES and MPTMS.

PP an organic material, exhibits tendency to wet and cover the surface of inorganic zeolite particles during the film production in the extruder. This problem can be overcome by the improvement of PP-zeolite compatibility. The increase in hydrophobicity of zeolite with surface modification causes the improvement of compatibility between apolar PP and polar zeolite. As a result, the wettability between hydrophobic polypropylene and hydrophilic zeolite improves with the increase in

hydrophobicity of zeolite using silane coupling agents due to the enhancement of compatibility between PP and zeolite.

### 7.3. Water sorption of PP-Zeolite Composites

The incorporation of zeolite into the hydrophobic PP matrix makes the PP composite as a water sorbing material. The effects of zeolite loading, type and concentration of surface modifier and plasticizer type on the water sorption properties of PP-zeolite composites were studied. Water sorption results of PP-zeolite composites with different compositions were given in Appendix A.1. Figure 7.3 shows the water sorption data of the PP-untreated zeolite and PP-PEG treated zeolite composites with two different plasticizers (DOP, EPS). As seen in the figure, the addition of zeolite into the PP matrix increased the water sorption as expected. It was also observed that the water sorption of the PP-untreated zeolite composites was lower than that of the PP-PEG treated zeolite composites. PP composites having untreated zeolite and epoxidized soybean oil (EPS) sorbed less water than those of having untreated zeolite and dioctylphthalate (DOP). PP composites having 6 wt% untreated zeolite and EPS sorbed 0.15 wt% water, on the other hand PP composites having 6 wt% untreated and PEG treated zeolite with DOP and PEG treated zeolite with EPS sorbed 0.2, 0.27, and 0.17 wt% water respectively. It is concluded that surface treatment of zeolite with PEG did not assist to decrease the water sorption of PP-zeolite composites.

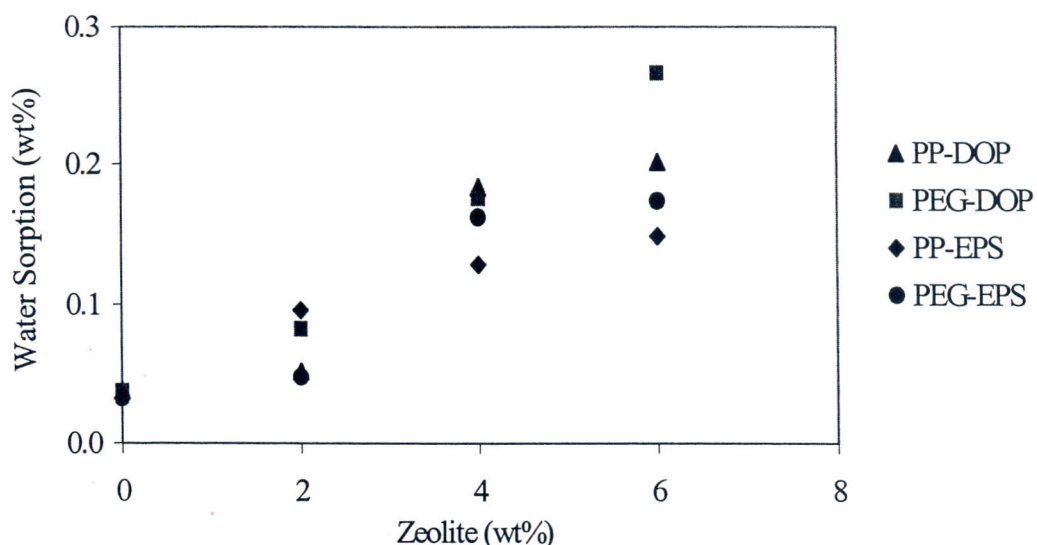


Figure 7.3. Water Sorption of PP-Untreated and PEG Treated Zeolite Composites with Different Plasticizers.

Surface treatment of the zeolite with silane coupling agents changed the hydrophilic nature of zeolite to the more hydrophobic one as seen in the contact angle measurements of silane treated zeolites. Figure 7.4 illustrates the water sorption of PP-zeolite composites as a function of zeolite loading for three different types of silane coupling agents. Water sorption of PP-zeolite composites was decreased by the surface modification of zeolite with silane coupling agents confirming contact angle results as given in Figure 7.4 and Table A.1 in Appendix. PP composites consisting of 6 wt% untreated and treated zeolite with 1wt% AMPTES, 1 wt% MTES and 0.5 wt% MPTMS sorbed 0.15, 0.048, 0.095 and 0.057 wt% water respectively. It was observed that there was no significant difference between water sorption of PP composites consisting of treated zeolite with AMPTES and MPTMS. The water sorption of PP composites having MTES treated zeolite was less than that of the composites with untreated zeolite, but more than that of the composites with AMPTES or MPTMS treated zeolite. The decrease in water sorption of the composites treated with silane coupling agents can be explained by reducing the hydrophilicity of zeolite's surface due to the decrease in the number of hydroxyl groups of zeolite's surface as shown in Figure 7.5. In addition, silane-coupling agents may provide a water-resistant bond between the zeolite and the polymer matrix. The water-resistant bond between apolar PP and zeolite requires the presence of polar groups of the polymer such as carboxyl group (-COOH). Carboxyl groups may also form by oxidation of apolar PP during the extrusion process.

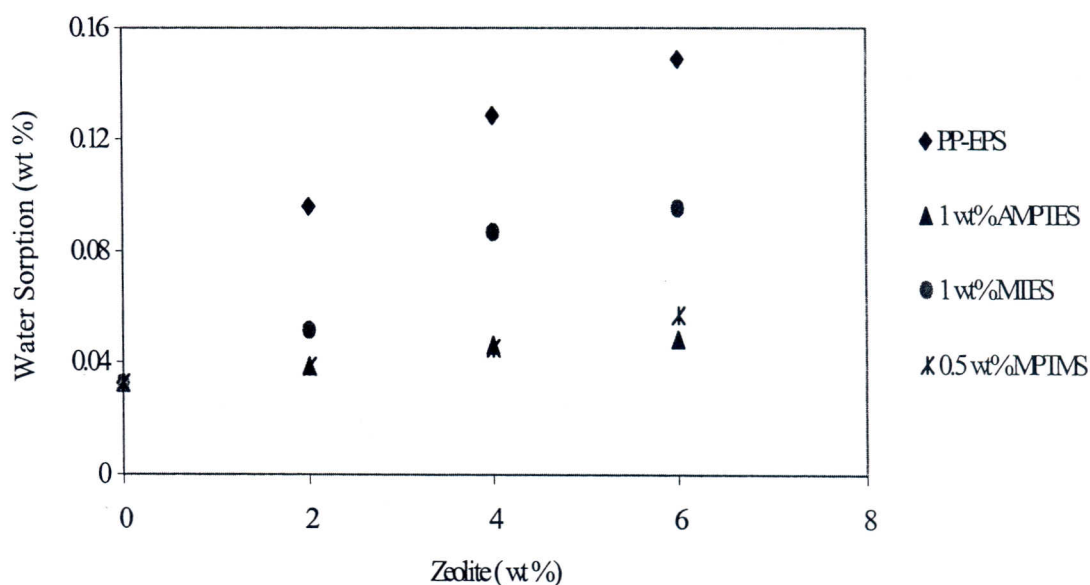
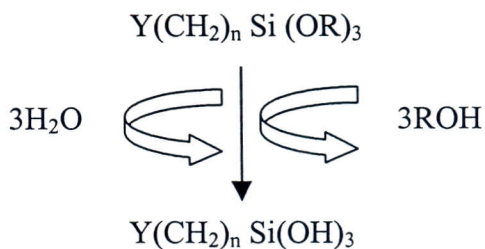
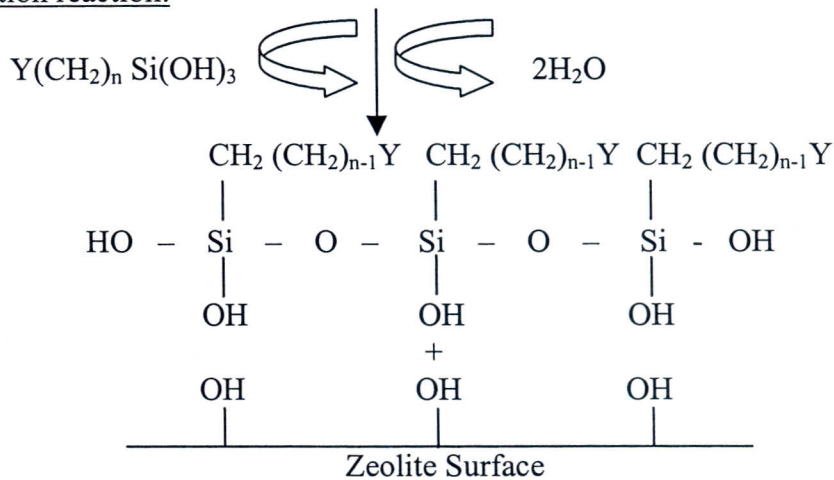


Figure 7.4. Water Sorption of PP Composites Containing Untreated and Treated Zeolite with Silane Coupling Agents as a Function of Zeolite Loading.

Hydrolysis reaction:



Condensation reaction:



Hydrogen Bonding:

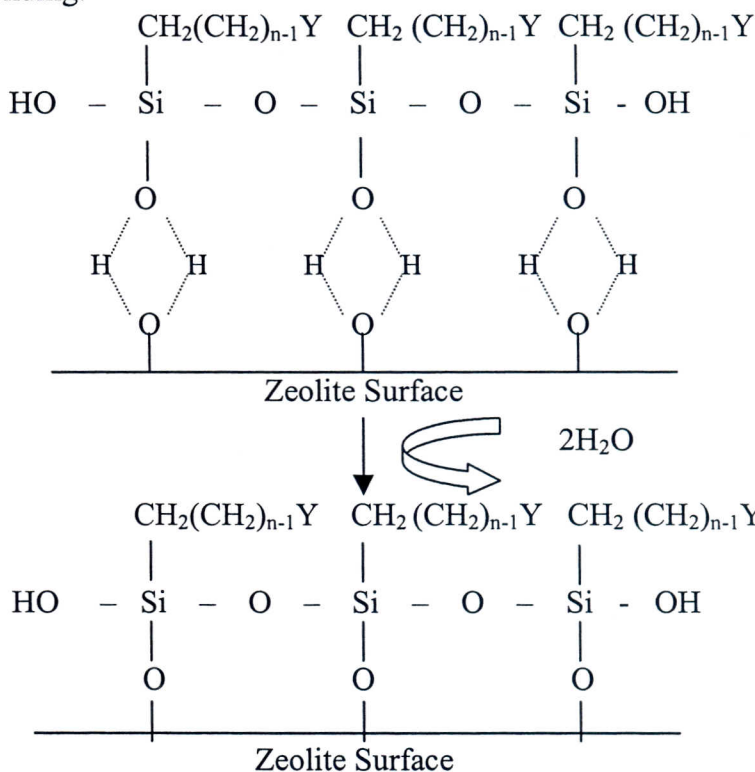


Figure 7.5. Chemical Reactions of Silane Coupling Agents with Zeolite Surface.  $\text{Y(CH}_2)_n$  denotes  $\text{NH}_2\text{-CH}_2\text{-CH}_2\text{-CH}_2$ ,  $\text{SH-CH}_2\text{-CH}_2\text{-CH}_2$  and  $\text{CH}_3$  for AMPTES, MPTMS and MTES, respectively.

As a result of water sorption experiments, it was found that the composites consisting 2, 4, and 6 wt% treated zeolite with 1wt% amino functional silane sorbed 59.3, 64.3, 67.8 wt% less amount of water compared to the 2, 4, and 6 wt% filled untreated composite. However, AMPTES does not have maximum hydrophobization according to contact angle measurement.

## 7.4. FTIR Spectroscopy Results

### 7.4.1. Characterization of Zeolite by FTIR Spectroscopy

FTIR spectroscopy provides determination of structural groups as well as chemical reactions at the interface between zeolite and silane coupling agents. FTIR spectra of AMPTES, MTES and MPTMS coupling agents used in this study were given in Figures 7.6 to 7.8 respectively. The characteristic peaks of silane coupling agents related to Si-O-C bonds given in Table 5.3 were observed at 800-850  $\text{cm}^{-1}$  and 1100  $\text{cm}^{-1}$  in these figures. The 1080, 1105 and 960  $\text{cm}^{-1}$  peaks in AMPTES and MTES stand for double, asymmetric and symmetric stretch of Si-O-C<sub>2</sub>H<sub>5</sub> group of AMPTES and MTES respectively. The 1166  $\text{cm}^{-1}$  peak is attributed to ethoxy in silyl ester of AMPTES and MTES, while the 1390  $\text{cm}^{-1}$  peak indicates the CH bond in CH<sub>3</sub>.

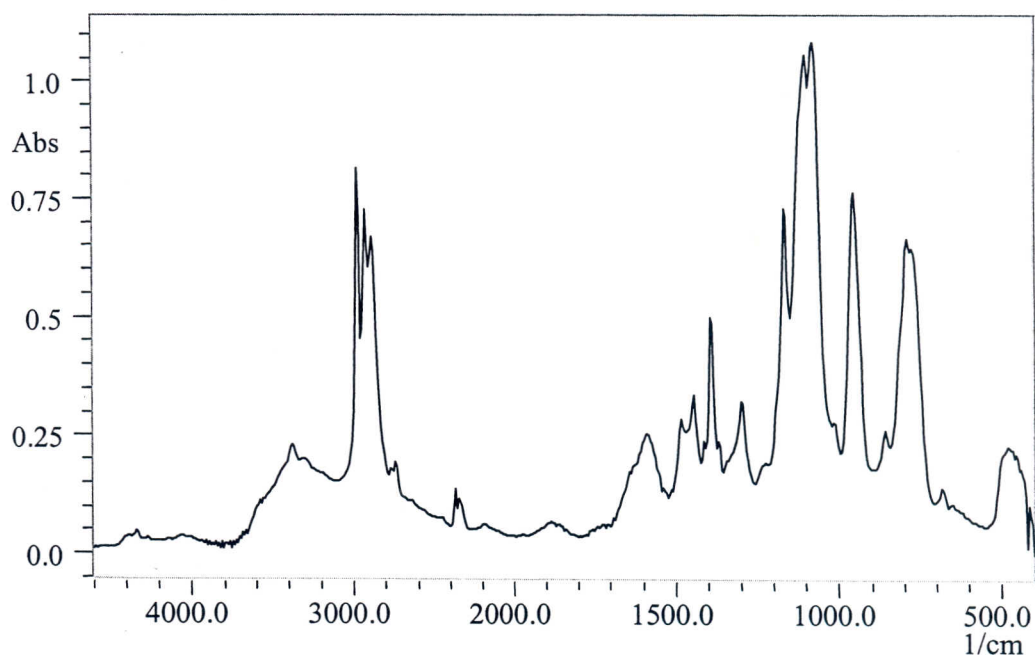


Figure 7.6. FTIR Spectrum of AMPTES.

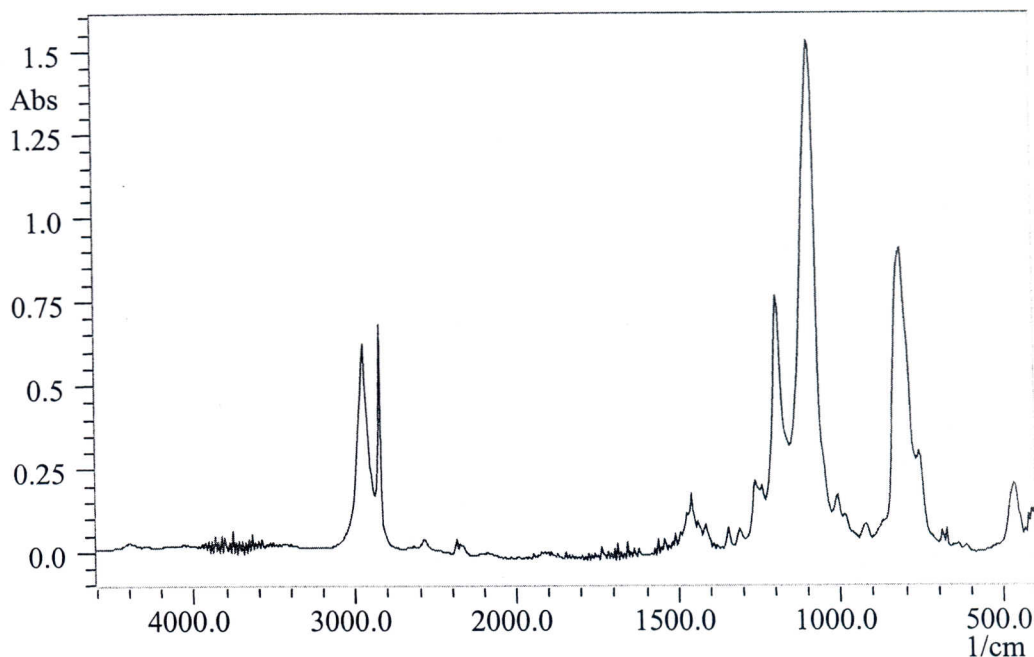


Figure 7.7. FTIR Spectrum of MTES.

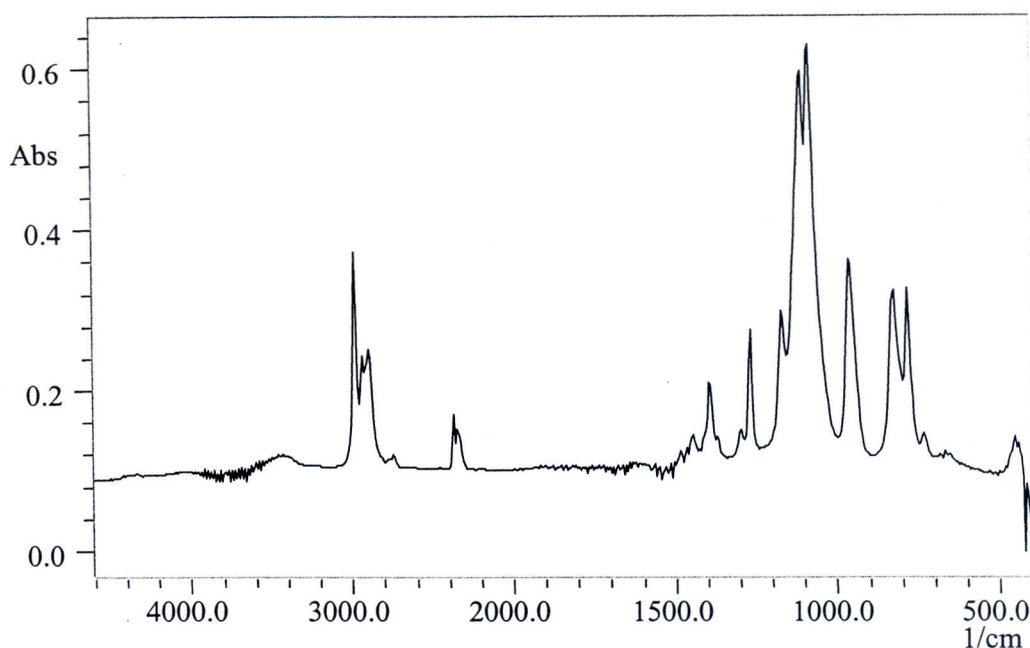


Figure 7.8. FTIR Spectrum of MPTMS.

The  $1591\text{ cm}^{-1}$  peak refers to primary amine in AMPTES can be regarded as a characteristic peak of AMPTES. The  $1265\text{ cm}^{-1}$  peak in MTES is assigned to the symmetric deformation of  $\text{Si-CH}_3$ . The  $\text{Si-CH}_3$  group present only in MTES can be regarded as a characteristic group of MTES without functional group. In MPTMS, having SH functional group, the  $1195\text{ cm}^{-1}$  peak stands for the  $\text{Si-O-CH}_3$  group. The weak band at  $2570\text{ cm}^{-1}$  peak indicates the SH stretch in MPTMS. The 2940 and

2850  $\text{cm}^{-1}$  peaks stand for the asymmetric and symmetric stretch of  $\text{CH}_2\text{-S}$  bands (Colthoupe et al, 1990).

Figure 7.9 shows the FTIR spectra of untreated and 1 wt% treated zeolite with three different silane coupling agents. The characteristic peaks of zeolite given in Table 5.2 are observed in the spectra of untreated and treated zeolite samples. The 450  $\text{cm}^{-1}$  and 609  $\text{cm}^{-1}$  peaks were assigned to the internal and external Si(or Al)-O double ring respectively. The IR spectra of all treated zeolite samples show the fluctuations near 1600  $\text{cm}^{-1}$  caused by deformation of water molecules (Akdeniz, 1999). The strong symmetric and asymmetric stretch vibrations are present at 1065  $\text{cm}^{-1}$  and around 1200  $\text{cm}^{-1}$  respectively. As seen in Figure 7.9, the peak intensities of the strongest vibrations of zeolite present in the range of 1300  $\text{cm}^{-1}$  and 840  $\text{cm}^{-1}$  decreases with silane treatment. The decrease in the peak intensities of the treated zeolite samples is related to the amount of sample used in the analysis. The silanol deformation (Si-OH) and siloxanes (Si-O-Si) bonds formed as a result of the reaction between the zeolite surface and silane coupling agents absorbs near 1030  $\text{cm}^{-1}$  and 1130-1000  $\text{cm}^{-1}$  respectively. These characteristics groups indicating the reaction between the silane and zeolite was not observed in the silane treated zeolite due to the presence of the strong vibrations of zeolite in the range of 1300  $\text{cm}^{-1}$  and 840  $\text{cm}^{-1}$ . This indicates that the signals were simply too weak to be distinguished. However, the new weak bands in the surface treated zeolites appear as a result of the characteristic peaks of silane coupling agents.

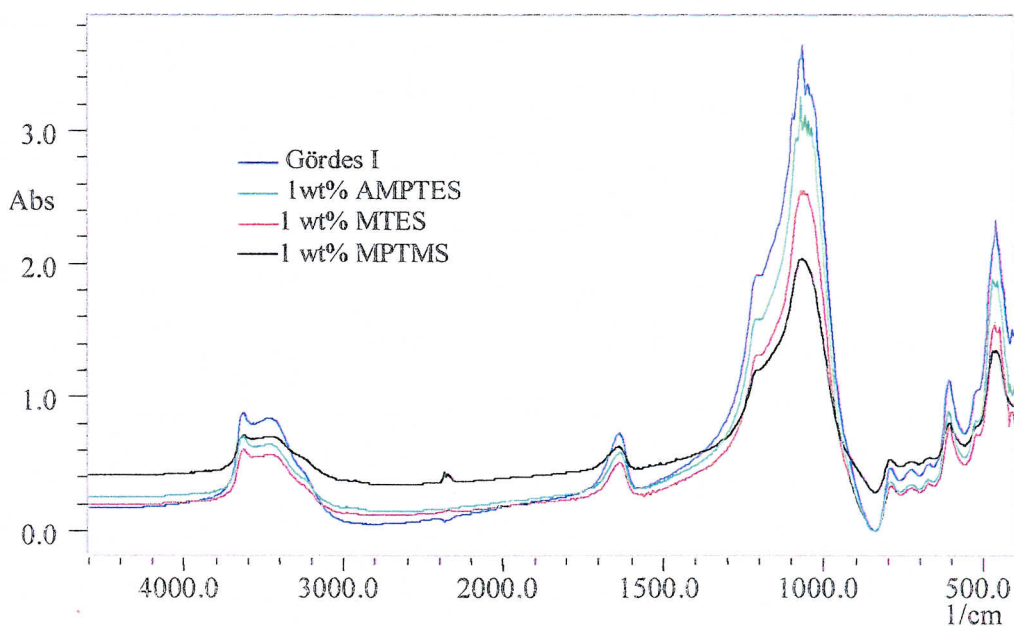


Figure 7.9. FTIR Spectra of Untreated, and Treated Zeolites with 1wt% AMPTES, MTES and MPTMS.

Alonso et al. (1997) observed the slight decrease in both the OH stretching ( $3678\text{ cm}^{-1}$ ) and OH libration ( $673\text{ cm}^{-1}$ ) bands of talc with silane coupling agents. From the spectra of untreated and treated zeolites, it was observed that the peak intensities of  $\text{H}_2\text{O}$  bending and OH stretch vibrations at  $1620\text{ cm}^{-1}$ ,  $3700\text{ cm}^{-1}$  and  $3400\text{ cm}^{-1}$  bands respectively decrease with silane treatment. The change of characteristic peak of zeolite at  $450\text{ cm}^{-1}$  with respect to  $\text{H}_2\text{O}$  bending at  $1620\text{ cm}^{-1}$  was compared to investigate the concentration effects of different silane coupling agents. Figure 7.10 shows b/a calibration curve with respect to the coupling agent content. Here b and a represent the absorbance values of zeolite peaks at  $450\text{ cm}^{-1}$  and  $1620\text{ cm}^{-1}$  respectively. As seen in Figure 7.10, surface treatment increases b/a values until the optimum of coupling agent concentration. The maximum b/a value was obtained at 1 wt% AMPTES. This result indicates that the maximum hydrophobization of zeolite surface can be obtained by the treatment with 1 wt% amino functional silane-coupling agent.

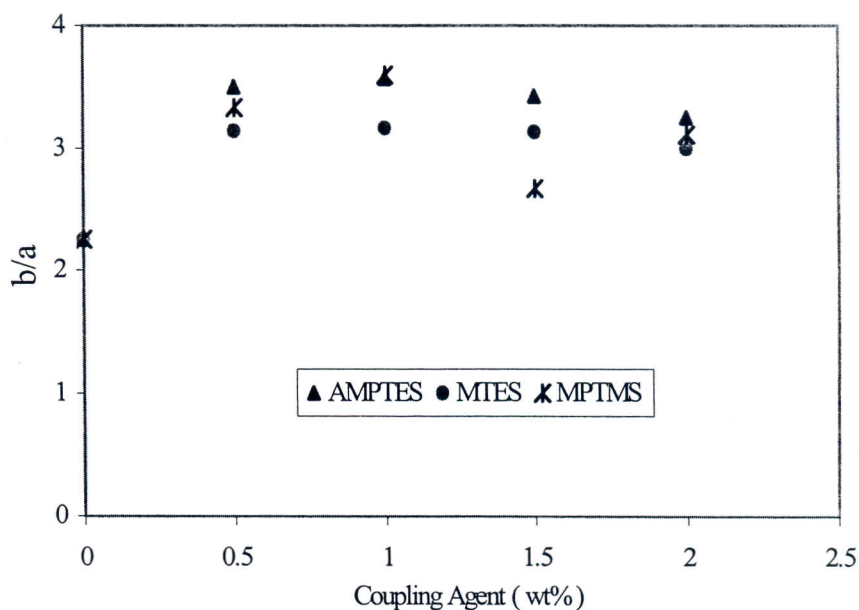


Figure 7.10. Variation of b/a with Respect to Silane Coupling Agents.

#### 7.4.2. Characterization of PP-Zeolite Composites by FTIR Spectroscopy

FTIR spectroscopy was used to investigate the effects of the surface treatment and plasticizers on the chemical structure of the PP-zeolite composites. Figure 7.11 shows the FTIR spectra of PP composites containing 6 wt% zeolite with DOP and EPS. Figures 7.12 to 7.14 illustrate the comparison of the FTIR spectra of the PP-EPS matrix

consisting of untreated and 1 wt% treated zeolite with three different silane coupling agents at the constant zeolite loading of 6 wt%. The characteristic peaks of polypropylene and zeolite given in Table 5.1 and 5.2 were observed in the spectra of the composites. In these figures, the broad peaks at  $3100\text{ cm}^{-1}$  and  $1640\text{ cm}^{-1}$  are due to the antioxidants used in polypropylene (Pehlivan, 2001). The  $1750\text{ cm}^{-1}$  peak refers to the carbonyl group of dioctylphthalate (DOP) and epoxidized soybean oil (EPS) used as plasticizers. As seen from the figures, surface treatment of zeolite did not change the spectra of the PP composites due to the low vibration intensity of silane coupling agents.

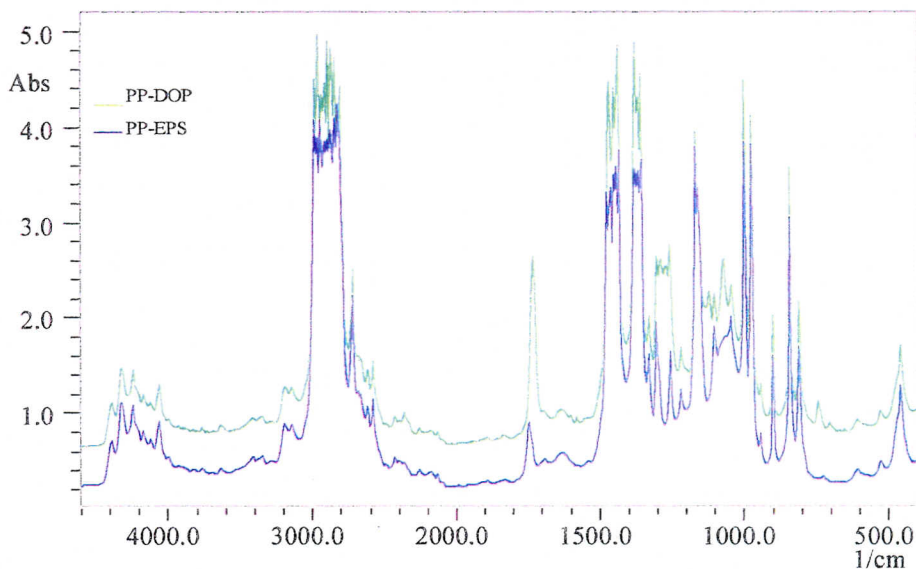


Figure 7.11. FTIR Spectra of PP Composites Containing 6 wt% Zeolite with DOP and EPS.

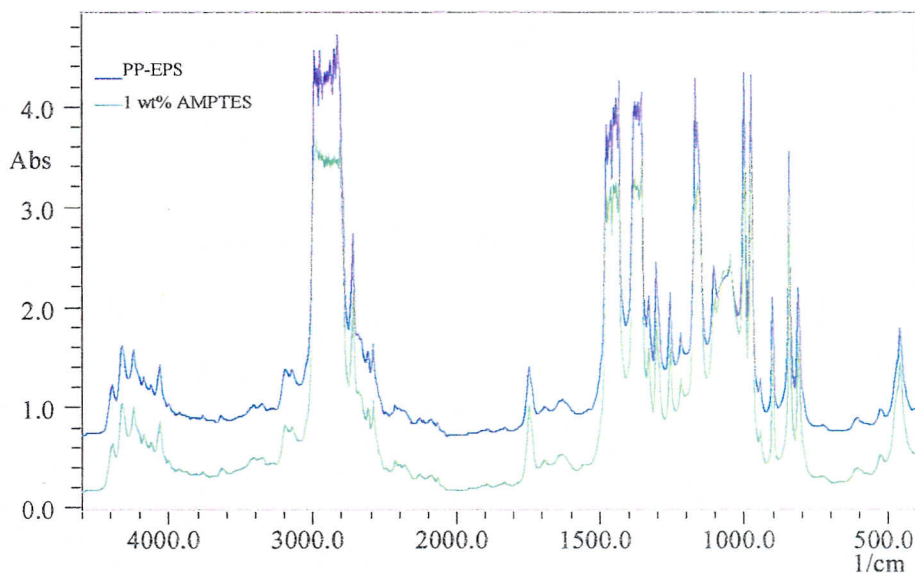


Figure 7.12. FTIR Spectra of PP-EPS Composites Containing 6 wt% Untreated and Treated Zeolite with 1 wt% AMPTES.

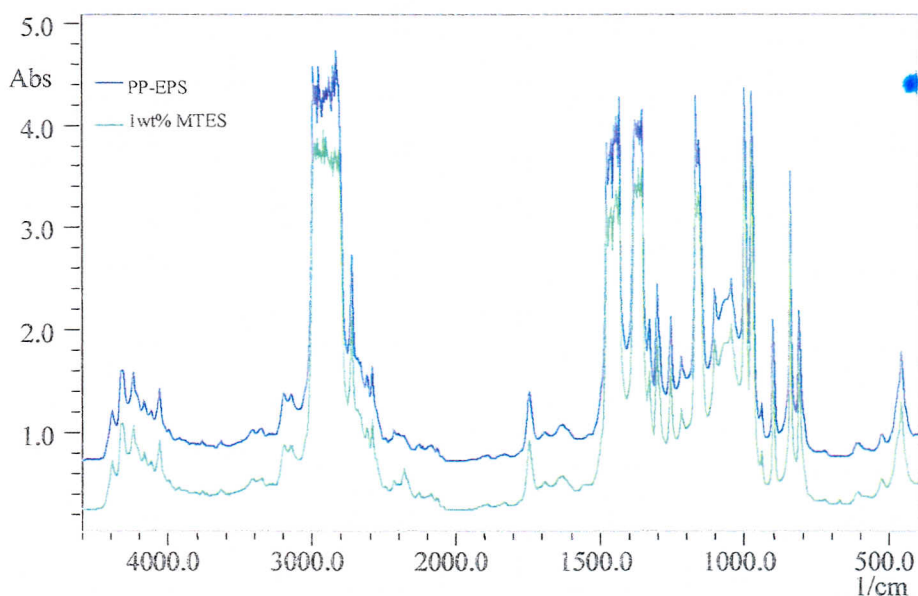


Figure 7.13. FTIR Spectra of PP-EPS Composites Containing 6 wt% Untreated and Treated Zeolite with 1 wt% MTES.

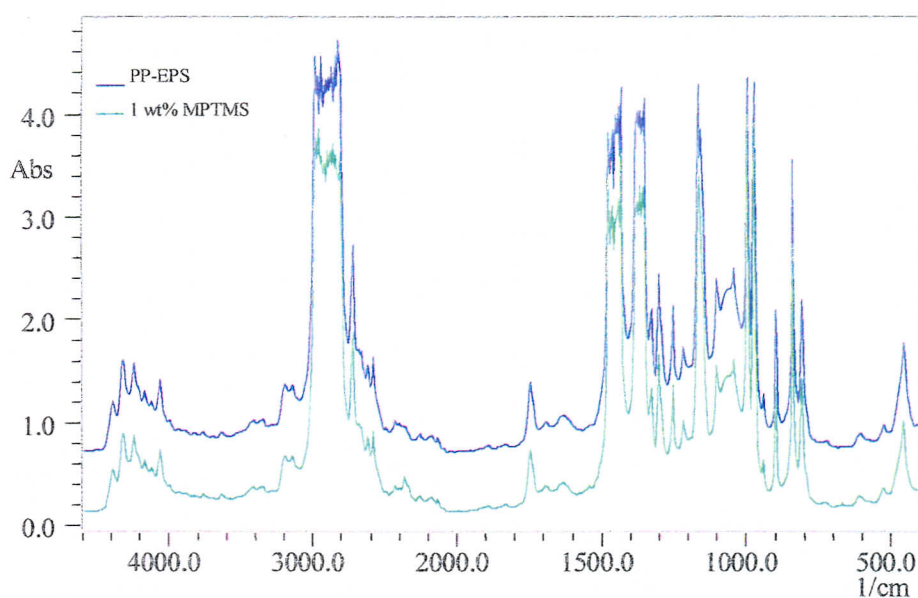


Figure 7.14. FTIR Spectra of PP-EPS Composites Containing 6 wt% Untreated and Treated Zeolite with 1 wt% MPTMS.

### 7.5. Results of Thermal Analyses

In this study, TGA and DSC were used for the thermal characterization of PP composites consist of untreated and treated zeolite with different surface modifiers. The

effects of surface modifiers on melting, degradation and crystallization behavior of PP composites were investigated.

### 7.5.1. Characterization of PP-Zeolite Composites by TGA

TGA based on the measuring the temperature dependence of the loss of the sample weight was performed to investigate the thermal degradation behavior of PP-zeolite composites. The weight losses, onset and termination of degradation temperatures of PP composites containing 2 wt% untreated and treated zeolite with 4 different surface modifiers at different concentrations were given in Table 7.1 and 7.2. As seen in Table 7.1, the onset and the termination of degradation temperatures of the composites decrease with the addition of plasticizers (DOP and EPS). The onset of degradation temperatures of the PP decreases from 257 °C to 247 and 248 °C with the addition of DOP and EPS, respectively.

Table 7.1. TGA Results of PP–Untreated Zeolite Composites.

Plasticizer	Zeolite Content (wt %)	Surface Modifier	Surface Modifier Content (wt %)	Onset of Degradation (°C)	Termination of Degradation (°C)	Weight Loss (wt %)
-	-	-	-	257	537	100
DOP	-	-	-	247	535	99.4
	2	-	-	216	533	98
EPS	-	-	-	248	536.5	99.4
	2	-	-	249	532	99

Thermogravimetric analysis allows the determination of the zeolite content of the composites. All substances in the composite except the zeolite particles decomposes until 600°C. TGA curve of Gördes 1 zeolite is shown in Figure 7.15. The water content of zeolite only decreases until 600 °C. The total amount of water loss was found as 12.75 % of the zeolite. For that reason, the relationship between the mass at the end and beginning of the analysis allows the determination of the zeolite content of the composites. It was observed that the weight loss of the 2 wt% untreated and treated

zeolite filled composites change considerably in the range of 99 and 88.7 %. The difference in the weight losses of the filled composites indicates the uneven distribution of zeolite in the matrix. The weight loss values below 98 % shows that the filler content in the composite is higher than 2 wt%. As seen in Table 7.1, the onset of degradation temperature for the PP-EPS composites increases with the decrease in the weight loss or the increase in the filler content. The zeolite retards the onset temperature, however termination temperature shifts to the lower temperatures. This indicates that addition of zeolite to the PP-EPS matrix slightly accelerate the degradation. DOP addition to the matrix also showed the same effect on the degradation termination temperature of PP.

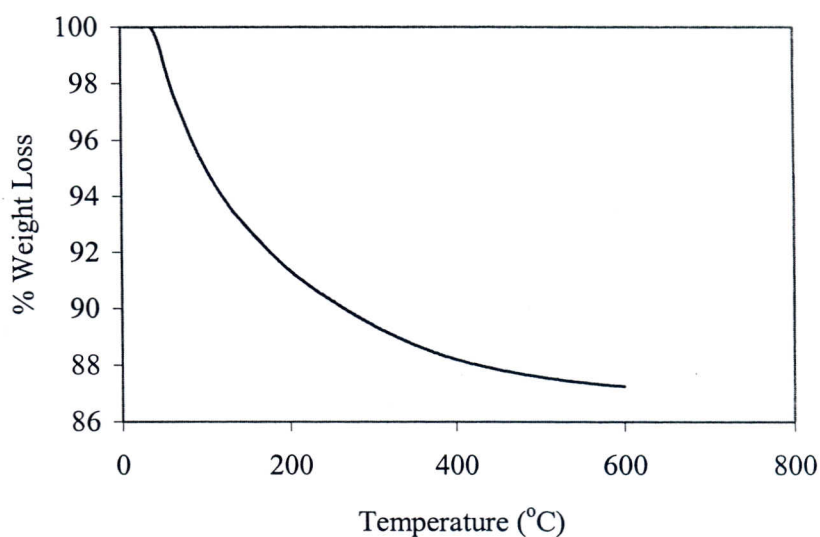


Figure 7.15. TGA Curve of Gördes 1 Zeolite.

TGA curves of the composites containing PP-EPS matrix and 2 wt% untreated and treated zeolite with PEG, 1 wt% AMPTES, MTES and MPTMS are shown in Figure 7.16. As seen in the figure, degradation of all samples starts around 250 °C and terminates around 535 °C. The weight losses of the composites containing untreated and treated zeolite with PEG and 1 wt% AMPTES, 1 wt% MTES and 1 wt% MPTMS are found as 99.7, 88.7, 98.8 and 92.1 % respectively. The onset and termination of degradation temperatures of the composites depend on the weight loss of the composites due to the zeolite content. For that reason, the effects of surface modifiers on the degradation behavior of PP-zeolite composites were not observed because of the difference in the weight losses of the composites. As seen in the table, there is a slight difference in the weight losses of (0.5, 1, 1.5 and 2 wt%) MPTMS treated zeolite filled

composites. Thus, the effect of MPTMS concentration on the degradation behavior of the composites can be observed. The onset of degradation temperature and termination of degradation temperature of the composites decrease with the increase of MPTMS concentration at a constant zeolite loading.

The effect of surface modifier and its concentration on the degradation behavior of the composites could not be observed easily from the TGA analysis because of the non-homogenous distribution of the zeolite in the PP matrix. Since the amount of filler in the matrix was not constant, it was difficult to understand which effect caused the degradation temperature fluctuations. The difference in the weight losses of the composites indicated that thermal stability of the composites was also improved by grafting of PP on to the zeolite surface.

Table 7.2. TGA Results of PP - 2 wt% Treated Zeolite Composites.

Plasticizer	Surface Modifier	Surface Modifier Content (wt%)	Onset of Degradation (°C)	Termination of Degradation (°C)	Weight Loss (wt%)
DOP	PEG	3	256	532	91.9
EPS	PEG	3	251	540	99.7
EPS	-	-	249	532	99
EPS	AMPTES	0.5	255	532	91.1
		1	257	533	88.7
		1.5	252	534	91.7
		2	254	531	90.2
	MTES	0.5	245	533	99.4
		1	250	535	98.8
		1.5	247	533	99
		2	241	531	90.5
	MPTMS	0.5	256	530	92.2
		1	254	538	92.1
		1.5	251	534	92
		2	253	534	93.7

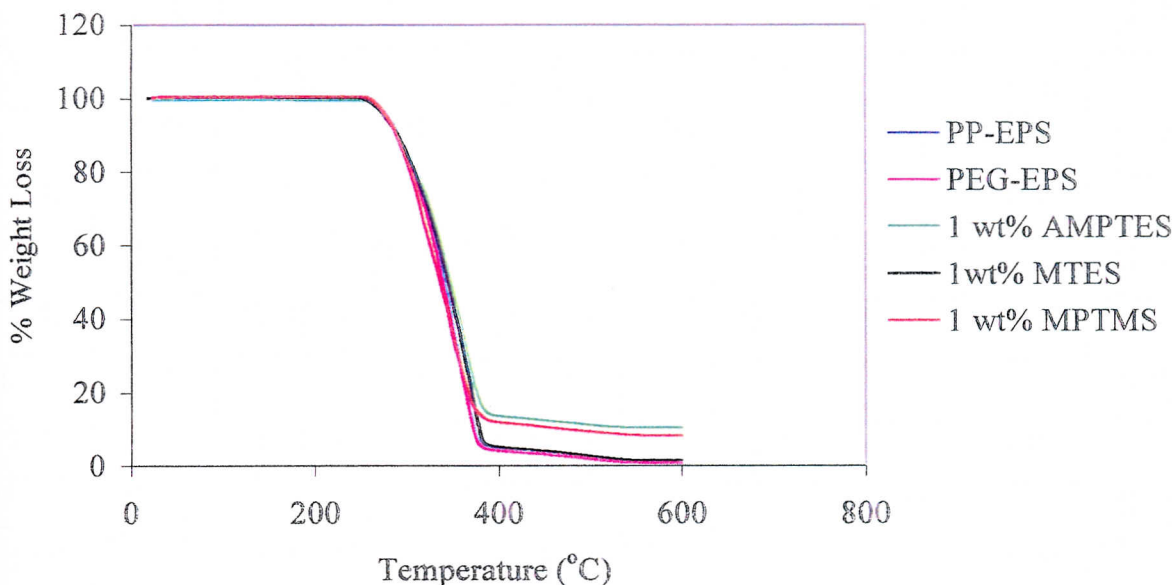


Figure 7.16. TGA Curves of PP-EPS Composites Containing 2 wt% Untreated and Treated Zeolite.

### 7.5.2. Characterization of PP-Zeolite Composites by DSC

The effects of plasticizers and surface modifiers on melting, degradation and crystallization behavior and crystallization kinetics of PP-zeolite composites were investigated.

#### 7.5.2.1. Melting and Degradation Behavior of PP-Zeolite Composites

Thermal analyses of PP composites containing plasticizers (DOP and EPS) and 2 wt% untreated and treated zeolite with PEG, AMPTES, MTES and MPTMS were carried out from room temperature to 500 °C at a heating rate of 10 °C/min. The DSC results of PP composites containing untreated zeolite are given in Table 7.3. As shown in the table, melting temperature of PP was decreased from 165 °C to 162.8 and 163 °C by the addition of DOP and EPS respectively. It was observed that the incorporation of untreated zeolite did not change the melting temperature of the composites. The thermal degradation temperature of PP was decreased from 459.9 to 457.4 °C by the addition of DOP. The degradation temperature of PP-EPS does not change with the addition of untreated zeolite, however, that of the PP-DOP shows a slight increase with the addition of zeolite from 457.4 to 463.9 °C.

Table 7.3. DSC Results of PP - Untreated Zeolite Composites.

Plasticizer	Zeolite Content (wt %)	Surface Modifier	Surface Modifier Content (wt %)	1 <sup>st</sup> Peak Temp. (°C)	2 <sup>nd</sup> Peak Temp. (°C)	$\Delta H_f$ (kJ/kg)	$\Delta H_d$ (kJ/kg)	% Cryst.
-	-	-	-	165	459.9	59.57	258.2	28.5
DOP	-	-	-	162.3	457.4	76.13	360.4	36.4
	2	-	-	162.8	463.9	84.2	416.8	40.3
EPS	-	-	-	162.8	459.1	81.7	396.5	39.1
	2	-	-	162.8	459.2	75.81	414.4	36.3

At a heating rate of 10 °C/min, the quantitative information about peak temperatures for melting and degradation, heat of fusion ( $\Delta H_f$ ), heat of degradation ( $\Delta H_d$ ) and % crystallinity values are tabulated in Table 7.4 for the composites treated with PEG and silane coupling agents. It was found that there was a slight change in melting temperatures of the composites treated with PEG and silane coupling agents compared to the untreated ones. The melting points of composites are between 162.3 and 164.8 °C.

Figure 7.17 shows the DSC curves of the composites containing 2 wt% untreated and silane treated zeolite. In the figure, the first and the second peak temperatures show the melting and the degradation temperatures of the composites, respectively. As seen in the figure and tables, the silane treatment indicates no effect in the melting and thermal degradation peak temperatures of the composites except thermal degradation temperature of the composites containing treated zeolite with 1.5 wt% MPTMS and MTES. The thermal degradation temperatures of the composites consist of 2 wt% treated zeolite with 1.5 wt% MPTMS and MTES shows a slight decrease from 459.9 °C to 454.8 °C.

The % crystallinity values of the composite films listed in Table 7.3 were determined using Equation (5.5).  $\Delta H_f$  value for the isotactic PP was taken as 209 kJ/kg (Horrocks and D'Souza, 1991). As shown in the Table, although % crystallinity of pure PP film was 28.5 %, the addition of plasticizer was found to increase crystallinity of PP film to 36.4 and 39.1 % for DOP and EPS, respectively. Also the crystallinity of the films increases with the addition of zeolite from 28.5 up to 40.3.

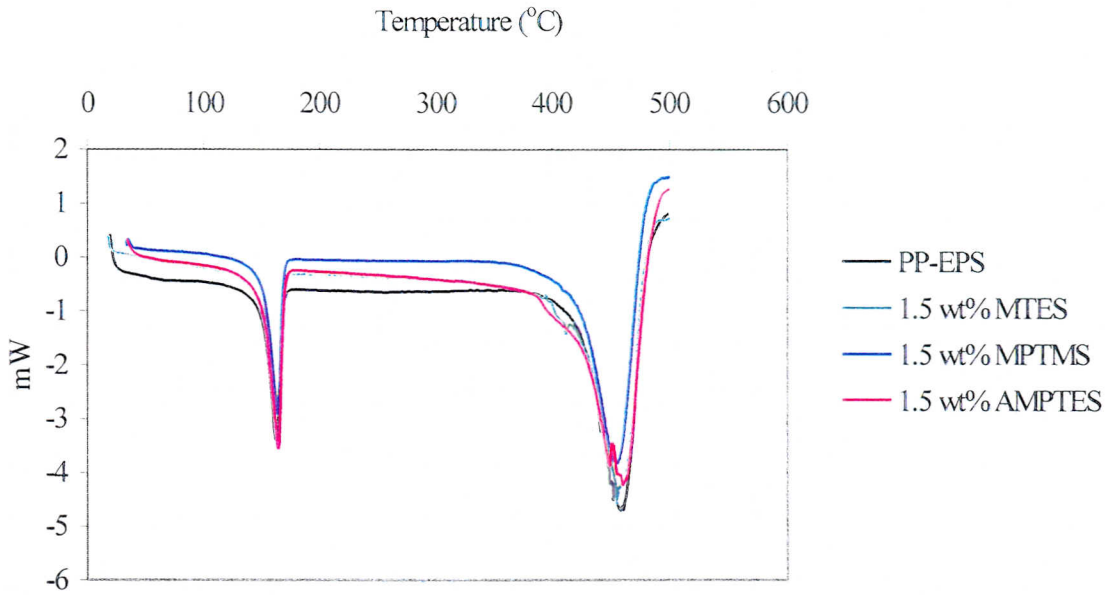


Figure 7.17. DSC Curves of PP-EPS Composites Containing 2 wt% Untreated and Treated Zeolite

Although the addition of zeolite had an insignificant effect on the melting behavior of the composites, % crystallinity of the composites increases with the addition of zeolite. It is concluded that zeolite acts as a nucleating agent in the PP matrix. The higher the zeolite content, the higher the crystallinity values were obtained in the composites. Özmihçı (1999) and Pehlivan (2001) have also observed this behavior. As shown in Table 7.4, crystallinity values of the composites containing silane treated zeolite were in the range of 34 and 43.2 %. This shows that silane treatment does not affect the crystallinity values of the composites significantly. In addition, the maximum % crystallinity was found as 48.3 % for the PP-PEG treated zeolite composites. This high crystallization value can be due to the non-homogeneous distribution of zeolite in the composite. The heat of melting values of the composites can also confirm the non-homogeneous distribution of zeolite in the composite. As seen in the table, the high heat of melting values of the composites lead to the high values of % crystallinity due to the nucleation effect of the composite.

Table 7.4. DSC Results of PP- 2 wt% Treated Zeolite Composites.

Plasticizer	Surface Modifier	Surface Modifier Content (wt %)	1 <sup>st</sup> Peak Temp. (°C)	2 <sup>nd</sup> Peak Temp. (°C)	$\Delta H_f$ (kJ/kg)	$\Delta H_d$ (kJ/kg)	% Cryst.
DOP	PEG	3	163.5	460.7	99.0	472.3	47.4
EPS	PEG	3	163.03	461.9	100.9	487.5	48.3
EPS	AMPTES	0.5	163.6	459.3	84.72	455.3	40.5
		1	163.6	461.4	90.3	478.42	43.2
		1.5	164.3	460.0	83.1	469.3	39.7
		2	163.9	458.84	88.3	504.6	42.2
	MTES	0.5	164.8	460.6	82.4	477.6	39.4
		1	163.1	459.1	74.2	444.3	35.5
		1.5	164.5	454.8	71.2	410.6	34
		2	163.7	458.3	77.8	435.9	37.2
	MPTMS	0.5	163.2	458.9	81.0	403.2	38.8
		1	164.2	460.2	89.5	441.0	42.8
		1.5	163.6	454.8	77	424.4	36.8
		2	162.8	458.0	72.5	422.5	34.7

### 7.5.2.2. Crystallization Behavior of PP-Zeolite Composites

Crystallization temperature of composites is an important parameter that affects the quality of the PP films such as permeability and mechanical properties. Polymer processing occurs in the melt phase and crystallization of the polymer from the melt influences the distribution of the crystallites developed upon cooling from the melt that determine the final properties of the materials. For that reason, the effects of surface modification of zeolite with silane coupling agents on the crystallization temperature of the composites were studied. The PP-EPS composites containing 4 wt% untreated and treated zeolite with 1 wt% silane coupling agents were heated to 200 °C at a heating rate of 20 °C/min and cooled to 50 °C at three different cooling rates of 5, 10, and 20 °C/min.

The melting and crystallization peak temperatures, the onset crystallization temperatures, heat of fusion ( $\Delta H_f$ ), heat of crystallization ( $\Delta H_c$ ) and % crystallinity

values of the PP composites are tabulated in Table 7.5. % crystallinity values were found from  $\Delta H_f$  and  $\Delta H_c$  of the composites using Equation (5.5). As seen in the table, silane coupling agents and zeolite loading do not quite affect the melting peak temperatures of the composites. It was observed that the onset and peak temperatures of crystallization of the composites containing silane treated zeolite show a slight increase at a constant cooling rate compared to the untreated ones and decrease with increase in the cooling rate. The crystallization temperature of the composites shows a slight increase. This could be due to the weak nucleating ability of zeolite or non-homogeneous distribution of zeolite in the composite. The onset crystallization temperature of the composites containing AMPTES treated zeolite shows a significant increase at all cooling rates. The onset temperature of the composites containing 4 wt% untreated zeolite increases from 122.3 to 129.2°C with the treatment of zeolite with AMPTES at a cooling rate of 20 °C/min. As seen in the table, the crystallization temperatures of the composites shift to the higher temperatures at lower cooling rates.

Figure 7.18 shows that the DSC curves of PP-EPS composites containing 4 wt% MPTMS treated zeolite at cooling rates of 5, 10 and 20 °C/min. As seen in the figure, although the melting temperature shows a slight increase from 162.7 to 163.4 °C, the crystallization temperature decreases from 118.4 to 114.4 °C with increase in the cooling rate. The heat of melting and heat of crystallization values show no significant change with increase in the cooling rate. The heat of melting and the heat of crystallization values were found as around 81 and 94 kJ/kg, respectively.

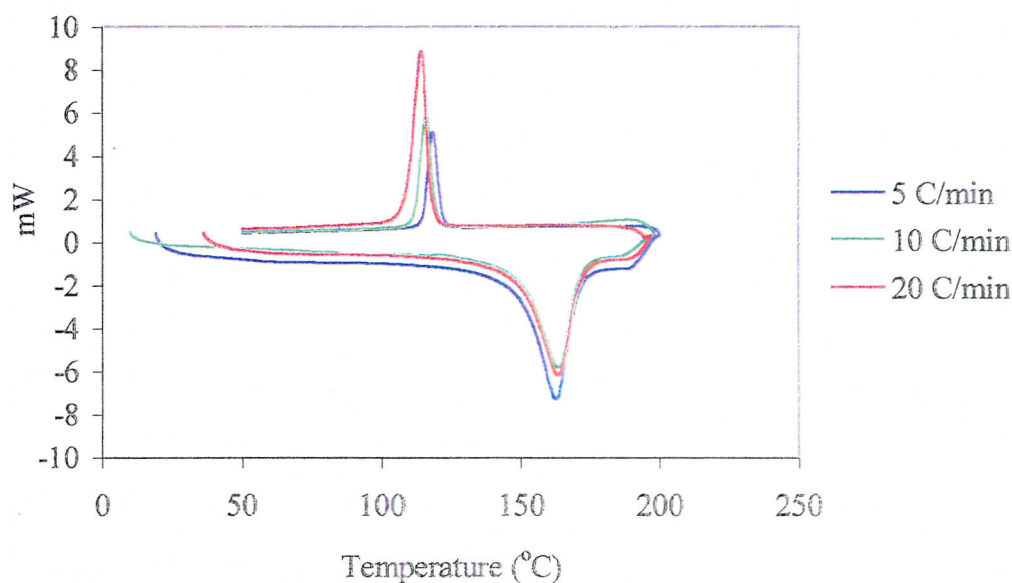


Figure 7.18. DSC Curves of PP Composites Containing 4 wt% MPTMS Treated Zeolite at Different Cooling Rates.

As seen in Table 7.5, % crystallinity values also show no significant change with increase in the cooling rate and silane treatment. However, it was observed that the heats of melting of the composites were lower than the heats of crystallization. For that reason, % crystallinity values of quenched composites calculated from the heat of melting were lower than those of the composites calculated from the heat of crystallization. This difference between % crystallinity values can be explained by the thermal analysis conditions. The % crystallinity of the quenched composites was a direct indication of the crystallinity of the composites obtained from the extruder. The % crystallinity values of the composites obtained from crystallization peak were affected by thermal history of the composites. For that reason, the composites in the analyses were heated up to 200 °C for 4 min in order to erase any previous thermal history.

Table 7.5. Crystallization Results of PP-EPS Composites Containing 4 wt% Zeolite.

Cooling Rate (°C/min)	Surface Modifier	Zeolite Content (wt%)	Melting Temp. (°C)	Cryst. Temp. (°C)	Onset Cryst. Temp. (°C)	$\Delta H_f$ (kJ/kg)	$\Delta H_c$ (kJ/kg)	% Cryst Of Quench Film	% Cryst Of Cryst. Peak
5	-	-	162.8	118.2	121.6	73.3	96.8	35.1	46.3
	-	4	163.8	117.8	122.5	81.5	93.3	38.9	44.6
	AMPTES	4	163.1	117.8	126.8	78	92.3	37.3	44.2
	MTES	4	163.3	119.3	123.3	80.1	92.5	38.3	44.3
	MPTMS	4	162.7	118.4	122.7	82.3	96.7	39.4	46.3
10	-	-	162.5	112.4	124.9	77.2	91.8	36.9	43.9
	-	4	164.3	113.6	118.5	77.7	91.4	37.2	43.7
	AMPTES	4	162.5	113.5	126.7	83.5	95.5	40	45.7
	MTES	4	163.5	115.3	120.5	83.2	98.3	39.8	47
	MPTMS	4	163.5	115.9	120	80.3	94	38.4	45
20	-	-	161.8	109.5	122.3	77.2	93.9	37	45
	-	4	165.5	111.1	119.8	75.9	85.6	36.3	41
	AMPTES	4	162.2	111.7	129.2	80.9	97.2	38.7	46.5
	MTES	4	164	114.4	121	73.1	88.2	35	42.2
	MPTMS	4	163.4	114.4	119.5	81.9	94	39.2	45

Although an increase in crystallinity of the composites was observed with the addition of untreated and treated zeolite, the crystallization behavior of the composite from the melt shows a slight effect. This may be due to the non-homogeneous distribution of the zeolite in the composite and/ or activity of zeolite. It is concluded that the onset and the peak crystallization temperatures of PP composites remain unaffected by the presence of untreated and silane treated zeolite except the composite containing AMPTES treated zeolite. Crystallization of the composites having high onset values starts earlier than that of the composites having low onset values. For that reason, the improvement in the mechanical properties of the composites containing AMPTES treated zeolite was expected due to the high onset crystallization values.

The effect of inorganic fillers on the crystallization of PP is related to the filler type according to the inactive or active type filler such as carbon black and talc respectively (Alonso et al, 1997 and Mucha, 2000). Although inactive fillers have little effect on the rate of crystallization, active fillers can be applied to accelerate the crystallization of the composites.  $\Phi$  values, indicating the activity of the filler in Equation (5.14) for untreated and surface treated zeolite with silane coupling agents were calculated from B values found from the experimental slopes in the representation of  $\log q$  versus  $1/\Delta T^2$ , according to Equation (5.12). The lower value of  $\Phi$  represents a higher value of activity. Figure 7.19 represents a plot of  $\log q$  versus  $1/\Delta T^2$  for the PP-EPS composites having unfilled and filled 4 wt% untreated and treated zeolite with silane coupling agents. B values obtained from the slopes in the curves were 8190, 10568, 11002, 11205 and 15839 for the composites having unfilled and filled 4 wt% untreated and treated zeolite with AMPTES, MTES and MPTMS coupling agents, respectively.  $\Phi$  values of the PP composites containing 4 wt % untreated zeolite and treated zeolite with 1 wt% AMPTES, MTES, and MPTMS were found as 1.29, 1.34, 1.37 and 1.93, respectively. The increase in the  $\Phi$  values of the treated zeolite was observed for PP-EPS-zeolite composites with silane treatment contrary to the literature. Alonso and coworkers (1997) and Guitierrez et al (1999) observed the decrease in the  $\Phi$  values of talc with surface modification. They obtained that the activity of filler was increased with silane treatment and the nucleating effect was increasing with silane treatment. This contrary result can be explained by the particle size distribution of the zeolite in the composites. Mitsubishi et al. (1991) reported that the activity values of fillers increase with a decrease in particle size.

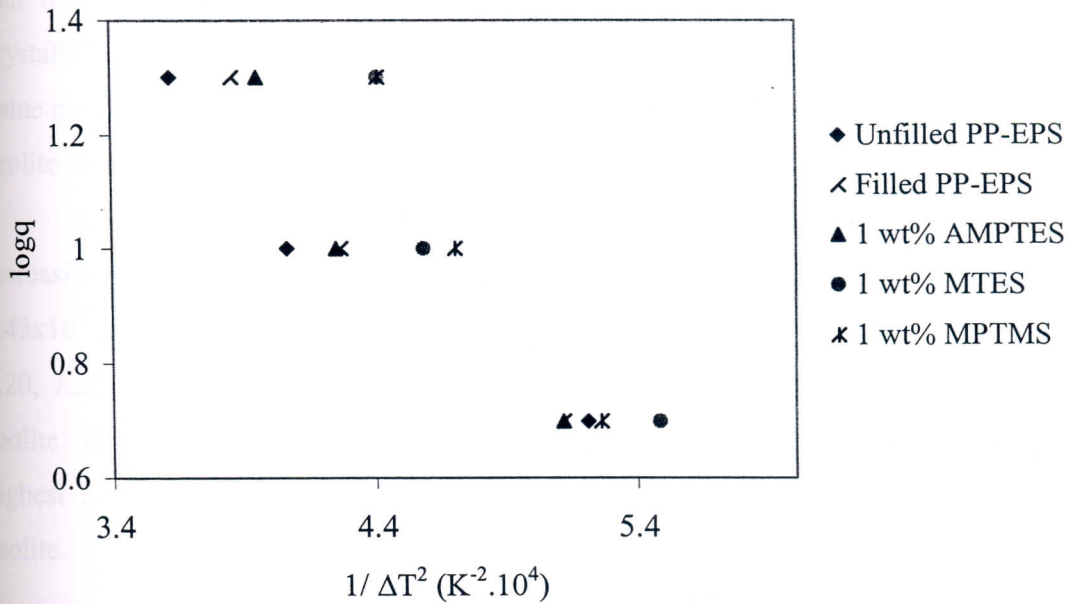


Figure 7.19. The  $\log q$  versus  $1/\Delta T^2$  Plot for Unfilled and Filled PP-EPS Composites Containing 4 wt% Untreated and Treated Zeolite with Silane Coupling Agents.

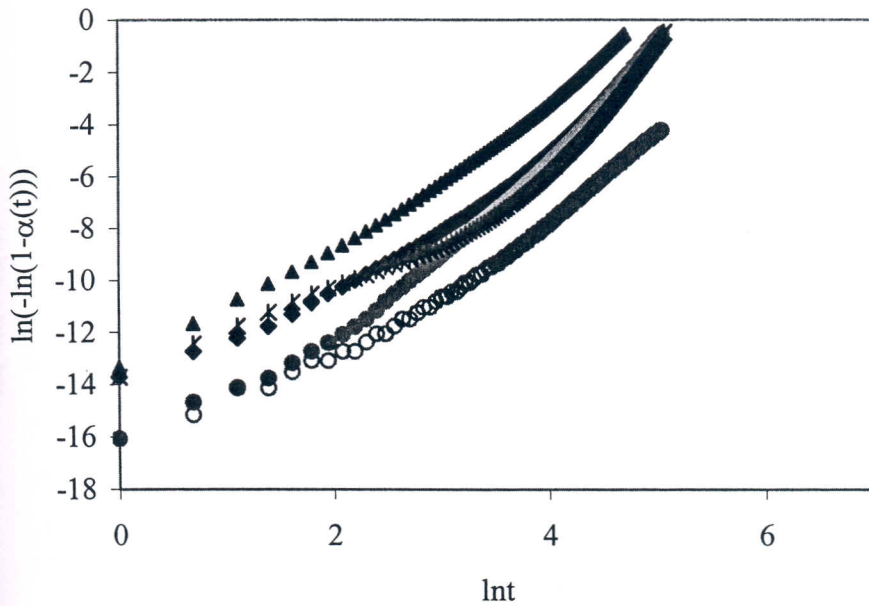
### 7.5.2.3. Crystallization Kinetics of PP-Zeolite Composites

Crystallization kinetics of PP-EPS composites containing 4 wt% untreated and treated zeolite with 1 wt% silane coupling agents was determined according to both Avrami and Kissinger methods. The double logarithmic plot of  $\ln(-\ln(1-X_t))$  versus  $\log t$ , known as Avrami plot, for unfilled and filled PP-EPS composites with 4 wt% untreated and treated zeolite with different silane coupling agents at a cooling rate of 5 °C/min is shown in Figure 7.20. 7.21 also shows Avrami plot for the composites containing 4 wt% treated zeolite with 1 wt% MTES at a cooling rate of 10 °C/min. Avrami parameters,  $n$  and  $K$ , in Equation (5.7) can be determined from the slopes and intercepts of the linear portion. Avrami parameters of the composites for three different cooling rates were calculated and tabulated in Table 7.6.

The  $n$  values of the composites depend on the form of crystal growth. The  $n$  values can vary between 1 and 4, related with the size of crystals. The shape of the crystal changes from rod like to three-dimensional spherulite in this range (Progelhof and Throne, 1993). The  $n$  values obtained from this study were between 2.68 and 3.66 as seen in Table 7.6. The change in the value of  $n$  from 2.68 to 3.66 indicated that the nature of crystal growth was changing from one-dimensional disk to three-dimensional

spherulite. The number of nucleation sites increase with the decreasing of  $n$  values. For that reason, those have minimum  $n$  values at different cooling rates show rapid crystallization. Since  $n$  is related to the crystal growth and geometry, the higher the value means the larger the crystals in the composites. It was found that PP-silane treated zeolite composites had larger crystal sizes compared to the untreated ones.

As seen in Table 7.6, the rate constant,  $K$ , in the Avrami Equation increases with increasing of cooling rate. The  $K$  parameters of PP-EPS increase from  $5.66 \times 10^{-9}$  to  $2.43 \times 10^{-7}$  with the increase in the cooling rate from 5 to 20 °C/min. As seen in Figure 7.20, 7.21, and in Table 7.6,  $K$  values increase with the surface modification of the zeolite. This shows that the rate of crystallization increases with the treatment and the highest  $K$  value was obtained for the composites having 1 wt% AMPTES treated zeolite.



○ PP-EPS ◆ Filled PP-EPS ▲ 1 wt% AMPTES ● 1 wt% MTES ✱ 1 wt% MPTMS

Figure 7.20. Avrami plots of Unfilled and Filled PP-EPS Composites Containing 4 wt% Untreated and Treated Zeolite with Silane Coupling Agents at a Cooling Rate of 5 °C/min.

Kissinger method was also used to determine the activation energy of the composites filled with untreated and treated zeolite with silane coupling agents. According to the Kissinger method given in Chapter 5, crystallization activation

energies of the composites were determined from the slope of the graph of  $\ln(Q/Tp^2)$  versus  $1/Tp$ . Figure 7.22 shows the graph of  $\ln(Q/Tp^2)$  versus  $1/Tp$  for the PP-EPS. The crystallization activation energies of PP-EPS composites tabulated in Table 7.7 were found as 194.9, 259.6, 275.91, 325.7, and 254.4 kJ/mol for the unfilled, filled with untreated and treated zeolite with 1wt% AMPTES, MTES and MPTMS, respectively. As seen in Table 7.7, the crystallization activation energies of the composites increase with the addition of zeolite and silane treatment. The higher activation energies indicate the faster change of crystallization rate with temperature. Surface modification resulted the higher activation energy values, thus the faster change of crystallization with temperature compared to untreated zeolite. It is concluded that nucleating effect increased with the addition of both untreated and treated zeolites to the PP matrix and the nucleating effect of the composites having treated zeolites was more pronounced than that of the untreated composite.

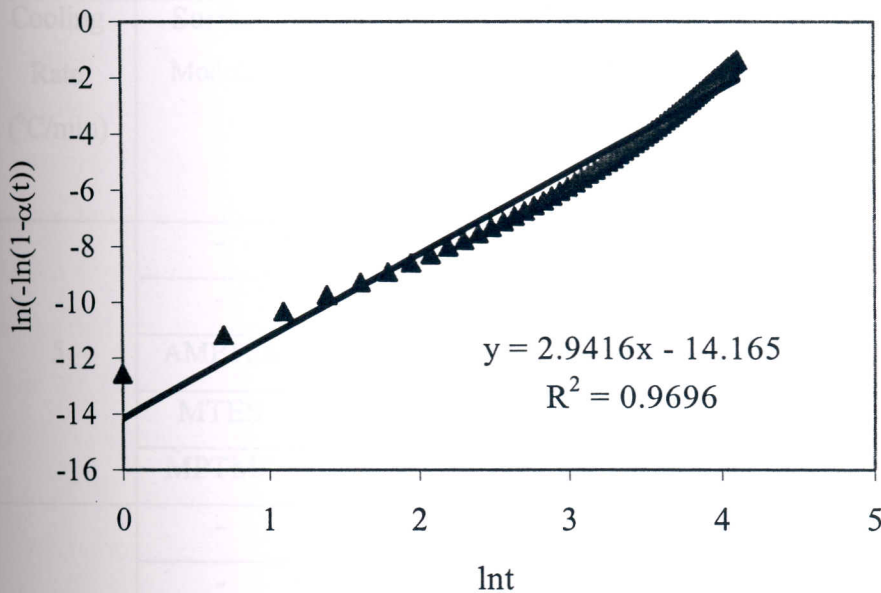


Figure 7.21. Avrami Plot of the PP-EPS Composites Containing 4 wt% Treated Zeolite with 1 wt% MTES at a Cooling Rate of 10 °C/min.

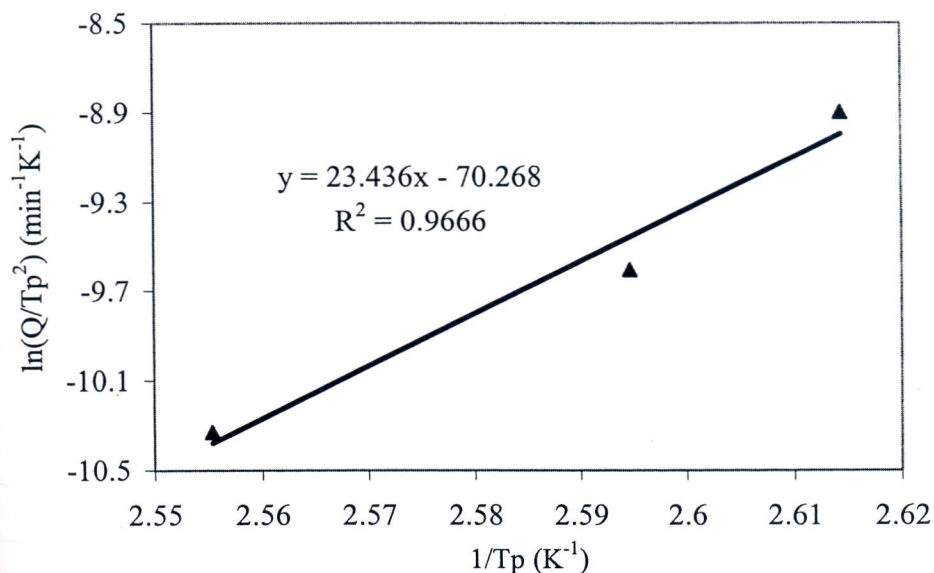


Figure 7.22. Kissinger Plot of PP-EPS.

Table 7.6. Avrami Parameters of the PP-Zeolite Composites for Non-isothermal Crystallization.

Cooling Rate (°C/min)	Surface Modifier	Amount of Surface Modifier (wt%)	Zeolite Content (wt %)	Avrami Method	
				n	K (s <sup>-n</sup> )
5	-	-	-	2.87	$5.7 \times 10^{-9}$
	-	-	4	3.08	$2.6 \times 10^{-8}$
	AMPTES	1	4	2.87	$2.7 \times 10^{-7}$
	MTES	1	4	3.59	$2 \times 10^{-9}$
	MPTMS	1	4	3.07	$1.8 \times 10^{-8}$
10	-	-	-	3.45	$9.36 \times 10^{-8}$
	-	-	4	2.71	$2.96 \times 10^{-6}$
	AMPTES	1	4	3.39	$9.6 \times 10^{-8}$
	MTES	1	4	2.94	$7.05 \times 10^{-7}$
	MPTMS	1	4	3.49	$6.08 \times 10^{-8}$
20	-	-	-	3.66	$2.43 \times 10^{-7}$
	-	-	4	3.41	$8.59 \times 10^{-8}$
	AMPTES	1	4	3.45	$4.88 \times 10^{-7}$
	MTES	1	4	3.53	$1.49 \times 10^{-6}$
	MPTMS	1	4	2.68	$4.88 \times 10^{-7}$

Table 7.7. Activation Energy Values of the PP-Zeolite Composites for Non-isothermal Crystallization.

Surface Modifier	Amount of Surface Modifier (wt%)	Zeolite Content (wt%)	Kissinger Method $\Delta E$ (kJ/mol)
-	-	-	194.9
-	-	4	259.6
AMPTES	1	4	275.9
MTES	1	4	325.7
MPTMS	1	4	254.4

## 7.6. Mechanical Properties of PP-Zeolite Composites

Tensile tests of (2, 4, and 6 wt%) the untreated and treated zeolite filled PP composites were conducted to determine how mechanical properties were influenced by the presence of surface modifiers (AMPTES, MTES, MPTMS or PEG) at the interface between the polymer matrix and zeolite. In addition, tensile tests of wet samples obtained from immersion of the composites in water for 24 hours at room temperature were carried out to determine the interfacial strengths of the composites. Experimental tensile test results of the dry and wet composites were given in Table A.3 and A.4 in the Appendix. Young's modulus, yield stress, tensile stress at break and elongation at break values of PP-zeolite composites were investigated as a function of zeolite loading, type of surface modifier, and surface modifier concentration for both dry and wet samples.

### 7.6.1. Young's Modulus of PP-Zeolite Composites

The effects of filler content, plasticizers, water and surface treatment on Young's modulus of PP-zeolite composites were studied and shown in Figures from 7.23 to 7.26. It was observed that Young's modulus of the composites increased as the filler content increases. The increase in Young's modulus of the zeolite-filled composites indicated an increase in the rigidity of PP related to the restriction of the mobility in PP matrix. Zeolite particles in the composite restrict the mobility and

deformability of PP matrix. Young's modulus of PP decreased with addition of plasticizer but it is not significantly different than that of PP containing DOP and EPS. The Young's modulus values of PP, PP-DOP, and PP-EPS were found as 1169, 1167 and 1152 MPa respectively. The Young's modulus values of 6 wt% zeolite filled PP-DOP and PP-EPS composites increased by 24 and 25.9 %, compared to the unfilled PP-DOP and PP-EPS matrix respectively. When the composites were exposed to water, Young's modulus of the composites decreased as seen in Figure 7.23. The Young's modulus values of wet PP, PP-DOP and PP-EPS were found as 1126.7, 1095.1 and 1096.5 MPa respectively. The Young's modulus values of wet PP, PP-DOP and PP-EPS were 3.6, 6.2 and 4.8 % lower than that of the dry samples, respectively. The Young's modulus values of wet PP-DOP and PP-EPS composites containing 6 wt% untreated zeolite increased by 21.1 and 23.7 %, when compared to the dry unfilled PP-DOP and PP-EPS matrix respectively.

The effect of surface treatment on Young's modulus of the composites is contradictory to the literature. According to the some references, improved adhesion leads to increased stiffness (Maiti and Sharma, 1992), other references claim that modulus is independent of treatment compared to the composites prepared with untreated filler, and occasionally a decrease in modulus is reported on increasing surface coverage (Demjen and Pukanszky, 1997).

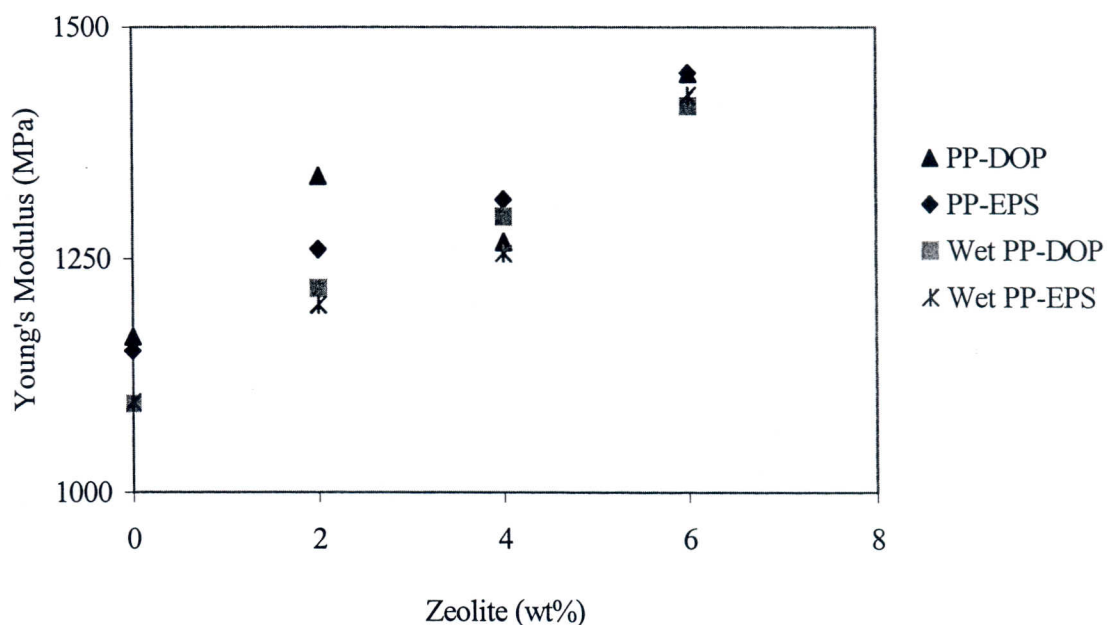


Figure 7.23. Young's Modulus of Dry and Wet PP-Zeolite Composites with Respect to Plasticizers and Zeolite Content.

Özmişçi (1999) and Pehlivan (2001) observed a decrease in Young's modulus of PP-zeolite composites with an increase in zeolite loading. The decrease in modulus of PP composites indicates the formation of voids around filler due to poor bonding between the zeolite particles and PP matrix in the absence of a coupling agent. Surface treatment of zeolite with PEG and silane coupling agents increases the Young's modulus of the composites with increase in zeolite loading. The Young's modulus values of dry PP-DOP and PP-EPS composites containing 6 wt% PEG treated zeolite were 22.5 and 22.3 % higher than those of the unfilled PP-DOP and PP-EPS respectively. However, the Young's modulus values of the wet PP-DOP and PP-EPS composites containing 6 wt% PEG treated zeolite increased by 17 and 19.2 % as compared to the unfilled dry PP-DOP and PP-EPS matrix respectively.

Figures 7.24 and 7.25 show the influence of the surface treatment concentration of silane coupling agents on Young's modulus of the dry and wet composites containing 6 wt% zeolite, respectively. Young's modulus of the composites were measured for four different types of silane concentrations (0.5, 1, 1.5, and 2 wt%). As seen in the figures, silane treatment leads to the increase in Young's modulus due to improvement of adhesion between zeolite and PP matrix. Although 1 wt% coupling agent concentration shows a maximum in the Young's modulus of dry and wet composites, Young's modulus decrease somewhat with increasing silane coupling agent concentration in all cases after 1 wt% coupling agent concentration due to the plasticizing effect of the surface modifier. The maximum Young's modulus values for 1 wt% coupling agents concentration indicate the maximum strength of interaction between zeolite and PP matrix. Although the decrease in Young's modulus is almost the same for all silane coupling agents, the composites modified with AMPTES are always stiffer than the one containing untreated filler. Young's modulus of dry composites containing 6 wt% treated zeolite with 1 wt% AMPTES, MTES and MPTMS increased by 56.7, 45.6 and 44.3 % as compared to the unfilled PP-EPS matrix respectively.

As seen in Figure 7.25, the increase in wet Young's modulus values of the composites containing 6 wt% treated zeolite with 1 wt% AMPTES, MTES and MPTMS was found as 32.4, 25.53 and 33.1 % compared to the unfilled PP-EPS matrix respectively. Although dry and wet tensile modulus of the silane treated composites are higher than those of the untreated and PEG treated composites, wet tensile modulus of silane treated composites was decreased due to the water absorption by reduction of the chemical bonding strength at the interface. This decrease in wet modulus of silane

treated composites indicates that there is no perfect interfacial adhesion between the zeolite and PP matrix. However, dry and wet PP composites containing 1 wt% AMPTES treated zeolite have higher modulus values than the others at the constant zeolite loading. This indicates that the better interfacial adhesion between PP matrix and zeolite particles is obtained by surface treatment of zeolite with 1 wt% AMPTES.

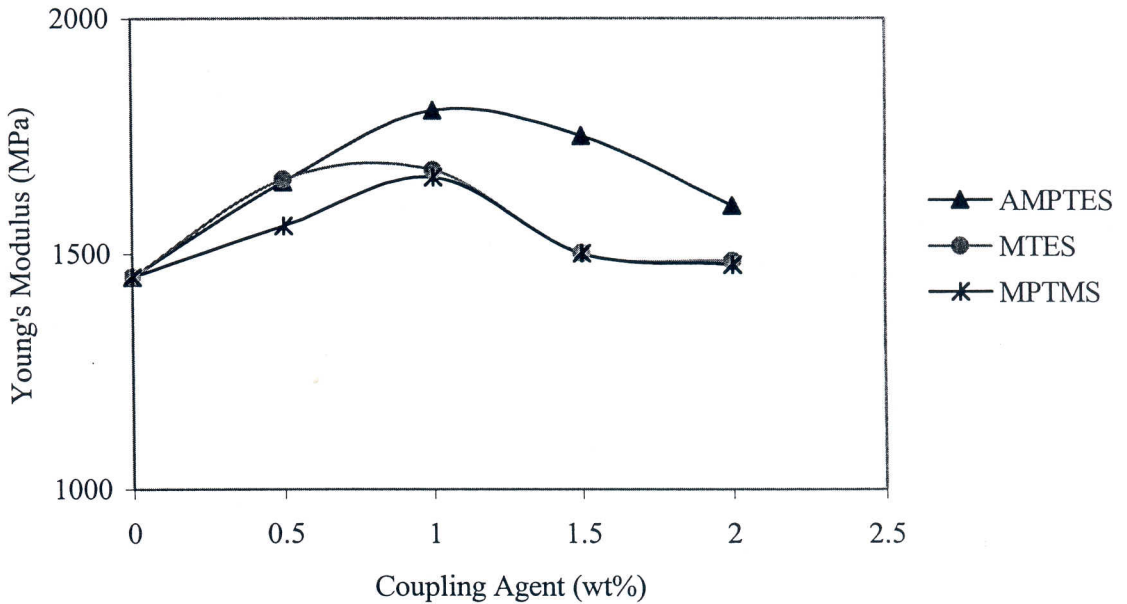


Figure 7.24. Effect of Silane Coupling Agents on the Young's Modulus of Dry PP Composites Containing 6 wt% Zeolite.

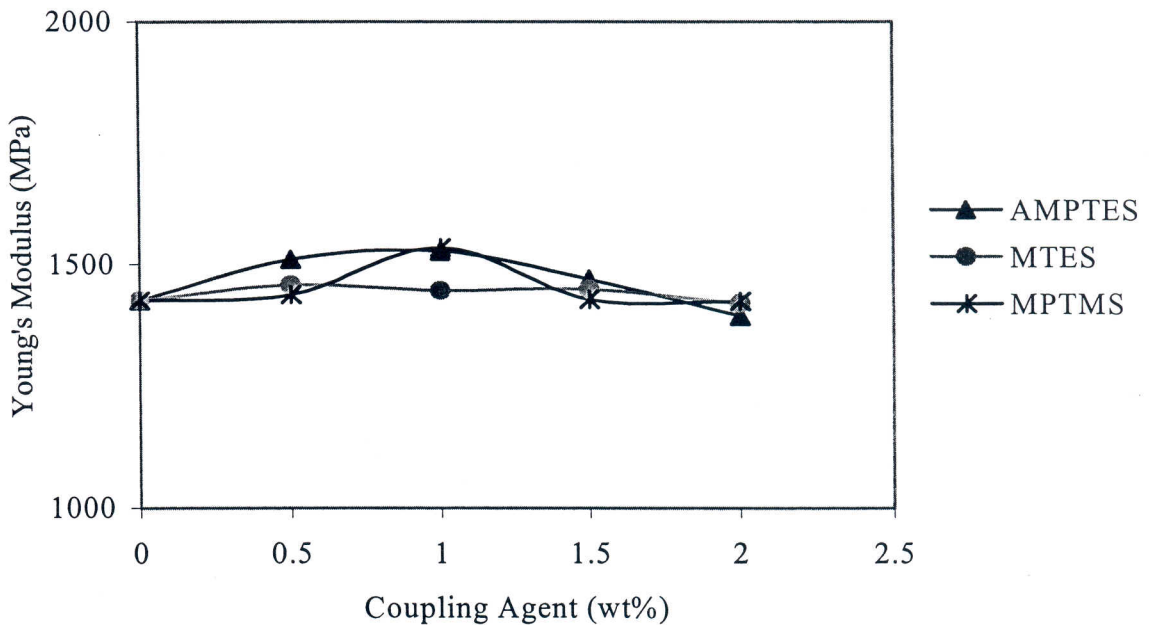


Figure 7.25. Effect of Silane Coupling Agents on the Young's Modulus of Wet PP Composites Containing 6 wt% Zeolite.

The dry and wet theoretical Young's modulus values of the composites given in Table A.9 and A.10 in Appendix were predicted using Kerner Equation (5.16). Figure 7.26 shows the comparison of experimental and theoretical modulus values of dry PP-EPS with respect to the untreated zeolite content. As seen in the figure, Kerner model didn't predict the experimental Young's modulus data for PP-EPS- zeolite composites. The model predicted lower values as compared to the experimental data. Also, deviation increases as zeolite loading increases.

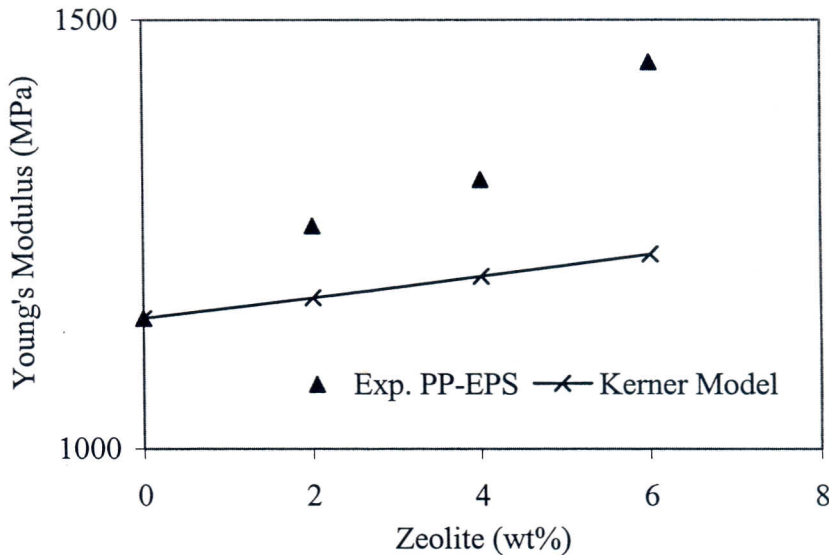


Figure 7.26. Experimental and Theoretical Young's Modulus Values of PP-EPS with Respect to Zeolite Content.

### 7.6.2. Tensile Yield Stress of PP-Zeolite Composites

The tensile yield stress data for dry and wet composites are tabulated in Table A.2 and A.3 in Appendix. Figure 7.27 shows the dry and wet yield stress values of PP-untreated zeolite composites as a function of zeolite loading. As seen in the figure, the yield stress of PP composites decreases with increasing zeolite loading. The dry yield stress of PP decreases from 28 MPa to 25.2 MPa with the addition of plasticizer. Although dry yield stress values of PP-DOP and PP-EPS are not significantly different from wet values, the addition of zeolite and water sorption cause a slight decrease in these values. It was observed that the dry and wet yield stress of filled PP-DOP composites are higher than those of filled PP-EPS composites. The yield stress of 6 wt% zeolite filled PP-DOP and PP-EPS composites decreased by 16 and 33 % for dry samples and 20 and 30.5 % for wet samples when compared to the unfilled dry PP-DOP

and PP-EPS matrix respectively as seen in Figure 7.27. It was observed that the decrease in yield stress increased with water effect due to poor bonding between zeolite and matrix. PEG does not significantly affect on yield stress of the composites. In addition, the decrease in the yield stress of PP-DOP and PP-EPS composites containing 6 wt% PEG treated zeolite were found as 13 and 24 % for dry samples and 15.4 and 25 % for wet samples compared to the dry unfilled matrix respectively.

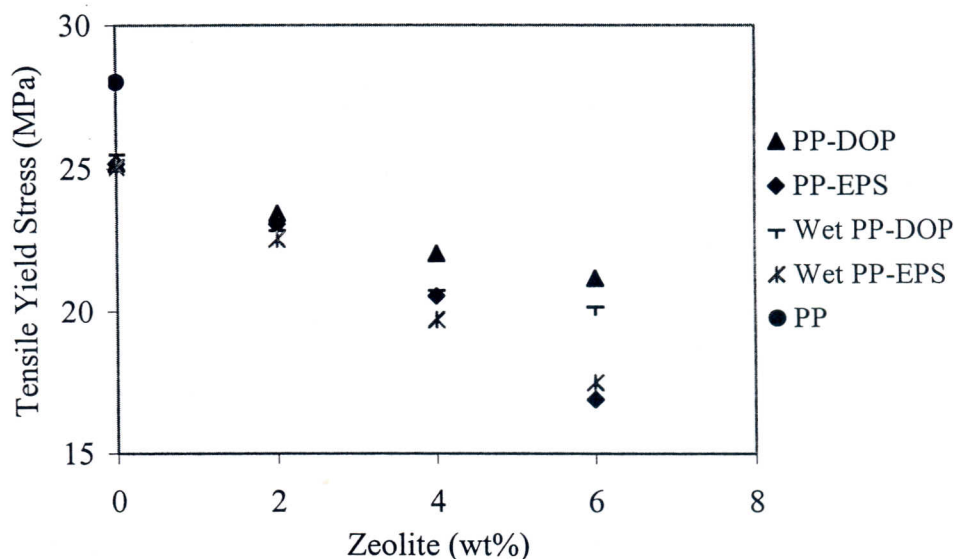


Figure 7.27. Dry and Wet Tensile Yield Stress Values of PP-Zeolite Composites with Respect to Zeolite Content for two Different Plasticizers.

The effect of various coupling agents on dry and wet yield stress of the composites is shown in Figures 7.28 and 7.29, respectively. The yield stress of the composites containing treated filler with silane coupling agents increased similar to the Young's modulus. As seen in the figures, addition of small amount of silane coupling agents leads to a sharp increase in the tensile yield strength of the composites. The increase in the yield stress values of the composites indicates that the strength of PP-zeolite composite is improved by silane coupling agent. Coupling agents show a maximum in the yield stress at the coupling agent concentration of 1 wt% for AMPTES and MTES and 0.5 wt% for MPTMS. These concentration levels for each silane coupling agent are the optimum concentrations which reflect the highest strength of interaction between zeolite and PP-EPS matrix. When coupling agent is used in large amounts such as 1.5 and 2 wt%, tensile yield stress decreases. This could be due to the formation of physisorbed layers, which decrease the strength of interaction between the zeolite and the PP matrix. This type of behavior was seen by Demjen and coworkers

(1997 and 1998) for PP-CaCO<sub>3</sub> composites. They observed a maxima on the tensile properties of the composites around at 1 wt% silane concentration for various silane coupling agents such as (3-methacryloxypropyl)trimethoxysilane and aminopropyltriethoxysilane.

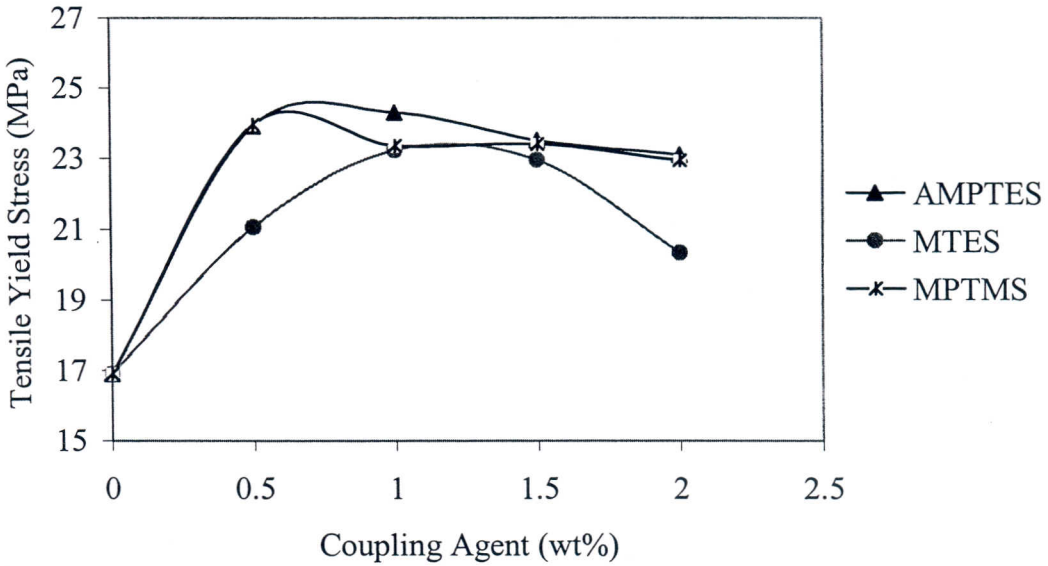


Figure 7.28. Effect of Silane Coupling Agents on the Dry Yield Stress of PP Composites Containing 6 wt% Zeolite.

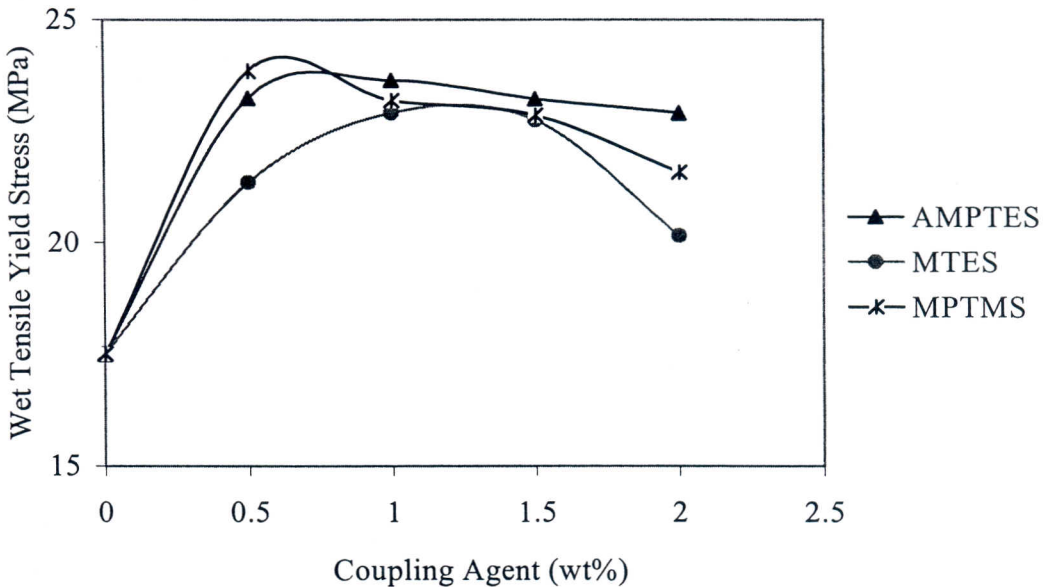


Figure 7.29. Effect of Silane Coupling Agents on the Wet Yield Stress of PP Composites Containing 6 wt% Zeolite.

Dry tensile yield stress values of the composites containing 6 wt% treated zeolite with 1 wt% AMPTES, 1 wt% MTES and 0.5 wt% MPTMS increased by 43.8, 37.5 and 41.8 % compared to the dry yield stress of 6 wt% untreated zeolite filled PP-EPS composite respectively. Also, the increase in wet tensile yield stress of these composites were found as 35.1, 30.9 and 36.3 % compared to the wet yield stress of untreated filled PP-EPS matrix respectively. It was observed that there was a slight decrease in wet yield stress of the composites treated with silane coupling agents compared to the untreated ones. This result shows that interfacial adhesion between zeolite and PP was improved by silane coupling agents and AMPTES was found as the most appropriate coupling agent.

Figure 7.30 and 7.31 illustrate the dry and wet tensile yield stress values of PP composites containing untreated and treated zeolite with PEG and silane coupling agents at optimum silane concentration as a function of zeolite content, respectively. All coupling agents used at optimum concentration show a reactive coupling effect that results in higher yield stresses compared to the untreated ones. As seen in Figure 7.24, wet theoretical tensile test results of 1 wt% AMPTES treated composites overlap with that of 0.5 wt% MPTMS treated composites.

Figure 7.30 and 7.31 also show the comparison of the experimental data with the Pukanszky model for dry and wet tensile yield stress values of PP-zeolite composites, respectively. Pukanszky model given in Equation 5.24. was explained in detail in Chapter 5. As seen in the figures, the model predicts the data of PP-silane treated composites very well. B parameter in the model characterizes the interaction between PP and zeolite, and the higher the B values indicate the better interaction. Significant difference exists in the slope of lines, i.e. in the parameter B, especially with the untreated case, indicating differences in the reactivity or coupling efficiency. As seen in the figures, the differences in the interaction become more pronounced, appearing as larger deviation in B of untreated and PEG treated zeolite filled composites than in B of silane treated zeolite filled composites, with increasing the zeolite content.

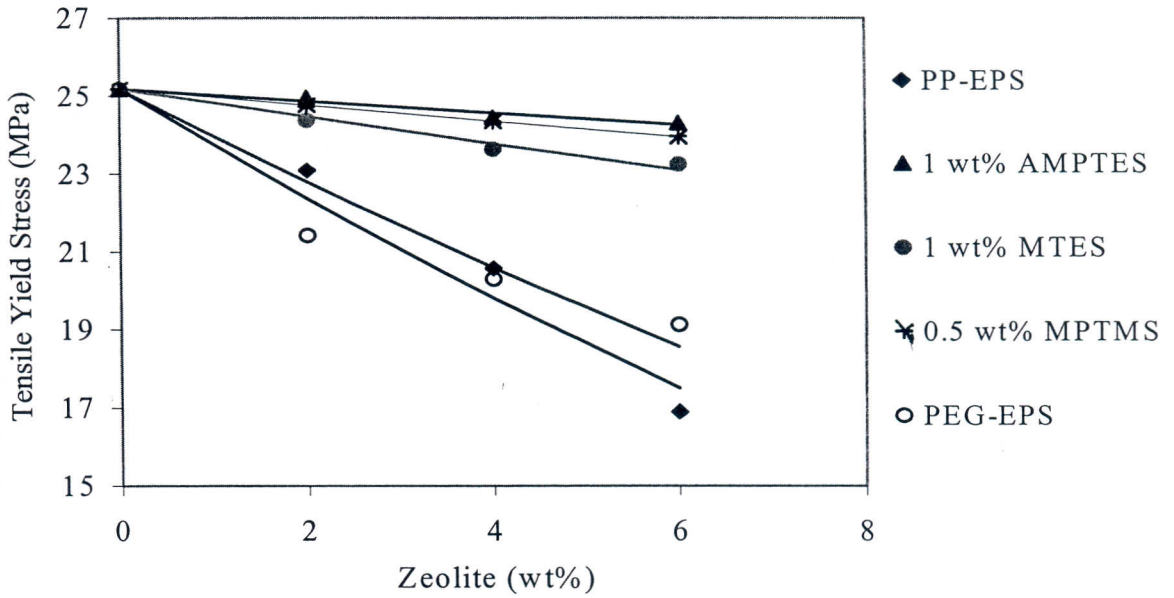


Figure 7.30. Effect of Surface Modifiers on the Experimental and Theoretical Dry Yield Stress Values of PP Composites with Respect to Zeolite Content and Pukanszky Model.

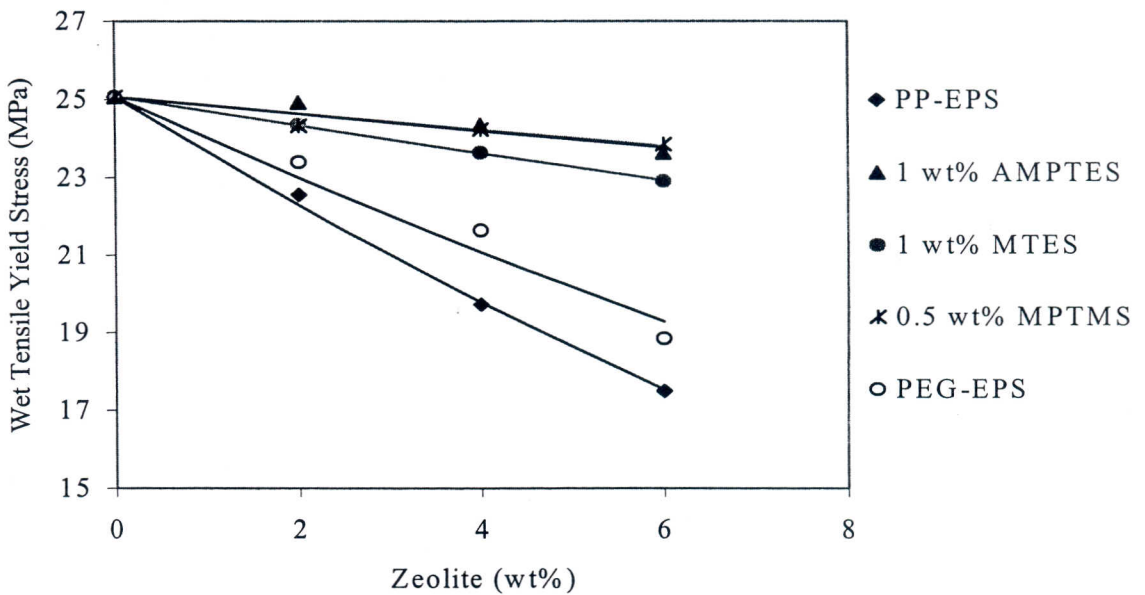


Figure 7.31. Effect of Surface Modifiers on the Experimental and Theoretical Wet Yield Stress Values of PP Composites with Respect to Zeolite Content and Pukanszky Model.

B parameter can be effectively used as a quantitative measure of the efficiency of surface treatments on each filler-matrix interface. Calculated B parameters in Pukanszky model for dry and wet yield stress of the composites are tabulated in Table A.5 in the Appendix. According to the dry yield stress of the composites, B values of the PP-EPS composites containing untreated and treated with PEG and silane coupling

agents at optimum silane concentrations: 1 wt% AMPTES, 1 wt% MTES and 0.5 wt% MPTMS were found as -9, -6.99, 2.15, 0.47 and 1.7 respectively. Also, B values of these composites were found as -8.8, -5.53, 1.67, 0.38, and 1.71 from the wet tensile test results respectively. Negative B values indicate the nonhomogeneous distribution of the zeolite particles in the composites. As seen in the table, AMPTES has the highest B value that shows again strongest strength of interaction compared to the others studied in this work. The maximum B value for AMPTES treated composites found as 2.15 in this study is in good agreement with the results of Demjen and coworkers (1997). The maximum B value was found as 2 for the PP composites containing AMPTES treated  $\text{CaCO}_3$  through eight different silane coupling agents and stearic acid by Demjen.

Nicholais and Narkis model was also used to compare the experimental data with this model. "a" value in the Nicholais and Narkis model known as adhesion parameter denotes a constant related to filler-matrix interaction and adhesion. Mean value of this constant "a" was calculated for dry and wet yield stress of PP containing untreated and treated zeolite composites at each silane concentration listed in Table A.6. in Appendix. The values for PP untreated and PEG treated zeolite composites were found as higher than 1.21. Since a value of "a"=1.21 represents the poor adhesion and the lower value of "a" than 1.21 reflects the better adhesion, the results indicate that the absence of adhesion between PP and untreated and PEG treated zeolites. However, the "a" values for PP containing silane treated zeolite composites except 2 wt% AMPTES, MPTMS and 0.5 and 2 wt% MTES were found as lower than 1.21. This result shows that surface treatment of zeolite with silane coupling agents increases the adhesion between zeolite and PP matrix due to the formation of a chemical bond between zeolite and PP matrix. The "a" values were found as 2.62, 0.32, 0.80 and 0.46 for the dry yield stress of PP composites containing untreated and treated zeolite with optimum coupling agent concentrations of; 1wt% AMPTES and MTES and 0.5 wt% MPTMS respectively. The "a" values for the wet yield stress of PP-zeolite composites are higher than those of the dry yield stress of PP composites due to the water effect in the interface between PP and zeolite. However, the a values of all silane treated composites were found as lower than 1.21. This indicates that silane treatment provides adhesion between PP and zeolite in the presence of water. The composites should be prepared at the optimum silane coupling agent concentration that is why in order to enhance the interaction between zeolite and PP. The increase in "a" values of composites containing 2 wt% silane treated zeolite may be explained by the formation of physisorbed layers on the surface of

zeolite with large amount of silane coupling agents which decreases the strength of interaction, hence “a” value increases.

Figure 7.32 shows the predictions of dry yield stress of PP composites containing 0.5 wt% MPTMS treated zeolite with respect to zeolite content. The experimental data were compared to Nicholais-Narkis and Pukanszky models. As seen in the figure, experimental and predicted yield stress values show a decreasing trend as the zeolite loading increases. Pukanszky model predicted the data well, and deviation of the theoretical values in Nicholais-Narkis model increased with an increase in zeolite loading. For that reason, the theoretical yield stress values of the composites given in Table A.9 and A.10 were predicted using Pukanszky model given in Equation 5.24.

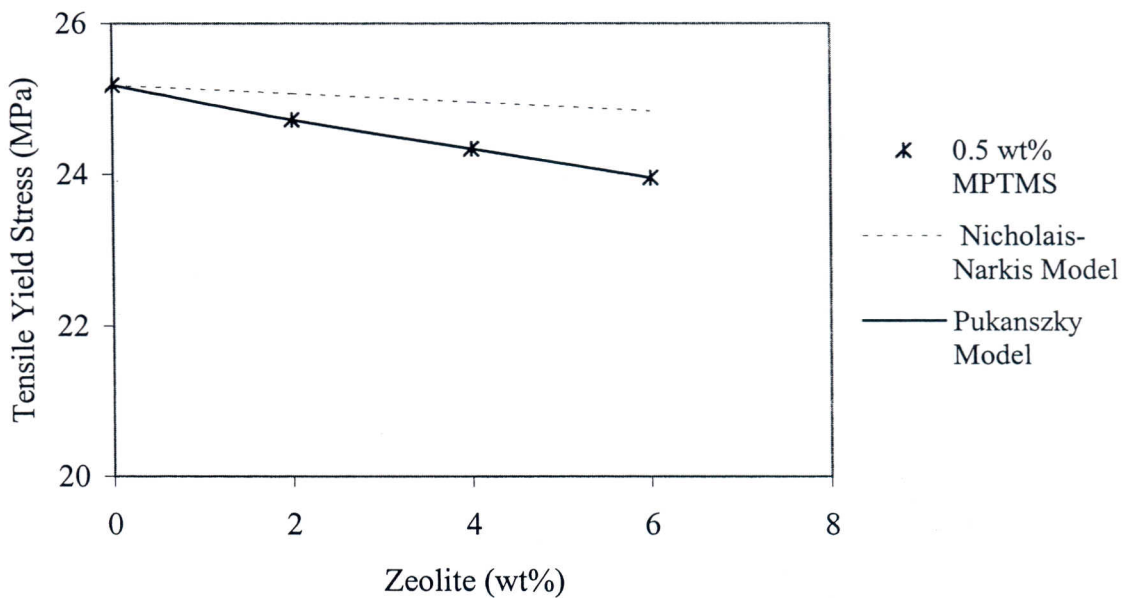


Figure 7.32. Experimental and Theoretical Dry Yield Stress Values of PP Composites Containing Treated Zeolite with 0.5 wt% MPTMS.

### 7.6.3. Tensile Stress at Break of PP-Zeolite Composites

The tensile stress at break of the composites gives information about the allowable load to composite failure and the final break. The tensile stress of the composites depends on its microstructure including the interfacial structure since load transfer and stress concentration between zeolite and PP matrix. The dry and wet tensile stress at break values of PP composites are given in Table A.3 and A.4. The dry tensile stress of PP, PP-DOP and PP-EPS composites are the same, and not slightly different

from wet values. It was observed that the tensile stress of the composites decreased with increasing in zeolite loading. The reduction in the tensile stress with an increase of filler content can be explained by the reduction in the effective matrix cross section and formation of voids in the matrix. The effect of surface treatment can be again seen better in Figures 7.33 and 7.34 where the composition dependence of tensile strength is shown for three different silane coupling agents.

Figure 7.33 and 7.34 show the dry and wet tensile stress at break of PP composites containing untreated and treated zeolite with PEG and silane coupling agents at optimum concentration with respect to zeolite content, respectively. The tensile stress of 6 wt% zeolite filled PP-DOP and PP-EPS composites have decreased by 33 and 37 % for dry samples and 35 and 39 % for wet samples when compared to the unfilled dry PP-DOP and PP-EPS matrix respectively. It was observed that efficiency of PEG is not good as silane coupling agents. The decrease in the dry and wet tensile stress of PP composites containing 6 wt% PEG treated zeolite was found as 20.7 and 29 % for PP-DOP and 29 and 36 % for PP-EPS respectively. Also, the decrease in the tensile stress of PP composites has been increased by silane coupling agents as in the tensile yield stress of the composites. The dry tensile stress of the composites containing 6 wt% treated zeolite with 1 wt% AMPTES and MTES and 0.5 wt% MPTMS decreased by 11, 15 and 14 % respectively compared to the dry tensile stress of unfilled PP-EPS matrix. As seen in Table A.3 and A.4 in Appendix, the composites treated with silanes results in higher tensile strengths as well as smaller elongation of the composites compared to the untreated and PEG treated ones.

Also, the decrease in wet tensile stress at break of these composites were found as 11.2, 18 and 17 % compared to the dry stress of unfilled PP-EPS matrix respectively. It is observed that there is no significant difference between wet and dry stress of composites treated with amino functional silane coupling agents. This result indicated that interfacial enhancement between zeolite and PP matrix was achieved by silane coupling agents.

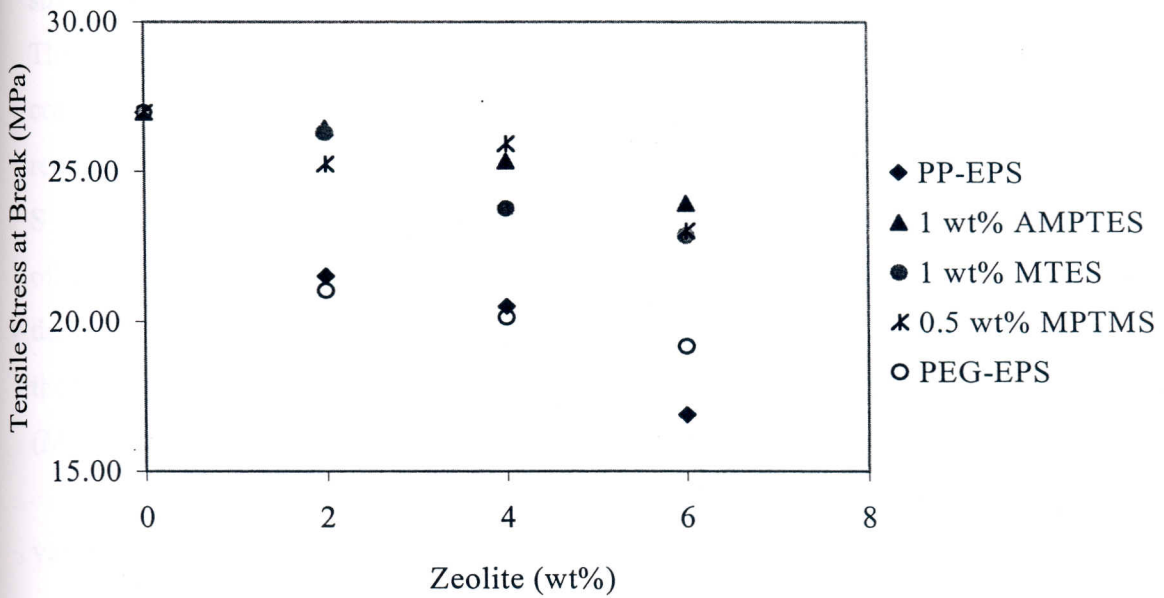


Figure 7.33. Dry Tensile Stress at Break of PP Composites with Respect to Zeolite Content.

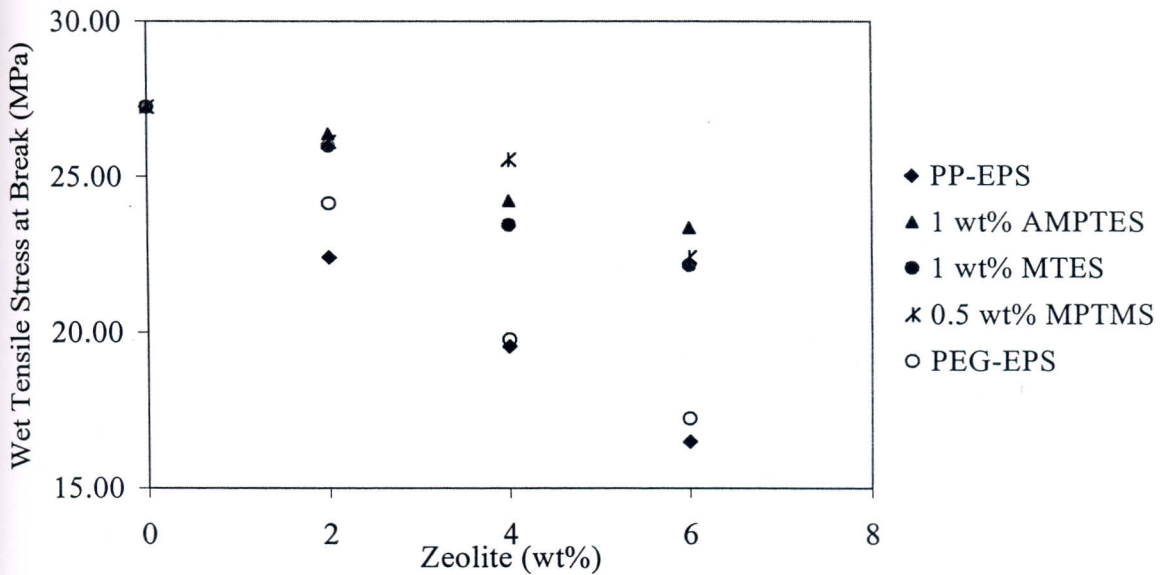


Figure 7.34. Wet Tensile Stress at Break of PP Composites with Respect to Zeolite Content.

The theoretical tensile stress at break values of the composites given in Table A.9 and A.10 were predicted using Nielsen model given in Equation 5.21. The parameter  $S$  in this model, known as stress concentration factor, describes the weakness in the structure of the composite. Calculated mean  $S$  values for each dry and wet yield

stress of PP containing untreated and treated zeolite composites are listed in Table A.7. The S values in dry and wet ultimate stress were determined as 0.78, 0.8 and 1 for PP containing untreated and PEG treated zeolite and 1 wt% AMPTES treated composites, respectively. S values increase with the treatment of the zeolite. As seen from the table, S values of amino functional and merkapto silane coupling agents are higher than that of the MTES. Approaching of S parameter to unity indicates that silane coupling agents decrease the stress concentration effect between zeolite and PP matrix. The decrease in the stress concentration leads to enhancement of adhesion between PP and zeolite (Maiti and Sharma, 1992).

Figure 7.35 shows the experimental and theoretical dry tensile stress at break values of PP composites containing 1 wt% AMPTES treated zeolite with respect to zeolite content. As seen in the figure, the tensile stress data fits Nielsen model well. Experimental and predicted tensile stress at break values show a decreasing trend as the zeolite loading increases.

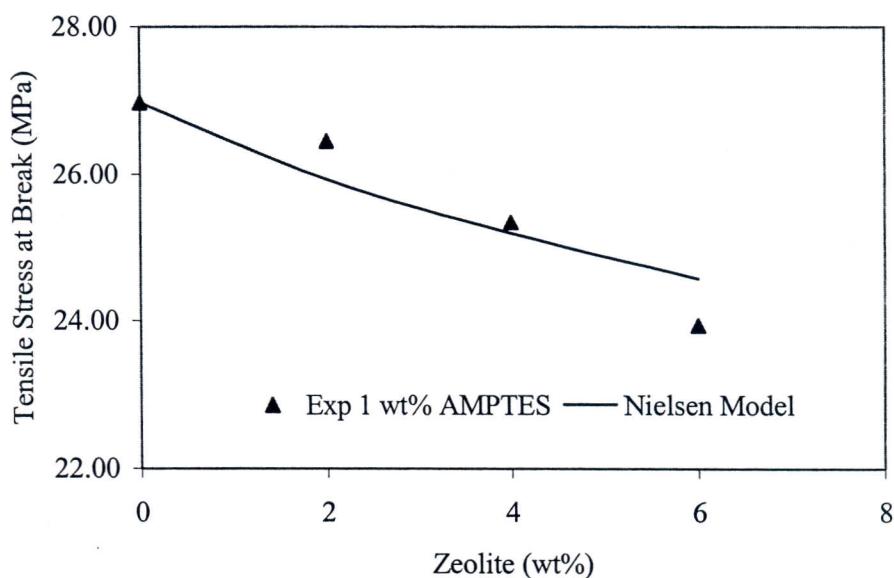


Figure 7.35. Experimental and Theoretical Dry Tensile Stress at Break Values of PP Composites Containing Treated Zeolite with 1 wt% AMPTES.

#### 7.6.4. Elongation at Break of PP- Zeolite Composites

Elongation at break values shown in Figure 7.36 and Table A.3 and A.4 increase with addition of plasticizer and decrease with addition of zeolite according to the dry and wet tensile test results. Elongation at break of PP increased by 4.5 and 4 % with

addition of DOP and EPS, respectively. As shown in the figure and Table A.3 and A.4, the elongation at break values for all composites containing 6 wt% zeolite show a sharp decrease. This decrease indicates that the composites become more brittle compared to the 4 % and 2 % zeolite loaded composites. In addition, the elongation at break values of the composites increase with the silane coupling agent treatment compared to the untreated case at the constant loading. According to the dry tensile test results, the decrease in the elongation values of composites containing 6 wt% zeolite were found as 98.7 % for untreated and PEG treated, 97, 96.7 and 94.4 % for 1 wt% AMPTES, MTES and 0.5 wt% MTES treated compared to the unfilled PP-EPS matrix respectively. The decrease in the elongation at break values of the composites in the presence of coupling agents was expected due to the enhancement of adhesion between PP and zeolite. However, the increase in the elongation values with silane coupling agents was observed due to the plasticizer effect of silane coupling agents.

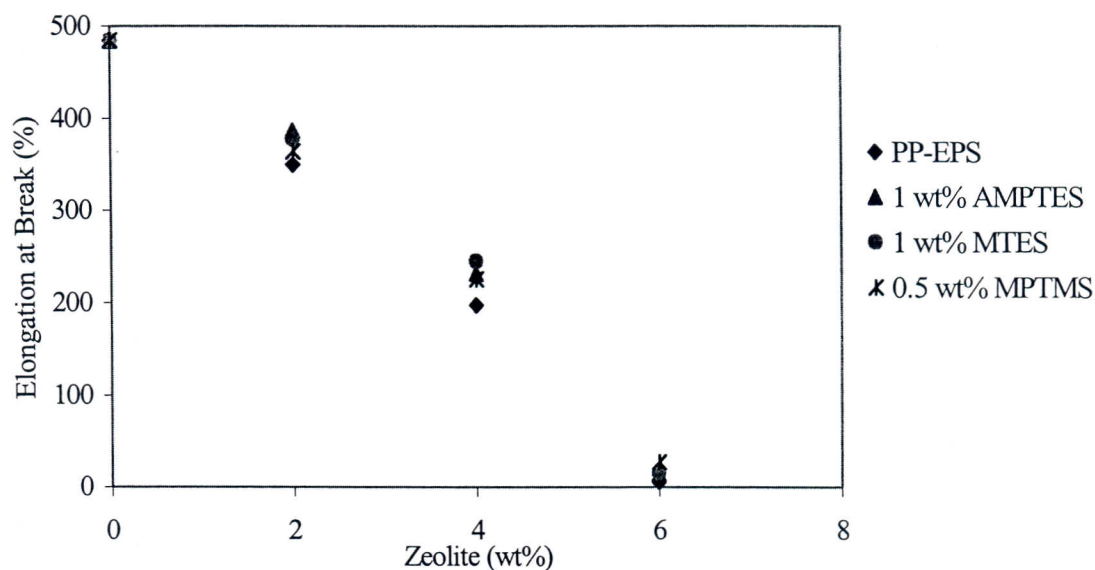


Figure 7.36. Effect of Silane Coupling Agents on the Elongation at Break of PP Composites with Respect to Zeolite Content.

Figure 7.37 shows the effect of silane coupling agents on the elongation at break of PP composites containing 4 wt% zeolite. As shown in the figure, elongation at break values increase with an increase in coupling agent concentration at constant zeolite loading. Deformability increases with increasing surface treatment concentration for all cases. This increase indicates that silane coupling agents provide a plasticizing/lubricating effect. Dry and wet elongation at break values of composites

given in Table A.3 and A.4 show some fluctuations due to the uneven distribution of zeolite particles in the matrix.

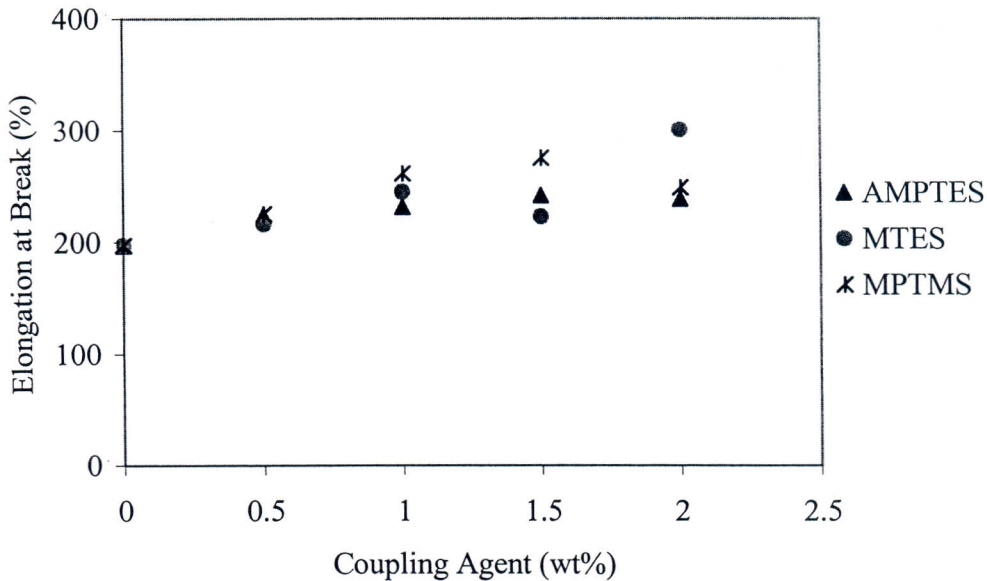


Figure 7.37. Effect of Silane Coupling Agents on the Elongation at Break of PP Composites Containing 4 wt% Zeolite.

Theoretical elongation at break values were predicted using Equation 5.27 to estimate the effect of filler-polymer interaction on elongation. In this model, interaction parameter value  $K$ , was calculated according to dry and wet tensile test results and given in Table A.8. As seen in the table, the mean  $K$  values in dry tensile test results were not significantly different than the values in wet tensile test results. It was observed that the mean  $K$  values determined for untreated zeolite filled composites are higher than those of the silane treated zeolite filled composites. The decrease in  $K$  parameter can be explained by the plasticizing effect of the coupling agent. The experimental and theoretical elongation at break values decrease with addition of zeolite according to the dry and wet tensile test results. Figure 7.38 shows the experimental and theoretical elongation at break values of the composites containing 1.5 wt% MPTMS treated zeolite with respect to the dry and wet tensile test results. Theoretical elongation values calculated from the mean  $K$  values underestimate the data for the composites containing 2 and 4 wt% zeolite and overestimate for the both dry and wet composites containing 6 wt% treated zeolite. As shown in the figure, and in Table A.3 and A.4, experimental results of composites containing 6 wt% zeolite show a large deviation

from predicted values. This deviation can be attributed to the nonhomogeneous distribution of zeolite in PP matrix as found in TGA.

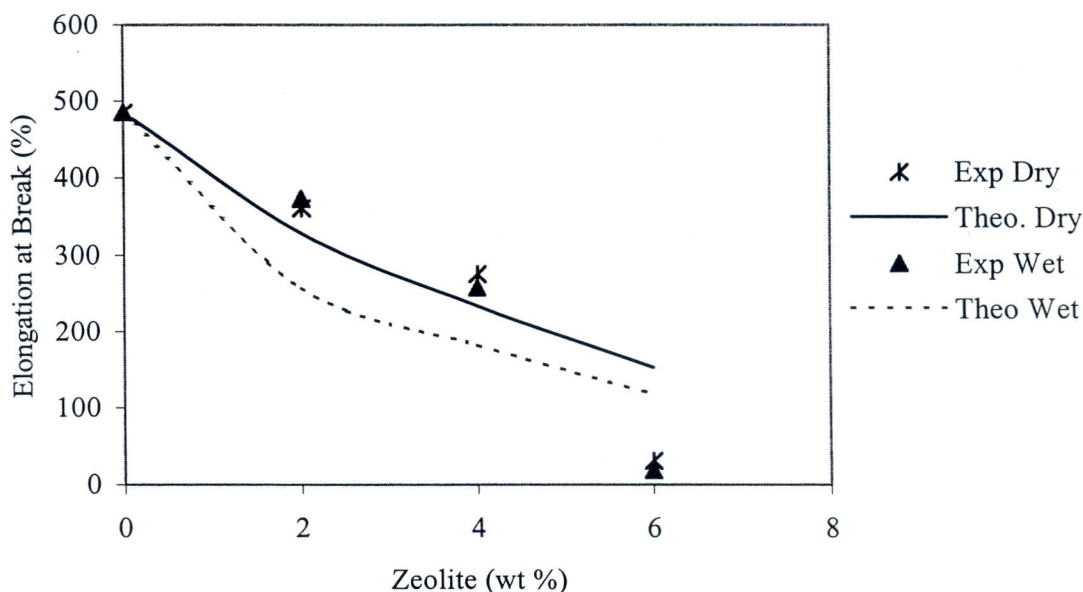


Figure 7.38. Experimental and Theoretical Elongation at Break Values of the Composites Containing Treated Zeolite with 1.5 wt% MPTMS.

## 7.7. Microstructure Analyses

### 7.7.1. Optical Microscopy

The surface treated zeolites and PP composite films containing 4 wt% untreated and treated zeolite with four surface modifiers (PEG, AMPTES, MTES and MPTMS) were examined by their optical micrographs.

Figure 7.39 shows the optical micrographs of untreated and treated zeolite with 3 wt% PEG. As shown in the figure, the formation of agglomerates was observed in both the untreated and PEG treated zeolite. The agglomeration of zeolite was not prevented by the surface modification of zeolite with PEG, a non-ionic surface modifier. The maximum agglomerate size of PEG treated zeolite was found as 19.2  $\mu\text{m}$ . Although it can not be seen a reduction in the size of agglomerates, Özmihçı (1999) observed a decrease in the agglomerations of the zeolite with 10 wt% PEG treatment. This contradictory result can be explained by the use of the different surface treatment methods or the amount of surface modifier. In this study, surface modification was

made by dry mixing of zeolite with PEG in the ball mill, however the surface modification was carried out by wet mixing of zeolite with PEG in ethanol solution by Özmihçi (1999).

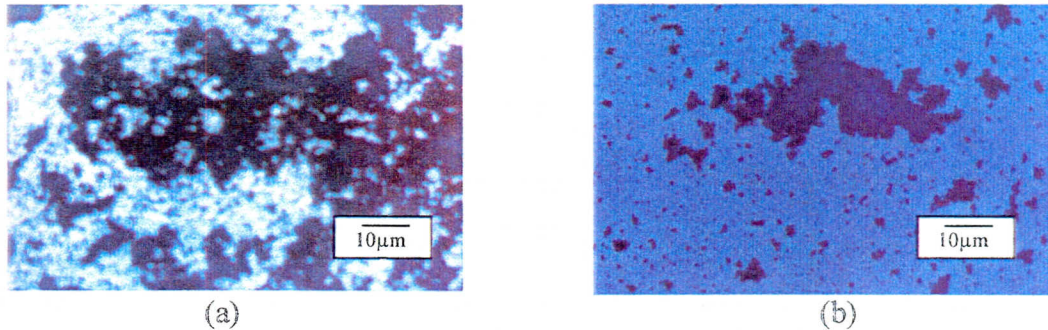


Figure 7.39. Optical Micrographs of 50 Times Magnified (a) Untreated Zeolite and (b) PEG Treated Zeolite.

Figure 7.40 shows the optical micrographs of treated zeolite with 1 wt% AMPTES, MTES and 0.5 wt% MPTMS. As shown in the figure, surface modification of zeolite with silane coupling agents reduces the agglomerate size of zeolite particles significantly. It was observed that amino functional and merkapto silane coupling agents (AMPTES and MPTMS) prevent the agglomeration of zeolite. The maximum agglomerate size of MTES treated zeolite was found as 11.4 µm.

The optical micrographs of PP composites consist of 4 wt% untreated and PEG treated zeolite are shown in Figure 7.41. As seen in the figure (a), as a result of agglomerations and voids, non-homogeneous distribution of zeolite particles in the PP-EPS matrix was observed. The presence of voids and agglomerates leads to the poor mechanical properties of the composites. The decrease in the size of agglomerations was observed by the use of PEG treated zeolite in the composite and also no void formation around filler was obtained.

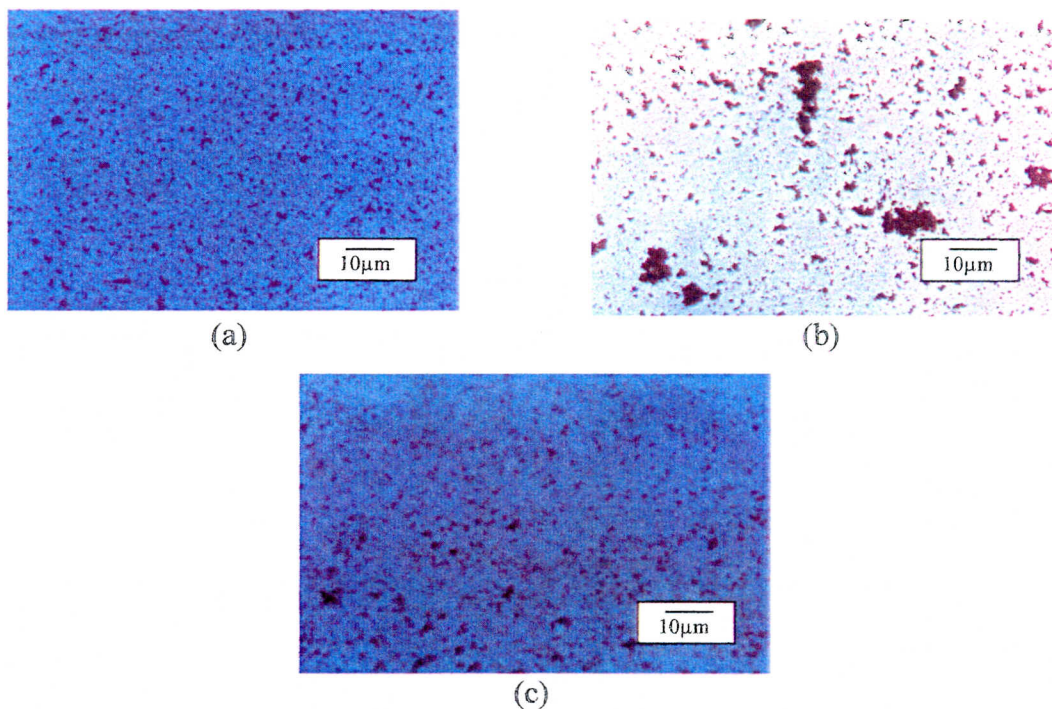


Figure 7.40. Optical Micrographs of 50 Times Magnified Treated Zeolite with (a) 1wt% AMPTES, (b) 1 wt% MTES and (c) 0.5 wt% MPTMS.

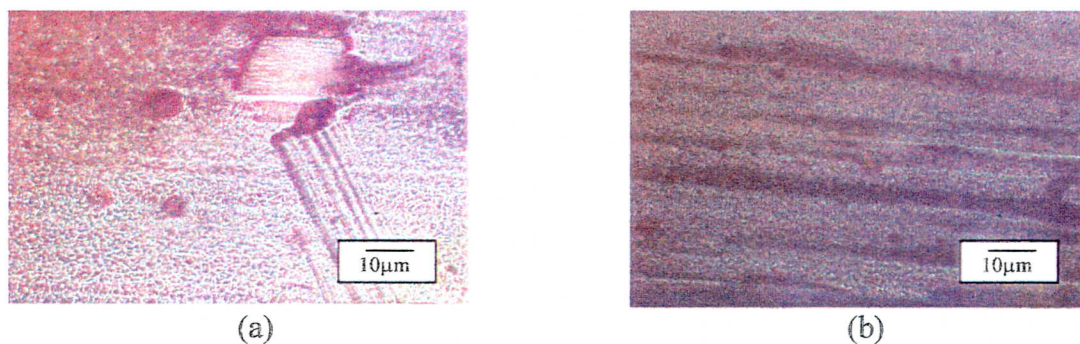


Figure 7.41. Optical Micrographs of 50 Times Magnified PP Composites Containing EPS and 4 wt% (a) Untreated Zeolite and (b) PEG Treated Zeolite

The optical micrographs of PP composites consist of 4 wt% treated zeolite with 1wt % AMPTES, 1wt % MTES and 0.5 wt% MPTMS are shown in Figure 7.42. Amino functional and merkapto silane coupling agents (AMP TES and MPTMS) show good dispersion of zeolite particles in the matrix. Particularly, good dispersion of zeolite particles in the matrix is required in order to obtain the composites having satisfactory mechanical properties. The agglomerate size of the treated zeolite with MTES in the matrix was lower than that of the treated zeolite with PEG. As seen in the figure, the

remarkable dispersion of zeolite was obtained with the amino functional silane coupling agent compared to the other surface modifiers used in this work.

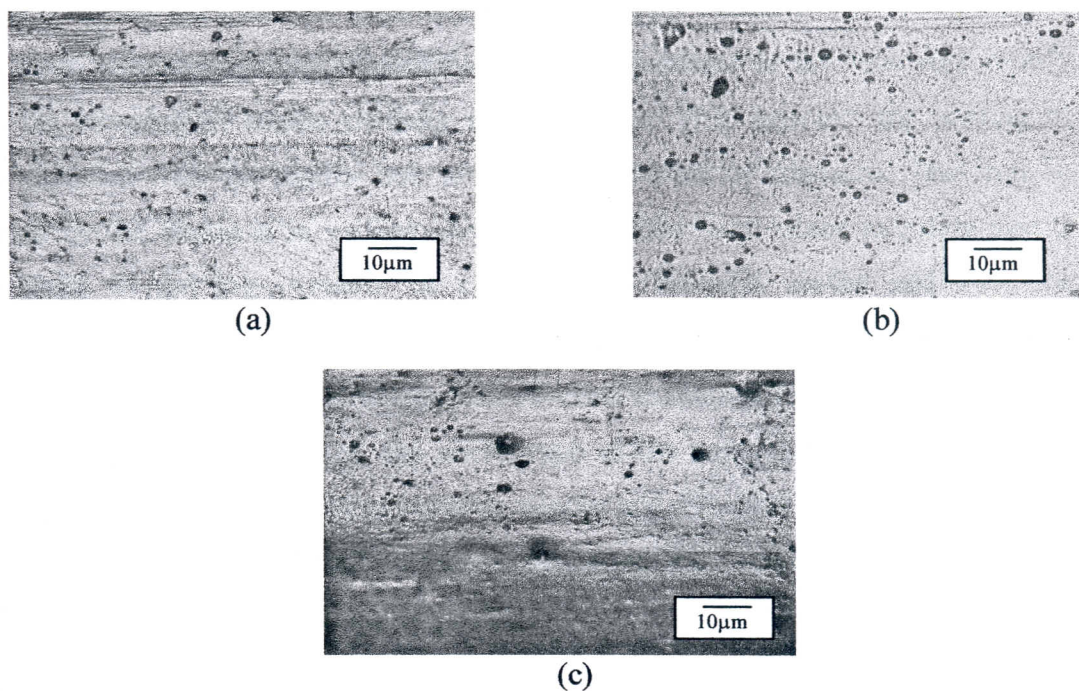


Figure 7.42. Optical Micrographs of 50 Times Magnified PP Composites Containing EPS and 4 wt% Treated Zeolite and (a) 1 wt% AMPTES, (b) 1 wt% MTES and (c) 0.5 wt% MPTMS

### 7.7.2. Scanning Electron Microscopy (SEM)

The effect of surface treatment on the interface between PP matrix and zeolite was studied by examining the fracture surfaces of tensile tested composites with SEM. Figure 7.43 shows the 5000 times magnified electron micrographs of fracture surfaces of PP composites containing 4 wt% untreated and treated zeolite with 1 wt% AMPTES, MTES and MPTMS. The weak interface between untreated zeolite and PP matrix can be clearly observed from the SEM micrograph in the Figure 7.43(a). The micrograph of PP composites containing 4 wt% untreated zeolite shows the clean surface of zeolite particles at the fracture surface. This indicates that PP can be separated completely from zeolite particles by breaking the interface due to the poor adhesion between zeolite and PP. The reason of poor adhesion between untreated zeolite and the polymer is the difference in surface free energy between zeolite and PP. Agglomeration of untreated zeolite particles in the matrix was also observed.

SEM micrograph of the composites containing 1 wt% AMPTES treated zeolite is significantly different from that of the composites containing untreated zeolite. The micrograph shows the enhanced modification of AMPTES treated composite's interface compared to the untreated zeolite composite. Zeolite particles do not seen very clearly due to the covering of zeolite particles by the matrix. This indicates the wetting of zeolite particles with the matrix due to the improvement of adhesion. This can be explained by the decrease in surface energy of the filler with silane coupling agents which leads to the improvement of compatibility between zeolite and PP. The improvement of adhesion between zeolite particles and PP led to the higher elastic moduli and yield strengths of the composites as found in section 7.6.

As seen in the figure (c), the micrograph of the composite containing MTES treated zeolite shows the adhesion between zeolite and PP. However it was observed that the agglomeration size of MTES treated zeolite particles was larger than that of the AMPTES and MPTMS treated zeolite particles.

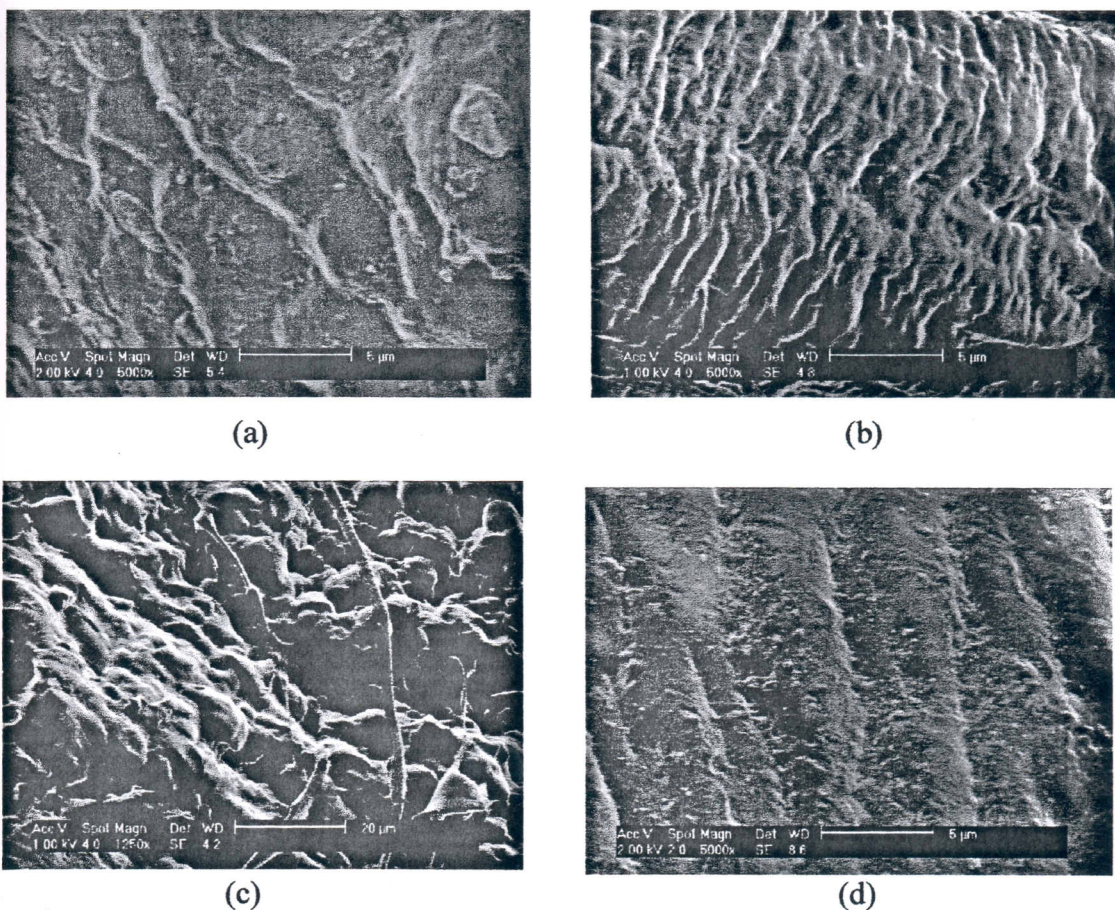


Figure 7.43. SEM Micrographs of the Fracture Surfaces of PP Composites Containing 4wt% (a) Untreated Zeolite and Treated Zeolite with (b) 1wt% AMPTES, (c) 1wt% MTES, and (d) 1 wt% MPTMS

The micrographs of the composites containing untreated and treated zeolite with merkapto silane coupling agents (MPTMS) indicate the brittle structure of the composite due to the observation of zeolite clearly. As seen in the SEM micrograph of the composite containing 1 wt% AMPTES, no particle agglomeration was observed in that of the composites containing 0.5 wt% MPTMS. The micrograph of the composites containing merkapto silane coupling agents (MPTMS) indicates that the filler dispersion is good and no void is present seen between the particles and the matrix. However, the micrograph of MPTMS treated composite show insufficient adhesion between zeolite particles and PP on the contrary to the mechanical tensile test results. The coupling agent layer in the PP-zeolite composites could not be seen since the magnification was not sufficient.

### 7.8. Density Measurements

Density measurements were performed by the displacement method using the Equation 6.2. Theoretical densities of the composites were calculated using equation below.

$$d_c = \frac{\sum M_i}{\sum (M_i / d_i)} \quad (7.1)$$

where

$d_c$ : theoretical density of composite

$M_i$ : mass of component i in the composite

$d_i$ : density of component i in the composite

$d_{zeolite} = 1.8 \text{ g/cm}^3$

$d_{PP} = 0.89 \text{ g/cm}^3$

$d_{DOP} = 0.981 \text{ g/cm}^3$

$d_{EPS} = 1.048 \text{ g/cm}^3$

All experimental and theoretical densities of the composites are listed in Table A.1. Figure 7.44 shows the experimental densities of the untreated and treated composites with PEG and silane coupling agents at optimum concentration as a function of zeolite content. Experimental densities were found as equal to 0.882 and 0.85 g/cm<sup>3</sup> for unfilled and filled 6 wt% untreated zeolite composite, respectively. As seen in the

figure, while experimental densities of the untreated composites decrease with increasing of zeolite loading, those of the treated composites increase with increasing of zeolite loading. This can be explained that surface treatment leads to the reduction in the voids around filler particles in the matrix by improvement of the interfacial adhesion between zeolite and PP.

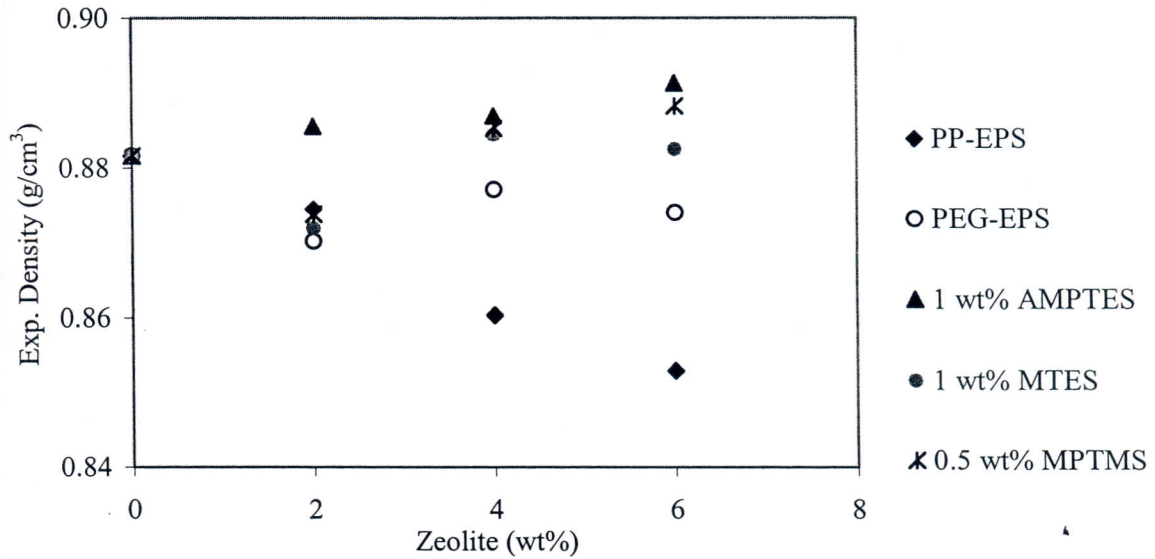


Figure 7.44. Effect of Surface Treatment on the Experimental Densities of PP Composites with Respect to Zeolite Content.

Experimental densities of the PP composites containing untreated zeolite are lower than the theoretical values. This can be explained by the presence of voids in the composites. Void fraction in the composite is an important parameter that leads to a poor of the mechanical properties of the composite. The void fractions in the composites were determined using Equation 7.2.

$$d_{c\text{exp}} = (1 - \varepsilon)d_{c\text{theo}} \quad (7.2)$$

where  $d_{c\text{exp}}$  and  $d_{c\text{theo}}$  are the experimental and the theoretical densities of the composite respectively, and  $\varepsilon$  denotes the void fraction in the composite.

Experimental densities of the composites consisting of treated zeolites are higher than those of the other composites. It is well known that higher crystallinity in the PP composites causes higher density of the composites. In addition, there are some fluctuations on the experimental densities because of uneven distribution of the

composites. Figure 7.45 shows the effect of surface treatment on the void fractions of PP composites at a constant zeolite loading of 6wt%. As seen in Figure 7.45, the optimum amount of coupling agents was found as 1 wt%, which shows the lowest void fractions among the others. The void fractions in the composites consisting of untreated and treated zeolite with PEG, 1wt% AMPTES, 1wt% MPTMS and 1wt% MTES were found as 0.076, 0.054, 0.035, 0.044 and 0.038 respectively. Void fractions of PP composites consisting of silane treated zeolite were lower than that of the others and the lowest void fraction value was found at 1 wt% AMPTES concentration. In addition, the void fractions in the composites are related to water sorption of the composites. Water sorption of the composites consisting of silane treated zeolite decreased due to the decreasing of void fraction of the composites as seen in Table A.1. These results also indicated that the surface treatment of zeolite with silane coupling agents increased the adhesion between polypropylene matrix and zeolite particles.

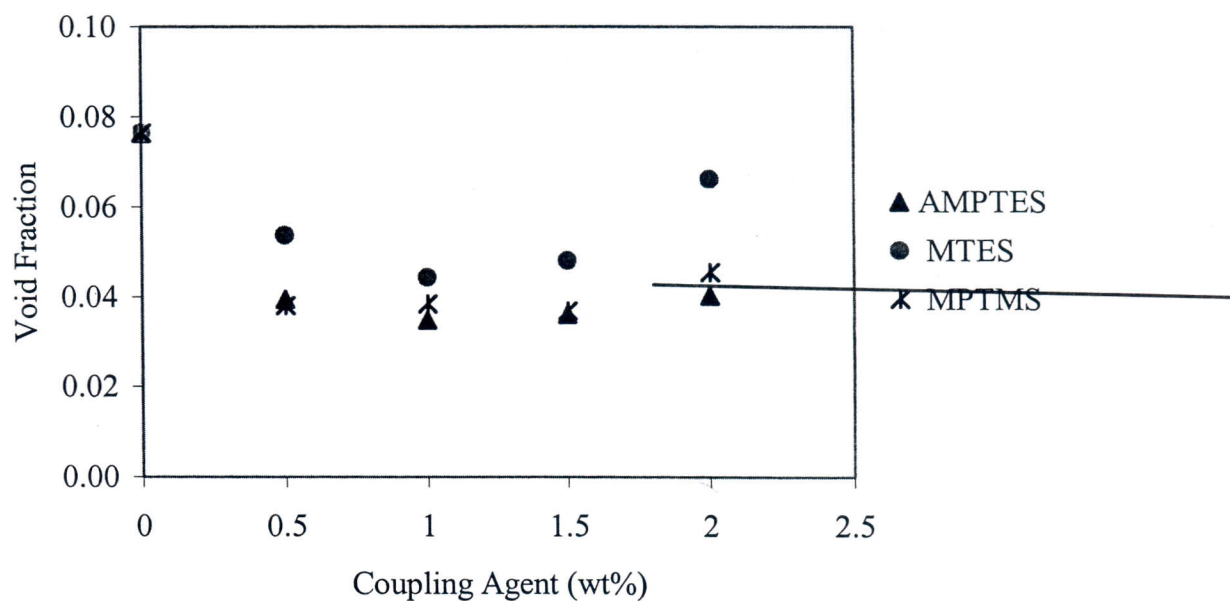


Figure 7.45. Effect of Silane Coupling Agents on the Void Fractions in the PP-Zeolite Composites.

## Chapter 8

### CONCLUSIONS AND RECOMMENDATIONS

In this study, the interfacial properties of a hydrophobic organic material, polypropylene, and a hydrophilic inorganic material, natural zeolite, were investigated and surface modification of zeolite with PEG and silane coupling agents was carried out to improve the compatibility of these two dissimilar materials.

Contact angle measurements and FTIR analyses of the silane treated zeolite samples and water sorption results of the PP-zeolite composites indicated that silane coupling agents increased the hydrophobization of zeolite significantly. The increase in contact angles of the treated zeolites was obtained for all silane coupling agents, but the change in contact angles was observed to be strongly dependent on the silane type and concentration. According to the contact angle measurements, 0.5 wt% MPTMS was found as the most effective coupling agent for hydrophobization of zeolite.

Water sorption of PP-zeolite composites was reduced by silane treatment significantly, since silane coupling agents provide a water-resistant bond between the zeolite and the polymer matrix. It was found that there was no significant difference between water sorption of PP composites consisting of treated zeolite with 1 wt% AMPTES and 0.5 wt% MPTMS. However, surface treatment of zeolites with amino functional silane 1 wt% provides maximum hydrophobization in the PP-zeolite composites.

FTIR spectra of untreated and silane treated zeolites also showed the hydrophobization of the zeolite samples. The peak intensities of H<sub>2</sub>O bending and OH stretch vibrations at 1620 cm<sup>-1</sup>, 3700 cm<sup>-1</sup> and 3400 cm<sup>-1</sup> bands decrease with silane treatment. FTIR spectra indicated that the maximum hydrophobization of zeolite surface was obtained by treating zeolite with 1 wt% amino functional silane coupling agents.

Thermal characterization studies pointed out that the addition of zeolite and silane treatment did not change the melting and degradation temperature of the composites, however it increased the crystallinity and crystallization temperature of the composites. Crystallization kinetics described by Avrami and Kissinger methods indicated that the composites containing silane treated zeolite had higher rate of crystallization with temperature compared to the composites containing untreated zeolite. However, some fluctuations were found in the thermal analysis results. This

could be due to the non-homogeneous distribution of the zeolite and plasticizer in the composite.

Although zeolite used as a filler improved stiffness of PP, untreated zeolite reduces the mechanical properties such as tensile yield stress and tensile stress at break values of the composites due to the weak adhesion between the zeolite particles and PP matrix. PEG and silane coupling agents were used to enhance the adhesion between zeolite and PP interface thereby improving the mechanical properties of the composites. PP containing PEG treated zeolite showed a significant weakness in the mechanical properties of the composites due to the absence of adhesion between PP and PEG treated zeolite. Surface treatment of zeolite with silanes improved the mechanical properties of the PP composites. According to the dry and wet tensile test results, the maximum improvement in the mechanical properties of the composites was observed in the PP composites containing 1 wt% AMPTES treated zeolite. Young's modulus, yield stress, tensile stress at break and elongation at break values of PP composite containing 6 wt% treated zeolite with 1 wt% AMPTES were found as 24.5, 43.8, 34.3 and 145 % higher than those of the 6 wt % untreated zeolite filled composites.

Pukanszky model, Nicholais and Narkis model, Nielsen model and the model derived by Mitsuishi et al (1985) were used to evaluate interfacial interactions and adhesion between PP and zeolite particles and to predict the experimental tensile test data for PP-zeolite composites. The improvement in adhesion between zeolite and PP with silane coupling agents was confirmed by these models.

Scanning Electron Microscopy studies showed that the adhesion between 1 wt% AMPTES treated zeolite and PP is better than that of the other composites. No agglomerations were observed in the optical micrographs of silane treated zeolite samples. This indicated that the formation of an organofunctional layer on zeolite led to its deagglomeration because of the reaction of the coupling agent with zeolite.

Consequently, the water sorption and mechanical test results, scanning electron micrographs and optical micrographs of the composites indicated that PP composites containing 1 wt% AMPTES treated zeolite improved compatibility and interfacial adhesion between zeolite particles and PP matrix.

According to the mechanical results of PP composites containing untreated and PEG treated zeolite and plasticizers (DOP and EPS), the composites containing DOP provided better mechanical properties than those of the composites containing EPS.

However, EPS was selected as an appropriate plasticizers due to the carcinogen effect of DOP and low water sorption values of PP-zeolite composites containing EPS.

In the future studies, ethylene-propylene-diene rubber (EPDM) and functionalized PP such as maleic anhydride grafted PP (MA-PP) can be used instead of EPS to provide the better improvement in the interfacial and mechanical properties of PP composites. Additionally, the homogeneous distribution of zeolite in PP matrix could be obtained using the plastograph (torque rheometer) or twin screw extruder.

## REFERENCES

1. Acosto J.L., Morales E., Ojeda M.C., Linares A., The Effect of Interfacial Adhesion and Morphology on the Mechanical Properties of Polypropylene Composites Containing Different Acid Surface Treated Sepiolites, *Journal of Materials Science*, 21, 1986, 725-728.
2. Agassant J.F., Avenas P., Sergent J.Ph., Carreau P.J., Polymer Processing Principles and Modeling, Hanser, New York, 1986.
3. Akdeniz Y., Cation Exchange in Zeolites, Structure Modification by Using Microwave, M.S. Thesis, İzmir Institute of Technology, Materials Science and Engineering, İzmir, 1999.
4. Akovalı G., The Interfacial Interactions in Polymeric Composites, Kluwer, 1993.
5. Akovalı G., Akman M.A., Mechanical Properties of Plasma Surface-Modified Calcium Carbonate Polypropylene Composites, *Polymer International*, 42, 1997, 195-202.
6. Akovalı G., Dilsiz N., Studies on the Modification of Interphase/Interfaces by Use of Plasma in Certain Polymer Composite Systems, *Polymer Engineering Science*, 36(8), 1996, 1081-1086.
7. Alonso M., Velasco J.I., Saja J.A., Constrained Crystallization and Activity of Filler in Surface Modified Talc Polypropylene Composites, *Eur. Polymer Journal*, 33(3), 1997, 255-262.
8. Bertalan G., Marosi G., Anna P., Ravadits I., Csontos I., Toth A., Role of Interface Modification in Filled and Flame-retarded Polymer Systems, *Solid State Ionics*, 141-142, 2001, 211-215.
9. Berry M.B., Libby B.E., Rose K., Haas K.H., Thompson R.W., Incorporation of Zeolites into Composite Matrices, *Microporous and Mesoporous Materials*, 39, 2000, 205-217.
10. Bledzki A.K., Gassan J., Composites Reinforced with Cellulose Based Fibres, *Prog. Polymer Science*, 24, 1999, 221-274.
11. Boluk M.Y., Schreiber H.P., Interfacial Interactions and Mechanical Properties of Filled Polymers, *Journal of Applied Polymer Science*, 40, 1990, 1783-1794.
12. Breck D.W., Zeolite Molecular Sieve: Structure, Chemistry and Use, by John Wiley and Sons, 1974, Newyork.

3. Chiang W.Y., Yang W.D., Polypropylene Composites I. Studies of the Effect of Grafting of Acrylic Acid and Silane Coupling Agent on the Performance of Polypropylene Mica Composites, *Journal of Applied Polymer Science*, 35, 1988, 807-823.
4. Colthup N.B., Daly L.H., Wiberley S.E., Introduction to Infrared and Raman Spectroscopy, Academic Press, 1990.
5. Demjen Z., Pukansky B., Jr J.N., Possible Coupling Reactions of Functional Silanes and Polypropylene, *Polymer*, 40, 1999, 1763-1773.
6. Demjen Z., Pukansky B., Nagy J., Evaluation of Interfacial Interaction in Polypropylene Surface Treated CaCO<sub>3</sub> Composites, *Composites Part A*, 29A, 1998, 323-329.
7. Dibenedetto, A.T., Tailoring of Interfaces in Glass Fiber Reinforced Polymer Composites: a review, *Material Science and Engineering A*, 302, 2001, 74-82.
8. Diez-Gutierrez S., Rodriguez-Perez M.A., De Saja J.A., Velasco J.I, Dynamic Mechanical Analysis of Injection Moulded Discs of Polypropylene and Untreated and Silane Treated Talc Filled Polypropylene Composites, *Polymer*, 40, 1999, 5345-5353.
9. Domka L., Modification Estimate of Kaolin, Chalk, and Precipitated Calcium Carbonate as Plastomer and Elastomer Fillers, *Colloid and Polymer Science*, 272, 1994, 1190-1202.
10. Dwyer J., Dyer A., Zeolites and introduction, *Chemistry and Industry*, 2, 1984, 237-240.
11. Dyer A., Uses of natural zeolites, *Chemistry and Industry*, 2, 1984, 241-245.
12. Fuad M.Y., Mustafah J., Mansor M.S., Ishak Z.A.M., Omar A.K.M., Thermal Properties of Polypropylene/Rice Husk Ash Composites, *Polymer International*, 38, 1995, 33-43.
13. Fuentes G.R., Ruiz-Salvador A.R., Mir M., Picazo O., Quintana G., Delgado M., Thermal and Cation Influence on IR Vibrations of Modified Natural Clinoptilolite, Microporous and Mesoporous Materials, 20, 1998.
14. Galli P., Danesi S., Simonazzi T., Polypropylene Based Polymer Blends: Fields of Application and New Trends, *Polymer Engineering and Science*, Mid-June, 24(8), 1984, 544-554.
15. Goryainov S.V., Stolpovskaya V.N., Likhacheva A.Y., Belitsky I.A., Fursenko B.A., Quantitative Determination of Clinoptilolite and Heulandite in Tuffaceous Deposits by Infrared Spectroscopy, Natural Zeolites, Mumpton F.A., 1995.
16. Gottardi G., Galli E., Minerals, Rocks, Natural Zeolites, by Goresy and Heidelberg Springer-Verlag, 1985, Berlin.
17. Grulke E.A., Polymer Process Engineering, Prentice Hall, New Jersey, 1994.

28. Gutowski W., Effect of Fibre-Matrix Adhesion on Mechanical Properties of Composites, Controlled Interphases in Composite Materials (ed H. Ishida), Elsevier, 1990, Newyork, 505-520.
29. Hatakeyama T., Quinn F.X., Thermal Analysis – Fundamentals and Applications to Polymer Science, Japan, 1994.
30. Hornsby P.R., Watson C.L., Interfacial Modification of Polypropylene Composites Filled with Magnesium Hydroxide, *Journal of Material Science*, 30, 1995, 5347-5355.
31. Hunt B.J., James M.I., Polymer Characterization, Blackie A & P, Glasgow, 1993.
32. Jancar J., Dibenedetto A.T., Effect of Morphology on the Behaviour of Ternary Composites of Polypropylene with Inorganic Fillers and Elastomer Inclusions Part I Tensile Yield Strength, *Journal of Material Science*, 30, 1995, 1601-1608.
33. Jancar J., Dibenedetto A.T., The Mechanical Properties of Ternary Composites of Polypropylene with Inorganic Fillers and Elastomer Inclusions, *Journal of Material Science*, 29, 1994, 4651-4658.
34. Jarvela P.A., Jarvela P.K., Multicomponent Compounding of Polypropylene, *Journal of Material Science*, 31, 1996, 3853-3860.
35. Jesionowski T., Krysztafkiewicz A., Comparison of the Techniques Used to Modify Amorphous Hydrated Silicas, *Journal of Non-Crystalline Solids*, 277, 2000, 45-57.
36. Jo H., Blum F. D., Characterization of the Interface in Polymer- Silica Composites Containing an Acrylic Silane Coupling Agent, *Chem. Materials*, 11, 1999, 2548-2553.
37. Karger-Kocsis, J., Polypropylene Structure, Blends and Composites by Chapman and Hall, V.3, 1995, Cambridge.
38. Khunova, V., Sain, M.M., Optimization of Mechanical Strength of Reinforced Composites 2. Reactive Bismaleimide-Modified Polypropylene Composites Filled with Talc and Zeolite, *Die Angewandte Makromolekulare Chemie*, 225, (1995), 11-20.
39. Kownlton G. D., White T. D., McKague H.L., Thermal Study of Types of Water Associated with Clinoptilolite, *Clays and Clay Minerals*, 29(5), 1981, 403-411.
40. Koh S.K., Cho J.S., Yom S.S., Beah Y.W., Hydrophilic Surface Formation on Polymers and its Applications, *Current Applied Physics*, 1, 2001, 133-138.
41. Koltuksuz G., Removal of Hydrocarbons From Wastewaters, M.S. Thesis, İzmir Institute of Technology, Environmental Engineering, Izmir, 2002.
42. Lee J.Y., Lee S.H., Kim S.W., Surface Tension of Silane Treated Natural Zeolite, *Material Chemistry and Physics*, 63, 2000, 251-255.

3. Liauv C.M., Filler Surface Modification with Organic Acids, *Plastics Additives & Compounding*, December, 2000, 26-29.
4. Lowell S., Shields J.E., Powder Surface Area and Porosity, 3<sup>rd</sup> edition, Chapman & Hall, 1991.
5. Maiti S.N., Sharma K.K., Studies on Polypropylene Composites Filled with Talc Particles Part I Mechanical Properties, *Journal of Material Science*, 27, 1992, 4605-4613.
6. Mareri P., Bastide S., Binda N., Crespy A., Mechanical Behaviour of Polypropylene Composites Containing Fine Mineral Filler: Effect of Filler Surface Treatment, *Composites Science and Technology*, 58, 1998, 747-752.
7. Mascia L., Thermoplastics Materials Engineering , 2<sup>nd</sup> edition, Elsevier Science, Newyork, 1989.
8. Mucha M., Marszalek J., Fidrych A., Crystallization of Isotactic Polypropylene Containing Carbon Black as a Filler, *Polymer*, 41, 2000, 4137-4142.
9. Ogasawara T., Yoshino A., Okabayashi H., O'Connor C.J., Polymerization Process of the Silane Coupling Agent 3-aminopropyltriethoxy silane- HNMR Spectra and Kinetics of Ethanol Release, *Colloids and Surfaces A: Physicochemical and Engineering Aspects*, 180, 2001, 317-322.
0. Özmiççi F., Polypropylene-Natural Zeolite Composite Films, M.S. Thesis, İzmir Institute of Technology, Chemical Engineering, İzmir, 1999.
1. Palaban T. R., Thermodynamics of ion exchange between clinoptilolite and aqueous solutions of  $\text{Na}^+/\text{K}^+$  and  $\text{Na}^+/\text{Ca}^{+2}$ , *Geochimica et Cosmochimica Acta*, 58(21), 1994, 4573-4590.
2. Parker A.A., A Technical Review of Organosilanes and Adhesion, <http://aaparkerconsulting.home.attt.net>.
3. Pehlivan H., Preparation and Characterization of Polypropylene Based Composite Films, M.S. Thesis, İzmir Institute of Technology, Chemical Engineering, İzmir, 2001.
4. Plueddemann E.P., Silane Coupling Agents, 2<sup>nd</sup> edition, Plenum Press, New York, 1992.
5. Progelhof R., Throne J., Polymer Engineering Principles, Properties, Processes, and Tests for Design, Hanser Publishers, 1993.
6. Pukanszky B., Tudos F., The Possible Mechanisms of Polymer-Filler Interaction in Polypropylene- $\text{CaCO}_3$  Composites, *Journal of Material Science Letters* 8, 1989, 1040-1042.
7. Rao K.H., Forssberg K.S.E., Forsling W., Interfacial Interactions and Mechanical Properties of Mineral Filled Polymer Composites: Wollastonite in PMMA Polymer

- Matrix, Colloids and Surfaces A: Physicochemical and Engineering Aspects, 133, 1998, 107-117.
58. Schaefer K.U., Theisen A., Hess M., Kosfeld R., Properties of the Interphase in Ternary Polymer Composites, *Polymer Engineering and Science*, 33 (16), 1993, 1009-1021.
59. Schnabel W., Polymer Degradation Principles and Practical Applications, Hanser International, 1981.
60. Schreiber H.P., 'Aspects of Components Interactions in Polymer Systems', The Interfacial Interactions in Polymeric Composites, Akovalı G., Kluwer, 1993.
61. Sibilıa J.P., A Guide to Materials Characterization and Chemical Analysis, Newyork, 1988.
62. Tang L. G., Kardos J.L., A Review of Methods for Improving the Interfacial Adhesion Between Carbon Fiber and Polymer Matrix, *Polymer Composites*, February, 18(1), 1997, 100-113.
63. Tjong S.C., Li R.K.Y., Cheung T., Mechanical Behavior of CaCO<sub>3</sub> Particulate-Filled  $\beta$ -crystalline Phase Polypropylene Composites, *Polymer Engineering and Science*, January, 37(1), 1997, 166-172.
64. Todd D.B., Improving Incorporation of Fillers in Plastics. A Special Report, *Advances in Polymer Technology*, 19(1), 2000, 54-64.
65. Ulutan S., Balköse D., Interfacial Enhancement of Flexible PVC-Silica Composites by Silane Coupling Agents, *Composite Interfaces*, 4(4), 1997, 223-237.
66. Vasant E.F., Pore Size Engineering in Zeolites, John Wiley & Sons, England, 1990.
67. Wang Y., Wang J.J., Shear Yield Behaviour of Calcium Carbonate- Filled Polypropylene, *Polymer Engineering and Science*, January, 39(1), 1999, 190-197.
68. Whelan A., Craft J.L., Developments in Plastics Technology-2, Elsevier Science, 1985.
69. Wightman J.P., "Reinforcing Fibers for Composites", The Interfacial Interactions in Polymeric Composites, Akovalı G., Kluwer, 1993.
70. Xanthos M., Interfacial Agents for Multiphase Polymer Systems: Recent Advances, *Polymer Engineering and Science*, Mid-November, 28(21), 1988, 1392-1399.
71. Xavier S.F., Schultz J.M., Friedrich K., Fracturepropagation in Particulate -filled Polypropylene Composites Part 3 Influence of Mica Surface Treatments, *Journal of Material Science*, 25, 1990, 2428-2432.

## APPENDIX

Table A.1. Density and Water Sorption Results of the PP –Zeolite Composites.

Plasticizer	Surface Modifier	Amount of Surface Modifier (wt%)	Zeolite (wt%)	Amount of water sorption (wt%)	Exp. Density (g/cm <sup>3</sup> )	Theo. Density (g/cm <sup>3</sup> )	Void Fraction
-	-	-	-	0.033	0.87	0.89	0.03
DOP			-	0.038	0.88	0.89	0.01
			2	0.052	0.77	0.90	0.15
			4	0.184	0.81	0.91	0.11
			6	0.202	0.74	0.92	0.20
	PEG	3	2	0.083	0.83	0.90	0.08
			4	0.176	0.81	0.91	0.11
			6	0.267	0.81	0.92	0.12
EPS			-	0.033	0.88	0.90	0.02
			2	0.096	0.87	0.91	0.03
			4	0.129	0.86	0.91	0.06
			6	0.149	0.85	0.92	0.08
	PEG	3	2	0.048	0.87	0.91	0.04
			4	0.162	0.88	0.91	0.04
			6	0.174	0.87	0.92	0.05
EPS	AMPTES	0.5	2	0.042	0.88	0.91	0.03
			4	0.041	0.88	0.91	0.03
			6	0.049	0.89	0.92	0.04
		1	2	0.039	0.89	0.91	0.02
			4	0.046	0.89	0.91	0.03
			6	0.048	0.89	0.92	0.03
		1.5	2	0.04	0.90	0.91	0.01
			4	0.041	0.89	0.91	0.02
			6	0.05	0.89	0.92	0.04
		2	2	0.045	0.88	0.91	0.02
			4	0.05	0.90	0.91	0.02
			6	0.052	0.89	0.92	0.04
EPS	MTES	0.5	2	0.043	0.88	0.91	0.03
			4	0.061	0.92	0.91	0.00
			6	0.069	0.87	0.92	0.05
		1	2	0.051	0.87	0.91	0.04
			4	0.087	0.88	0.91	0.03
			6	0.095	0.88	0.92	0.04
		1.5	2	0.044	0.87	0.91	0.04
			4	0.046	0.88	0.91	0.04
			6	0.094	0.88	0.92	0.05
		2	2	0.035	0.89	0.91	0.02
			4	0.052	0.89	0.91	0.03
			6	0.069	0.86	0.92	0.07

Plasticizer	Surface Modifier	Amount of Surface Modifier (wt%)	Zeolite (wt%)	Amount of water sorption (wt%)	Exp. Density (g/cm <sup>3</sup> )	Theo. Density (g/cm <sup>3</sup> )	Void Fraction
EPS	MPTMS	0.5	2	0.038	0.87	0.91	0.04
			4	0.045	0.89	0.91	0.03
			6	0.057	0.89	0.92	0.04
		1	2	0.040	0.88	0.91	0.03
			4	0.04	0.88	0.91	0.03
			6	0.054	0.89	0.92	0.04
		1.5	2	0.035	0.91	0.91	0.00
			4	0.050	0.89	0.91	0.03
			6	0.056	0.89	0.92	0.04
		2	2	0.046	0.88	0.91	0.02
			4	0.053	0.88	0.91	0.03
			6	0.056	0.88	0.92	0.05

Table A.2. Contact Angle Measurements.

Surface Modifier	Amount of Surface Modifier (wt%)	I. Run	II. Run	III. Run	IV. Run	V. Run	Mean Contact Angle (°)	Standart Deviation
-	-	0	0	0	0	0	0	0
AMPTES	0.5	30	40	30	35	30	33	1.79
AMPTES	1	40	40	35	40	40	39	0.89
AMPTES	1.5	30	35	30	36	40	34.2	1.71
AMPTES	2	32	30	30	30	30	30.4	0.36
MTES	0.5	30	25	25	25	30	27	1.10
MTES	1	40	38	25	25	25	30.6	3.08
MTES	1.5	40	38	38	35	35	37.2	0.87
MTES	2	25	30	30	30	35	30	1.41
MPTMS	0.5	90	90	90	90	90	90	0
MPTMS	1	85	85	85	85	85	85	0
MPTMS	1.5	78	78	78	78	79	78.2	0.18
MPTMS	2	75	75	75	75	75	75	0

Table A.3. Experimental Dry Tensile Test Results of PP-Zeolite Composites.

Plasticizer	Surface Modifier	Amount of Surface Modifier (wt%)	Zeolite (wt%)	Dry $E_c$ (MPa)	Dry $\sigma_{yc}$ (MPa)	Dry $\sigma_c$ at Break (MPa)	Dry $\epsilon_c$ at Break (%)
-	-	-	-	1169.4	28.02	27.9	466.13
DOP			-	1167.4	25.20	27.4	487.2
			2	1338.5	23.45	25.1	433.60
			4	1268.1	22.06	22.3	340.40
			6	1449.7	21.20	22.3	46.44
	PEG	3	2	1350.8	23.76	23.9	395.10
			4	1416.8	23.19	22.2	289.40
			6	1429.9	21.88	22.1	61.66
EPS			-	1152.2	25.18	26.9	484.6
			2	1260.3	23.08	23.7	349.73
			4	1313.6	20.56	21.4	197.06
			6	1450.4	16.90	17.8	5.89
	PEG	3	2	1360.8	21.41	21.0	405.90
			4	1428.2	20.29	19.2	137.96
			6	1409.1	19.13	20.1	6.09
EPS	AMPTES	0.5	2	1413.8	24.57	25.8	394.20
			4	1510.7	24.10	25.0	223.80
			6	1653.2	23.90	22.1	15.48
		1	2	1446.7	24.96	26.4	386.80
			4	1540.2	24.44	25.3	231.12
			6	1805.3	24.30	23.9	14.45
		1.5	2	1478.2	24.70	26.2	396.20
			4	1535.1	24.40	25.0	241.53
			6	1751.3	23.50	23.7	12.87
		2	2	1422.2	24.40	26.6	396.60
			4	1410.3	24.00	25.4	238.53
			6	1602.7	23.10	22.7	21.23
EPS	MTES	0.5	2	1295.6	24.60	25.8	381.40
			4	1444.4	23.69	21.7	216.20
			6	1658.9	21.05	20.7	32.43
		1	2	1443.9	24.37	26.3	377.20
			4	1449.4	23.62	22.2	244.60
			6	1678.15	23.23	23.9	15.66
		1.5	2	1540.6	24.41	26.3	389.40
			4	1585.4	23.64	23.3	222.60
			6	1501.5	22.95	22.9	30.72
		2	2	1491.0	24.23	24.2	340.40
			4	1563.9	23.89	20.1	300.60
			6	1484.5	20.34	19.0	27.97

Plasticizer	Surface Modifier	Amount of Surface Modifier (wt%)	Zeolite (wt%)	Dry $E_c$ (MPa)	Dry $\sigma_{yc}$ (MPa)	Dry $\sigma_{yc}$ at Break (MPa)	Dry $\epsilon_c$ at Break (%)
EPS	MPTMS	0.5	2	1336.3	24.72	25.2	364.00
			4	1434.9	24.34	25.9	225.00
			6	1560.0	23.96	23.0	27.09
		1	2	1348.1	24.46	26.2	370.20
			4	1443.3	23.77	25.3	261.05
			6	1663.1	23.35	23.9	24.00
		1.5	2	1337.6	24.64	26.3	360.12
			4	1526.1	24.13	24.6	275.00
			6	1500.5	23.40	23.0	30.48
		2	2	1301.2	24.51	25.2	402.20
			4	1439.7	23.87	24.4	248.40
			6	1475.9	23.20	23.2	15.34

Table A.4. Experimental Wet Tensile Test Results of PP-Zeolite Composites.

Plasticizer	Surface Modifier	Amount of Surface Modifier (wt%)	Zeolite (wt%)	Wet $E_c$ (MPa)	Wet $\sigma_{yc}$ (MPa)	Wet $\sigma_c$ at Break (MPa)	Wet $\epsilon_c$ at Break (%)
-	-	-	-	1126.7	27.40	27.4	484.8
DOP	PEG	3	-	1095.1	25.49	27.4	485.2
			2	1218.8	22.85	25.8	374.40
			4	1295.1	20.74	22.5	226.50
			6	1414.7	20.18	19.5	59.73
			2	1348.1	23.23	23.3	414.70
			4	1351.1	22.77	21.3	196.13
EPS	PEG	3	6	1365.6	21.31	19.6	58.74
			-	1096.5	25.06	27.2	485.4
			2	1201.1	22.55	22.6	370.30
			4	1255.9	19.72	22.3	196.61
			6	1425.8	17.49	19.9	7.96
			2	1222.2	23.39	24.8	380.80
EPS	AMPTES	0.5	4	1358.7	21.64	20.5	87.91
			6	1373.9	18.84	19.8	6.81
			2	1394.8	24.62	25.4	359.40
		1	4	1405.7	24.09	25.0	295.72
			6	1509.5	23.23	22.0	8.48
			2	1398.9	24.92	26.4	367.00
		1.5	4	1435.5	24.34	24.2	259.13
			6	1526.2	23.63	23.9	16.17
			2	1310	24.54	26.8	372.67
		2	4	1373.1	23.87	24.8	257.41
			6	1469.4	23.22	21.3	29.74
			2	1236.2	24.42	25.3	379.70
EPS	MTES	0.5	4	1359.1	23.75	24.3	329.57
			6	1394.2	22.91	21.8	11.93
			2	1266.8	24.30	25.9	394.9
		1	4	1349.1	22.70	25.1	249.60
			6	1457.9	21.35	20.1	11.68
			2	1327.2	24.35	26.0	330.10
		1.5	4	1370.2	23.63	23.4	230.33
			6	1446.4	22.91	23.5	48.21
			2	1191.5	24.23	25.2	319.30
		2	4	1383.2	23.59	23.5	273.67
			6	1449.2	22.74	22.3	23.18
			2	1372.6	24.37	25.1	374.40
			4	1366.5	23.42	24.0	281.40
			6	1419.9	20.15	20.5	17.59
			2	1419.9	20.15	20.5	17.59

Plasticizer	Surface Modifier	Amount of Surface Modifier (wt%)	Zeolite (wt%)	Wet $E_c$ (MPa)	Wet $\sigma_{yc}$ (MPa)	Wet $\sigma_c$ at Break (MPa)	Wet $\epsilon_c$ at Break (%)
EPS	MPTMS	0.5	2	1251.7	24.32	26.3	361.98
			4	1325.3	24.22	25.5	266.06
			6	1437.7	23.84	24.3	16.45
		1	2	1259.4	24.41	26.8	353.00
			4	1339.6	23.53	24.8	296.00
			6	1533.7	23.09	23.4	13.80
		1.5	2	1231.0	24.32	26.0	372.40
			4	1332.8	23.48	24.2	257.60
			6	1427.9	22.85	22.0	18.50
		2	2	1238.6	23.98	25.3	344.60
			4	1367.2	23.07	24.0	285.17
			6	1424.3	21.58	23.8	44.13

Table A.5. B Values in Pukanszky Model for Dry and Wet Yield Stress of PP-Zeolite Composites.

Plasticizer	Surface Modifier	Amount of Surface Modifier (wt%)	B value in Dry $\sigma_{yc}$	B value in Wet $\sigma_{yc}$
DOP	-	-	-2.86	-5.55
DOP	PEG	3	-1.33	-2.86
EPS	-	-	-9.02	-8.8
EPS	PEG	3	-6.99	-5.53
EPS	AMPTES	0.5	1.46	1.05
EPS	AMPTES	1	2.15	1.67
EPS	AMPTES	1.5	1.30	0.88
EPS	AMPTES	2	0.59	0.48
EPS	MTES	0.5	-1.59	-1.79
EPS	MTES	1	0.47	0.38
EPS	MTES	1.5	0.23	0.16
EPS	MTES	2	-2.35	-2.59
EPS	MPTMS	0.5	1.7	1.71
EPS	MPTMS	1	0.64	0.6
EPS	MPTMS	1.5	1.02	0.22
EPS	MPTMS	2	0.64	-1.41

Table A.6. Values of Adhesion Parameter “a” in Nicolais Nartis Model for Dry and Wet Yield Stress of PP-Zeolite Composites.

Plasticizer	Surface Modifier	Amount of Surface Modifier (wt%)	a value in Dry $\sigma_{yc}$	a value in Wet $\sigma_{yc}$
DOP	-	-	1.65	2.36
DOP	PEG	3	1.26	1.73
EPS	-	-	2.62	2.79
EPS	PEG	3	2.85	2
EPS	AMPTES	0.5	0.55	0.57
EPS	AMPTES	1	0.32	0.37
EPS	AMPTES	1.5	0.52	0.63
EPS	AMPTES	2	0.73	0.73
EPS	MTES	0.5	1.02	1.18
EPS	MTES	1	0.80	0.78
EPS	MTES	1.5	0.82	0.84
EPS	MTES	2	1.19	1.2
EPS	MPTMS	0.5	0.46	0.54
EPS	MPTMS	1	0.73	0.75
EPS	MPTMS	1.5	0.6	0.82
EPS	MPTMS	2	0.72	1.17

Table A.7. Values of Stress Concentration Parameter “S” in Nielsen Model for Dry and Wet Tensile Stress at Break Values of PP-Zeolite Composites.

Plasticizer	Surface Modifier	Amount of Surface Modifier (wt%)	S value in Dry $\sigma_c$	S value in Wet $\sigma_c$
DOP	-	-	0.83	0.74
DOP	PEG	3	0.88	0.77
EPS	-	-	0.78	0.76
EPS	PEG	3	0.8	0.78
EPS	AMPTES	0.5	0.96	0.95
EPS	AMPTES	1	1	0.97
EPS	AMPTES	1.5	0.996	0.96
EPS	AMPTES	2	0.993	0.94
EPS	MTES	0.5	0.92	0.94
EPS	MTES	1	0.97	0.94
EPS	MTES	1.5	0.96	0.93
EPS	MTES	2	0.87	0.92
EPS	MPTMS	0.5	0.99	0.98
EPS	MPTMS	1	1.06	0.96
EPS	MPTMS	1.5	0.98	0.95
EPS	MPTMS	2	0.97	0.92

Table A.8. Values of Interaction Parameter “K” in The Model Derived by Mitsuishi et al. (1985) for Dry and Wet Elongation at Break Values of PP-Zeolite Composites.

Plasticizer	Surface Modifier	Amount of Surface Modifier (wt%)	K value in Dry $\epsilon_c$ at Break	K value in Wet $\epsilon_c$ at Break
DOP	-	-	5.39	7.24
DOP	PEG	3	6.35	6.92
EPS	-	-	8.28	7.96
EPS	PEG	3	7.98	8.85
EPS	AMPTES	0.5	7.27	7.18
EPS	AMPTES	1	7.32	7.36
EPS	AMPTES	1.5	7.09	7.19
EPS	AMPTES	2	7.05	6.52
EPS	MTES	0.5	7.42	7.06
EPS	MTES	1	7.33	7.96
EPS	MTES	1.5	7.25	7.90
EPS	MTES	2	7.27	7.02
EPS	MPTMS	0.5	7.64	7.37
EPS	MPTMS	1	7.22	7.24
EPS	MPTMS	1.5	7.19	7.27
EPS	MPTMS	2	6.92	7.25

Table A.9. Theoretical Dry Tensile Tests Results of PP Composites.

Plasticizer	Surface Modifier	Amount of Surface Modifier (wt%)	Zeolite (wt%)	Dry $E_c$ (MPa)	Dry $\sigma_{yc}$ (MPa)	Dry $\sigma_c$ at Break (MPa)	Dry $\epsilon_c$ at Break (%)
-	-	-	-	1141.3	28.02	27.95	466.13
DOP	PEG	3	-	1167.4	25.20	27.41	487.2
			2	1191.8	23.72	21.69	369.00
			4	1217.2	22.30	21.07	298.34
			6	1243.6	20.96	20.55	238.08
			2	1191.8	24.07	23.11	347.93
			4	1217.2	22.98	22.46	264.68
EPS	PEG	3	6	1243.6	21.93	21.90	193.68
			-	1152.2	25.18	26.97	484.6
			2	1176.3	22.35	20.15	303.95
			4	1201.3	19.80	19.58	195.95
			6	1227.4	17.51	19.09	103.85
			2	1176.3	22.78	20.67	310.37
EPS	AMPTES	0.5	4	1201.3	24.23	24.22	230.97
			6	1227.4	23.77	23.62	150.05
			2	1176.3	24.70	24.92	325.87
		1	4	1201.3	24.56	25.20	229.21
			6	1227.4	24.26	24.57	147.72
			2	1176.3	24.66	25.65	329.82
		1.5	4	1201.3	24.16	24.93	237.29
			6	1227.4	23.66	24.31	158.38
			2	1176.3	24.50	25.58	330.65
		2	4	1201.3	23.83	24.86	238.61
			6	1227.4	23.18	24.24	160.12
			2	1176.3	23.99	23.75	322.70
EPS	MTES	0.5	4	1201.3	22.84	23.08	225.90
			6	1227.4	21.74	22.51	143.36
			2	1176.3	24.47	24.95	324.57
		1	4	1201.3	23.78	24.25	228.89
			6	1227.4	23.10	23.65	147.31
			2	1176.3	24.41	24.66	326.43
		1.5	4	1201.3	23.66	23.96	231.86
			6	1227.4	22.93	23.37	151.23
			2	1176.3	23.82	22.44	325.93
		2	4	1201.3	22.51	21.81	231.07
			6	1227.4	21.26	21.27	150.18

Plasticizer	Surface Modifier	Amount of Surface Modifier (wt%)	Zeolite (wt%)	Dry $E_c$ (MPa)	Dry $\sigma_{yc}$ (MPa)	Dry $\sigma_c$ at Break (MPa)	Dry $\epsilon_c$ at Break (%)
EPS	MPTMS	0.5	2	1176.3	24.76	25.40	317.89
			4	1201.3	24.34	24.69	218.22
			6	1227.4	23.94	24.08	133.23
		1	2	1176.3	24.53	25.40	326.98
			4	1201.3	23.88	24.69	232.76
			6	1227.4	23.26	24.08	152.40
		1.5	2	1176.3	24.60	25.29	327.56
			4	1201.3	24.03	24.58	233.68
			6	1227.4	23.47	23.97	153.61
		2	2	1176.3	24.51	24.93	333.64
			4	1201.3	23.85	24.22	243.40
			6	1227.4	23.21	23.62	166.44

Table A.10. Theoretical Wet Tensile Tests Results of PP Composites.

Plasticizer	Surface Modifier	Amount of Surface Modifier (wt%)	Zeolite (wt%)	Wet $E_c$ (MPa)	Wet $\sigma_{yc}$ (MPa)	Wet $\sigma_c$ at Break (MPa)	Wet $\varepsilon_c$ at Break (%)
-	-	-	-	1126.7	27.40	27.4	484.8
DOP	PEG	3	-	1095.1	25.49	27.46	485.2
			2	1118.0	23.39	19.51	327.01
			4	1141.8	21.43	18.96	232.43
			6	1166.6	19.60	18.49	151.79
			2	1118.0	23.99	20.37	333.95
			4	1141.8	22.57	19.79	243.53
EPS	PEG	3	6	1166.6	21.21	19.30	166.42
			-	1096.5	25.06	27.26	485.4
			2	1119.4	22.29	19.97	245.21
			4	1143.3	19.78	19.41	163.21
			6	1168.1	17.52	18.93	93.28
			2	1119.4	22.99	20.35	229.96
EPS	AMPTES	0.5	4	1143.3	21.07	19.78	138.84
			6	1168.1	19.28	19.29	61.14
			2	1119.4	24.49	24.78	258.70
		1	4	1143.3	23.93	24.08	184.76
			6	1168.1	23.38	23.49	121.71
			2	1119.4	24.63	25.31	255.64
		1.5	4	1143.3	24.21	24.60	179.88
			6	1168.1	23.80	23.99	115.27
			2	1119.4	24.45	24.95	258.54
		2	4	1143.3	23.85	24.25	184.50
			6	1168.1	23.26	23.65	121.37
			2	1119.4	24.35	24.43	270.03
EPS	MTES	0.5	4	1143.3	23.66	23.74	202.86
			6	1168.1	22.99	23.15	145.58
			2	1119.4	23.83	24.33	260.84
		1	4	1143.3	22.65	23.64	188.19
			6	1168.1	21.51	23.06	126.23
			2	1119.4	24.33	24.48	245.21
		1.5	4	1143.3	23.62	23.79	163.21
			6	1168.1	22.92	23.20	93.28
			2	1119.4	24.20	24.29	246.38
		2	4	1143.3	23.37	23.61	165.08
			6	1168.1	22.56	23.02	95.74
			2	1119.4	23.65	23.84	261.42
			4	1143.3	22.30	23.17	189.11
			6	1168.1	21.01	22.60	127.45
			2	1119.4	23.65	23.84	261.42

Plasticizer	Surface Modifier	Amount of Surface Modifier (wt%)	Zeolite (wt%)	Wet $E_c$ (MPa)	Wet $\sigma_{yc}$ (MPa)	Wet $\sigma_c$ at Break (MPa)	Wet $\epsilon_c$ at Break (%)
EPS	MPTMS	0.5	2	1119.4	24.62	25.45	255.50
			4	1143.3	24.19	24.73	179.65
			6	1168.1	23.77	24.12	114.96
		1	2	1119.4	24.36	24.87	257.73
			4	1143.3	23.68	24.16	183.21
			6	1168.1	23.01	23.57	119.67
		1.5	2	1119.4	24.29	24.69	257.10
			4	1143.3	23.55	24.00	182.20
			6	1168.1	22.82	23.40	118.34
		2	2	1119.4	23.92	23.84	257.52
			4	1143.3	22.82	23.17	182.88
			6	1168.1	21.76	22.59	119.23

